VOL. XI - Nº 4 1989 ISSN 0100-7386

REVISTA BRASILEIRA DE CIÊNCIAS MECÂNICAS

JOURNAL OF THE BRAZILIAN SOCIETY OF MECHANICAL SCIENCES

PUBLICAÇÃO DA ABCM
ASSOCIAÇÃO BRASILEIRA DE CIÊNCIAS MECÂNICAS

RBCM - J. of the Braz.Soc.Mech.Sc.
Vol. XI - nº 4 - pp. 293-305 - 1989

ISSN 0100-7386
Impresso no Brasil

RECENT DEVELOPMENTS IN EXPERIMENTAL MODAL ANALYSIS – TRENDS AND NEEDS

DESENVOLVIMENTOS RECENTES EM ANÁLISE MODAL TENDÊNCIAS E NECESSIDADES

H.G. Natke
Curt-Risch-Institut für Dynamik
Schall- u.Messtechnik - Universität Hannover
Appelstr. 9A, 3000 Hannover 1 - FRG

Guilherme Emanuel Costa Laux - Membro da ABCM
UFES/CT - Departamento de Engenharia Mecânica
Vitória, ES - Brasil - CEP 29100

ABSTRACT

Are discuted in time and frequency domain the general procedures of. Experimental Modal Analysis, considering the most recent development. Excitation, sensoring, effetive degrees of freedom are considered including the error investigation. As a conclusion, statistical investigations on the different methods is necessary, due to the parameters correlation, and the erro hounds. Finally the modal identification aspects thort need to be investigated are presented.

Keywords: Modal Analysis

RESUMO

Discute-se, de uma forma geral os métodos experimentais de Análise Modal, nos domínios da freqüência e do tempo, com os mais recentes desenvolvimentos. São feitas considerações sobre excitação, sensoramento, número efetivo de graus de liberdade e investigação de erro. Conclue-se da necessidade de investigações estatísticas nos diferentes métodos, devido a correlação dos parâmetros, bem como do limite de erro. Finalmente apresenta-se aspectos de identificação modal que necessitam investigação atenta em detalhe.

Palavras-chave: Análise Modal

Submetido em Julho/89 **Aceito em Agosto/89**

REVISTA BRASILEIRA DE CIÊNCIAS MECÂNICAS
JOURNAL OF THE BRAZILIAN SOCIETY OF MECHANICAL SCIENCES

Publicado pela / Published by

ASSOCIAÇÃO BRASILEIRA DE CIÊNCIAS MECÂNICAS, ABCM /
BRAZILIAN SOCIETY OF MECHANICAL SCIENCES

Secretária da ABCM: Sra. Simone Maria Frade
Av. Rio Branco, 124 - 18º Andar - Rio de Janeiro - Brasil
Tel. (021) 221-6177 R. 278, Telex (21) 37973 CGEN-BR

Presidente: Sidney Stuckenbruck
Secret. Geral: José Luiz de França Freire
Diretor de Patrimônio: José Augusto Ramos do Amaral
Vice-Presidente: Luiz Bevilacqua
Secretário: Tito Luiz da Silveira

PROGRAMA DE APOIO À PUBLICAÇÕES CIENTÍFICAS

MCT

CNPq

finep

INTRODUCTION

Experimental modal analysis is well understood and is very common today. It is sometimes used when it is not really required, and there are cases when experimental modal analysis is performed while other methods would be preferable. The knowledge of modal quantities is needed, if

i) the inner structure of the dynamic behavior is required (decompositions),

ii) particular (generalized) degrees of freedom are requested (stability investigations),

iii) they are used for mathematical handling (e.g. modal transformation).

In all other cases the engineer is interested in the predictions of dynamic responses using a mathematical model with known confidence within pre-given error limits.

The basic theory of experimental modal analysis can be found in [1-10]. The state of the art of its theory and applications are described in [1,11-16] and elsewhere, [17] is an extensive review. Another review paper [32] additionally contains practical rules.

The state of the art is not directly presented here (see e.g. [14,15]), but only some statements will be made which seem to be important from the authors' point of view. The main characteristics of experimental modal analysis today can be described briefly as follows: the various possible excitations are applied mostly in the search for good coherent output quantities. It is known that multi-point excitations and "suitably" chosen force shapes increase the confidence of estimates. An attempt is made to improve the accuracy of the measurements by a large signal-to-noise ratio, and by repeated tests and applications of (approximated, e.g. averaging) estimations. With regard to the measurement itself, improvement may be noted with the application of suitably chosen pickups and high-quality instrumentation. The selection of transducers depends on the task, frequency range etc., and wether rotating parts have to be measured and many other conditions have to be taken into account, as described, for instance, in [1] and elsewhere. The choice of pickup positions is generally determined by prior knowledge. The choice of actuators and their locations is done by prior knowledge and also by trial and error. Linearity checks are not always performed, though they are absolutely necessary to avoid biased estimates. Boundary conditions and their realizations are also important in this context and have to be investigated thoroughly. If necessary their influence has, of course, to be modelled.

Data acquisition and signal processing can be a hard job. However, the effects of the various manipulations in this context are known and can be assessed. In consequence, if the correct approximations and remedies are chosen, the additional inaccuracy introduced must not exceed a pre-given bound.

Free response measurements and dynamic responses due to a defined excitation are the basis of identification. One first step may be the non-parametric estimation of impulse response functions, frequency response functions (connected with the Fourier transform)

and transfer functions (with respect to the Laplace transform). With regard to this, the theory is well established [1,6]. Some improvements concerning error minimization have been developed and will be discussed later. However, in general the estimates are presented without any direct error statements.

Modal parameter estimation methods are well developed. They are defined in the time domain as well as in the frequency domain. Measurements of dynamic responses, random decrement functions and inverse FFT applied to frequency response fur..tions are provided as starting data in the time domain. The classic second order equation of motion as well as the state space formulation serve as a basis for this. Their solutions are taken directly decomposed in modal quantities. Approximation of the equation of motion (see e.g. ARMA models) as well as of its solutions is favored. For details see the available publications and the reviews and surveys mentioned here. They may be complemented by [16,18,26,28,33]. Some of them are also tutorial and re-confirm statements (e.g. concerning excitation, local and global procedures) which are well-known to the practising engineer and analyst and which have already been published (sometimes the statements are self-evident). Many procedures exist, and some methods are compared and assessed mainly taking benchmarks.

A comparison may be useful in order to express a preference for one method for the assistance of the non-expert, but this is hard to establish and one should ask whether such a comparison is really necessary. If the appliers were able to give some error bounds (estimates) of their results, they could decide by themselves whether their results are accurate enough within the requirements. If not, they have to consider why they failed and then improve the estimates. In this context it should be mentioned that it can be difficult to determine the effective number of degrees of freedom. This problem is also discussed later.

Recent developments can be obtained from the proceedings of national and international conferences on experimental modal analysis, such as the annual seminars in Hannover [15], IMAC, IFAC, the international seminar at Leuven and, for instance held at CALTECH, Pasadena 1988. These papers have been assessed and serve as the basis of the paper in hand. Comments are made on them by the authors.

TEST REQUIREMENTS

With regard to test requirements, less new essential work is noted. Only a few publications deal with the optimization of measurement and excitation. The limited number of pickups and actuators must be taken into account, and also the limited excitation energy available. The types of sensors and actuators and their locations should be optimized.

Excitation. The trend is again toward multi-point excitation, because it provides higher confidence in the estimates, allows one to estimate several columns of the frequency response

matrix at the same time, and decreases the danger of omitting eigenmodes. Fewer problems arise with unwanted phase shifts if the synchronous excitation is performed electronically with electrodynamic exciters, than when electronic control is combined with mechanical (e.g. hammer) or explosive excitation sources. Nowadays a renewed interest in harmonic excitation as a stepped sine can be noted with non-constant frequency increments [26]. The exciter-system interaction has also been rediscovered. It should be noted that it can be difficult to measure the input forces with sufficient accuracy.

A good survey of excitation signals is presented in [22].

The appropriated exciation of a multi-degree of freedom system so that the system vibrates in one pre-selected normal mode is theoretically well-defined. It uses the unknown modal quantities. Papers which deal with the problem of how to find out the appropriate excitation are, for example [44-50], which also include attempts to automatize a procedure of this kind. As far as the authors are aware, no general convergent procedure exists.

Optimization of the excitation concerns the force shape, the number and placement of the actuators [52] using Fisher's information matrix under simplifying assumptions.

It should be noted that the optimum excitation of modes (modal quantities) is quite different from the excitation needed for modelling critical load paths. In the latter, realistic loading is favorable [1] (p. 186 with respect to the design loads).

Measurement. Multi-point measurements are necessary for mode shape estimation. In European ground vibration testing for airplanes (≡ modal test at the ground) more than 200 pick-ups are used simultaneously. The Boeing company reports on 300 channels [53]. The difficulty here is calibration, and in consequence one has to look for easy but accurate methods for doing this [54,55].

Holographic interferometry is not new, but it needs some improvement because of the ambiguity in fringe interpretation. [36] presents a modulated fringe technique which removes the fringe ambiguity by superposing a linear phase variation on the phase change produced by the vibration displacements. As low cost transducers are used as spatially distributed transducers, piezoelectric films are discussed [38,41]. This can be a step towards measuring field quantities instead of their discretized approximations.

With regard to the sensor types, numbers and their postions, the first papers have appeared, such as [56,35].

NON-PARAMETRIC IDENTIFICATION

Non-parametric identification refers to the impulse response functions (and step response functions) in the time domain and to the frequency response functions in the frequency

domain and the transfer functions in the s-domain (s - Laplacian variable).

Estimation of the Impulse Response Function. The determination of the impulse response function is equivalent to the deconvolution, which is a numerically unstable process. Although some direct estimation procedures for the estimation of impulse response functions exist [57], in general it is done indirectly by inverse Fourier transformation (Laplace transformation) using estimated frequency response functions (transfer functions). (Frequency response functions need only matrix inversion instead of convolution.) The step response function then follows from the unit impulse response function by single integration, as is well known.

Estimation of the Frequency Response Function (Transfer Function). The estimation of frequency response functions uses spectral analysis and takes into account output noise as well as input noise [21]. Unbiased estimates are possible for multi-degree-of-freedom models [33]. The coherence function serves to indicate the quality of the input/output relationship and can be used for obtaining estimates with the pre-defined variances. The reader can find an extensive error discussion in the older paper by H. Schmidt [51].

MODAL PARAMETER ESTIMATION

Experimental modal analysis today ought to be based on parameter estimation methods.

Effective Number of Degrees of Freedom. The methods discussed here need the knowledge of the effective number of degrees of freedom hidden in the measured data. This number defines the order of the model used in estimation. With regard to frequency domain methods, various procedures are discussed in [58]. In [34] the fractional rational function of the elements of the frequency response matrix is used in terms of orthogonal polynomials. Curve fitting of the denominator by a polynomial with pre-given maximum power using LS yields a squared error which serves as proof of the statistical hypothesis.

Deterministic methods are investigated in [39,42]. [39] starts with an LS problem and states that adding a column to a matrix increases its largest singular value and decreases its smallest singular value, thus making it closer to rank deficiency. In consequence, the "true" parameters will converge to a small area bounding the true values, the remaining parameters will be arbitrary (and will change in each step). Time domain methods will use the generalized inverses or rank decomposition. The latter is discussed in [42]. Here, for example, the (generalized) Hankel matrix is taken and the singular value decomposition applied which extracts the eigenvalue of the system from measurements. Another

decomposition method applies the QR algorithm. The modal methods [59,60] should be mentioned in this context. Many time domain methods make use of overspecification (that means taking a larger number of degrees of freedom than contained in the measurements) if required. This is necessary for determining the model order, and serves to reduce the bias [43]. Concerning the order determination of ARMA models see [61].

A further development is the complex mode indication function (CMIF) [23]. It is based on the frequency response matrix and is defined as the plot of the eigenvalues of the frequency response matrix premultiplied by its Hermitian matrix (the result is equal to the normal matrix). The plot is done on a log scale over the frequency axis. Thus it is a method for detecting the effective number of modes within the measurements.

Time Domain Methods. A comparison of parameter estimation methods (LS, double LS, total LS, correlation fit and Smith LS - which includes a constant offset term in the basic equation) is made in [25] by means of aircraft test data, and is applied to the impulse response of a multi-degree of freedom model. The LS applied results in the polyreference method. This investigation does not result in clear statements with respect to what methods in general seems to be favorable.

In [26] the state space formulation is used to develop a frequency domain method. SVD is applied to extract valid state variables. A combination of known methods, such as the so-called Ibrahim Method with the random decrement method, can be found in [62]. A probabilistic time domain identification method is presented in [30]. The identification of distributed systems (continuously modelled) using the Rayleigh quotient and admissible functions for discretization is described in [31]. In paper [32] the recursive prediction error in the context of ARMAX models is compared with the maximum-likelihood estimation in the context of state space modal parametrization by their characteristics. The optimal experiment design is based on the information matrix. Simplifications can be achieved by the determinant-optimal experiments for identifying modal frequencies and damping parameters. Various practical rules are given in this paper.

Total LS methods are investigated from a statistical point of view in [40]. The advantage is the practically unbiased estimates compared with the LS (pseudoinverse) solutions.

Frequency Domain Methods. It is agreed in the "modal community" that these methods work well in a narrow frequency intervall (small effective number of degrees of freedom) and that they are suitable (predestined) for the separation of highly coupled modes.

Some methods result in the root determination of polynomials. In [19] the numerical conditioning is investigated by root sensitivity due to coefficient perturbation. A small effective number of degrees of freedom (5-7, see [1]) can be handled.

The ARMA model in the Laplace domain is taken in [37]. Multiple reference frequency

response measurements (emphasized due to multipoint excitation) serve for estimation. It is a rational fraction formulation of orthogonal polynomials (Forsythe) which is able to reduce ill-conditioning and decouple the normal matrix.

The complex mode indication function [23] is mentioned in the context of chapter 4.1. It is based on the frequency response matrix, applies the SVD, and in a second stage procedure (by applying a single degree of freedom modal parameter estimation algorithm and mass matrix information) all modal parameters can be obtained.

The optimization of experimental design in order to obtain estimates of minimum variance was started in [63]. It takes into account only the excitation and minimizes the Fisher's information matrix under the restriction of decoupling submatrices with respect to the degree of freedom. It is continued essentially with regard to updating mathematical models [64].

ERROR INVESTIGATIONS

Experimental modal analysis results are, in general, erroneuous and incomplete. It is (or should be) common practice that the (statistical) errors of the measurements on which the modal procedure is based, including those of the frequency response functions if used, are known (estimated). However, the estimates of modal quantities, in general, are not presented with their uncertainties, although early exceptions do exist [65]. For validation of the estimates it is absolutely necessary to know these uncertainties in addition to global checks, such as looking for residuals (prediction errors etc.).

One has to distinguish between deterministic (including bias coming from estimation) and random errors on one hand, and on the other hand between the physical and mathematical interpretation of the results within their error bounds (e.g. if an asymmetric mode is estimated for a symmetrical system). The latter and deterministic errors due to testing conditions can be handled by indicators (functionals) and (sometimes) by the errors in the estimates. Statistical errors from the test set-up should be avoided or detected and corrected computationally.

With regard to indicators, one should mention the orthogonality check of measured modes (if not directly a part of the procedure as a dynamic constraint) [1]. The application of the so-called model assurance criteria (little, big, multi MAC) is widespread. Here the cosine of the angle between two estimated eigenvectors are checked (see [18] and the references cited there). It is therefore a deterministic check (no correlation in the statistical meaning) and the analogy to the coherence function is purely formal.

In [28] the unmodelled residual modes are investigated applying the inclusion principle in the identification of distributed systems (continua). The inclusion principle exists in identification as well as in modelling.

The basic idea of paper [35] is very interesting. It deals with different sets of eigenmodes in the stat space domain and investigates the influence of external forces and number of sensors on the modal results.

Estimates of covariances and/or of variances can be obtained by the well-known methods, mainly using weighted averaging. This is necessary in order to verify the estimates [27,29]. The application of parameter estimation methods presumes that the structure of the used mathematical model is adequately valid. The structure of this linear model with a finite number of degrees of freedom is predetermined by this number (see Chapt. 4.1) and by the modelling of the damping forces.

CONCLUDING REMARKS

The cited references with their subjects should indicate the trend in the field of experimental modal analysis. However, it is very difficult to summarize it briefly. Time domain methods are favorably discussed, benchmarks seem to be popular, and error investigations (in the sense of indication functions) are widespread. Papers which summarize systematically the experience made with different methods and applied to various structures are rare.

In the experience of the authors it is necessary to present modal estimates with their error estimates. Deterministic errors have to be corrected mathematically (if detected) and random errors should be approximately determined. The assessment of modal estimates with respect to their confidence is indispensable for application. Statistical investigation of the various method seem to be needed in this context, because (statistical) correlations of the parameters can involve inherent error bounds which cannot be reduced.

Some problems which should receive more detailed attention within modal identification in future are

- direct estimation of impulse response functions
- test optimization in general
- realization and optimization of multiple transient excitation
- inclusion of knowledge from the prior mathematical model
- real time identification for control purposes
- systematic approaches for applying the estimated modal quantities.

REFERENCES

[1] NATKE, H.G. - Einführung in Theorie und Praxis der Zeitreihen- und Modalanalyse, Friedr. Vieweg & Sohn, Braunschweig, Wiesbaden, 2. Aufl., 1988.

[2] EWINS, D.J. - Modal testing: Theory and practice, Research Studies Press Ltd., 1984.

[3] BRAUN, S. (Ed.) - Mechanical signature analysis - Theory and applications, Academic Press, London, Orlando, San Diego, New York, Austin, Montreal, Sydney, Todyo, Toronto, 1986.

[4] ZAVERI, K. - Modal analysis of large structures - Multiple exciter systems, Brüel & Kjaer, Naerum, DK, 1984.

[5] EYKHOFF, P. - System identification - Parameter and state estimation, John Wiley & Sons, London, New York, Sydney, Toronto, 1974.

[6] BENDAT, J.S.; PIERSOL, A.G. - Random data: Analysis and measurement procedures, John Wiley & Sons, New York, London, Sydney, Toronto, 1971.

[7] BOX, G.E.P.; JENKINS, G.M. - Time series analysis forecasting and control, Holden-Day, 1970.

[8] BARD, Y. - Nonlinear parameter estimation, Academic Press, N.Y., London, 1974.

[9] CHATFIELD, C. - Tthe analysis of time series: An introduction; 2nd Ed., Chapman and Hall, London, New York, 1980.

[10] FAHRMEIER, L.; KAUFMANN, H.; OST, F. - Stochastische Prozesse, Eine Einführung in Theorie und Anwendungen, Hanser, 1981.

[11] NATKE, H.G. (Ed.) - Identification of vibrating structures, CISM Courses and Lectures nº 272, Springer-Verlag Wien, New York, 1982.

[12] NATKE, H.G. (Ed.) - Application of system identification in engineering, CISM Courses and Lectures nº 296, Springer-Verlag Wien, New York, 1988.

[13] NATKE, H.G. - Survey of the parameter identification of elasto-mechanical systems, in H. Neunzert (Ed.), Proc. of the Workshop on Road-Vehicle-System and Related Mathematics, B.G. Teubner Stuttgart, pp. 155-170, 1985.

[14] NATKE, H.G. - Survey on the identification of mechanical systems, in H. Neunzert *d.), Proc. of the 2nd Workshop on Road-Vehicle-Systems and Related Mathematics, B.G. Teubner Stuttgart and Kluver Academic Publ., pp. 69-116, 1989.

[15] NATKE, H.G. - Identifikation mechanischer Systeme, Teil 1: Versuchstechnik innerhalb der Identifikation, Automobilindustrie 2/89, pp. 171-182, Teil 2: Experimentelle Analyse von Konstruktionen (Identifikation schwingender elastomechanischer Systeme), Automobilindustrie 3/89, pp. 325-334 and Teil 3: Anwendungen in der Systemidentifikation, in Automobil-Industrie, will be published.

[16] NATKE, H.G.; YAO, J.T.P. (Eds.) - Structural safety evaluation based on system identification approaches, Proc. of the Internat. Workshop at Lambrecht/Pfalz, Friedr. Vieweg & Sohn, Braunschweig, Wiesbaden, 1988.

[17] DENMAN, E.E.; HASSELMAN, T.K. et al. - Methods for identification of large structures in space, Report AFRPL, 1986.

[18] ROST, R.; BROWN, D.L. - The use of spatial domain concepts in modal analysis, Proc. of the 13th Internat. Seminar on Modal Analysis, Leuven, Belgium, Part I, I-2, 1988.

[19] VOLD, H.; SHICH, C.Y. - On the numerical conditioning of some modal parameter estimation methods, Proc. of the 13th Internat. Seminar on Modal Analysis, Leuven, Belgium, Part I, I-4, 1988.

[20] ALLEMANG, R.J. - Classification methods for experimental modal analysis, Proc. of the 13th Internat. Seminar on Modal Analysis, Leuven, Belgium, Part I, I-8, 1988.

[21] PINTELON, R.; SCHOUKENS, J.; RENNEBOOG, J. - Application of ELIS in Modal Analysis, Proc. of the 13th Internat. Seminar on Modal Analysis, Leuven, Belgium, Part I, C-1, 1988.

[22] SCHOUKENS, J.; PINTELON, R., OUDERAA, E. VAN DER; RENNEBOOG, J. - Survey of excitation signals for FFT based signal analysers, Proc. of the 13th Internat. Seminar on Modal Analysis, Leuven, Belgium, Part II, C-25, 1988.

[23] SHIK, C.Y.; TSUEI, Y.G.; ALLEMANG, R.J.; BROWN, D.L. - Complex mode indication function and its application to spatial domain parameter estimation, Proc. of the 13th Internat. Seminar on Modal Analysis, Leuven, Belgium, Part III, C-29, 1988.

[24] PAN, J.; ALLEMANG, R.; VOLD, H. - An equivalent monophase representation of operating shapes, Proc. of the 13th Internat. Seminar on Modal Analysis, Leuven, Belgium, Part III, C-31, 1988.

[25] COOPER, J.E. - Comparison of modal analysis parameter estimation techniques on aircraft structural data, Proc. of the 13th Internat. Seminar on Modal Analysis, Leuven, Belgium, Part III, C-34, 1988.

[26] LEMBREGTS, F.; LEURIDAN J.; BRUSSEL, H. VAN - Frequency domain direct parameter identification for modal analysis, Proc. of the 13th Internat. Seminar on Modal Analysis, Leuven, Belgium, Part III, C-54, 1988,

[27] DENMAN, E.E.; HASSELMAN, T.K. et al. - Identification of large space structures on orbit - a survey, Model Determination for Large Space Systems, Workshop held at Calif. Inst. of Technology, pp. 36-53, 22-24 March 1988.

[28] NORRIS, M.A.; MEIROVITCH, L. - On the inclusion principle and spillover effect in the identification of distributed structures, Model Determination for Large Space Systems, Workshop held at Calif. Inst. of Technology, pp. 72-80, 22-24 March 1988.

[29] HASSELMAN, T.K. - Effects of model deficiencies on parameter estimation, Model Determination for Large Space Systems, Workshop held at Calif. Inst. of Technology, pp. 127-130, 22-24 March 1988.

[30] BECK, J.L. - Time domain method with probabilistic concept, Model Determination for Large Space Systems, Workshop held at Calif. Inst. of Technology, pp. 164-187, 22-24 March 1988.

[31] SILVERBERG, L.M.; NORRIS, M.A. - Variational modal identification of gyroscopic distributed parameter systems, Model Determination for Large Space Systems, Workshop held at Calif. Inst. of Technology, pp. 290-307, 22-24 March 1988.

[32] BAYARD, D.S. - Optimal experiment design for on-orbit identification, Model Determination for Large Space Systems, Workshop held at Calif. Inst. of Technology, pp. 616-642, 22-24 March 1988.

[33] ZHANG, L.; YAO, Y. - Advances of frequency response function estimation in modal analysis, Proc. 6th Internat. Modal Analysis Conf., Kissimee, FL, vol. I, pp. 107-112, 1988.

[34] WU, W.-Z.; LWO, T.-W. - Global modal parameter estimation combined with a statistical criterion, Proc. 6th Internat. Modal Analysis Conf., Kissimee, FL, vol. I, pp. 121-128, 1988.

[35] ZHENG, G.-T.; HUANG, W.-H; SHAO, C.-X - The Inherent Error of Modal Test and Countermeasures, Proc. 6th Internat. Modal Analysis Conf., Kissimee, FL, vol. I, pp. 185-188, 1988.

[36] SHERMAN, P.S.; HUNG, Y.Y.; GERHART, G. - Automated mode shape measurement by a modulated-fringe holographic interferometry technique, Proc. 6th Internat. Modal Analysis Conf., Kissimee, FL, vol. I, pp. 376-382, 1988.

[37] SHIH, C.Y.; TSUEI,Y.G.; ALLEMANG, R.J.; BROWN, D.L. - A frequency domain global parameter estimation method for multiple reference frequency response measurements, Proc. 6th Internat. Modal Analysis Conf., Kissimee, FL, vol. I, pp. 389-396, 1988.

[38] BROWN, R.H. - PIEZO film vibration sensors - New techniques for modal analysis, Proc. 6th Internat. Modal Analysis Conf., Kissimee, FL, vol. I, pp. 639-645, 1988.

[39] BRAUN, S.; RAM, Y. - On the fitting of structural models to data, Proc. 6th Internat. Modal Analysis Conf., Kissimee, FL, vol. I, pp. 789-793, 1988.

[40] TURUNEN, R. - Total least squares methods in modal software, Proc. 6th Internat. Modal Analysis Conf., Kissimee, FL, vol. I, pp. 805-811, 1988.

[41] HUBBARD, J.E., JR. - Distributed transducers for smart structural components, Proc. 6th Internat. Modal Analysis Conf., Kissimee, FL, vol. II, pp. 856-862, 1988.

[42] LIANG, Z.; INMAN, D.J. - Rank decomposition methods in modal analysis, Proc. 6th Internat. Modal Analysis Conf., Kissimee, FL, vol. II, pp. 1176-1179, 1988.

[43] COOPER, J.E. - Comparison of some time domain system identification techniques using approximate data correlations, Proc. 6th Internat. Modal Analysis Conf., Kissimee, FL, vol. II, pp. 1589-1595, 1988.

[44] HAWKINS, F.J. - GRAMPA - An automatic technique for exciting the principal modes of vibration of complex structures, TR 65142, R.A.E. Farnborough, Great Britain, 1965.

[45] TAYLOR, G.A.; GAUKROGER, D.R.; SKINGLE, C.W. - MAMA - A semiautomatic technique for exciting the principal modes of vibration of complex structures, TR 67211, R.A.E. Farnborough, Great Britain, Aug. 1967.

[46] KNAUER, C.D. JR.; PETERSON, A.J.; RENDAHL, W.B. - Space vehicle experimental modal definition using transfer function techniques, SAE Paper nº 751069, 1975.

[47] STROUD, R.C.; SMITH, S.; HAMMA, G.A. - MODALAB - A new system for structural dynamic testing, Shock and Vibration Bulletin, 46, 5, pp. 153-175, 1976.

[48] IBANEZ, P. - Force Appropriation by extended Asher's method, Aerospace, Eng. and Manufacturing Meeting, San Diego, CA, paper 760873, 1976.

[49] MOROSOW, G.; AYRE, R.S. - Modal test and analysis, The Shock and Vibration Bulletin, Part 1, pp. 39-48, 1978.

[50] ANDERSON, J.E. - Another look at sine-dwell mode testing, AIAA Paper nº 81-0532, 22nd Structures, Structural Dynamics and Materials Conf. Proc., p. 202, 1981.

[51] SCHMIDT, H. - Resolution bias errors in spectral density, frequency response and coherence function measurements, I-VI, Journal of Sound and Vibration, vol. 101, nº 3, 8, pp. 347-482, 1985.

[52] COTTIN, N. - Optimale Versuchsauslegung für die Identifikation elasto-mechanischer Systeme, Forschungsbericht aus dem Curt-Risch-Institut der Universität Hannover, CRI-F-1/1987, 1987.

[53] WATANABE, R.K.; CAMPBELL, A.C.; MOORE, J.W. - A new generation modal data system utilising distributed processing. Proc. 6th Internat. Modal Analysis Conf., Kissimee, FL, vol. II, pp. 1161-1171, 1988.

[54] LALLY, M.; BARNEY, P.S.; BROWN, D.L. - Preliminary results from a 256 channel simultaneous sensor calibrator, Proc. of the 13th Internat. Seminar on Modal Analysis, Leuven, Belgium, Part II, C-15, 1988.

[55] LALLY, R.; BROWN, D.L. - Structural gravimetric calibration, Proc. of the 13th Internat. Seminar on Modal Analysis, Leuven, Belgium, Part II, C-17, 1988.

[56] SHAH, P.C.; UDWADIA, F.E. - A methodology for optimal sensor locations for identification of dynamic systems, Transaction of ASME, vol. 45, March 1978.

[57] ISERMANN, R. - Prozeβidentifikation - Identifikation und Parameterschätzung dynamischer Prozesse mit diskreten Signalen, Springer-Verlag, Berlin, Heidelberg, New York, 1974.

[58] ZAMIROWSKI, M. - Some tests for determination of the effective number of modes, prepared for publication.

[59] JUANG, J.-N; PAPPA, R.S. - An eigensystem realization algorithm (ERA) for modal parameter identification and model reduction, J. Guidance, Control and Dynamics, vol. 8, nº 5, pp. 620-627, Sept.-Oct. 1985.

[60] GAWRONSKI, W.; NATKE, H.G. - Realization of the transfer function matrix, Int J. Systems Sci., vol. 18, nº 2, pp. 228-236, 1987.

[61] GAWRONSKI, W.; NATKE, H.G. - Order estimation of AR and ARMA models, Int J. Systems Sci., vol. 19, nº 7, pp. 1143-1148, 1988.

[62] IBRAHIM, S.R.; WENTZ, K.R.; LEE, J. - Damping identification from non-linear responses using a multi-triggering random decrement technique, Mech. Systems and Signal Processing, vol. 1, nº 4, pp. 389-397, 1987.

[63] COTTIN, N. - Final report for preparation of the Research Project: "Optimale Versuchsauslegung für die Identifikation elastomechnischer Systeme", Curt-Risch-Institute of the University Hannover, CRI-F-4/83.

[64] COTTIN, N. - Versuchsoptimierung für die parametrische Identifikation linearer elastomechanischer Systeme - Parameteranpassung des Rechenmodells, in: Dynamische Probleme - Modellierung und Wirklichkeit (Eds. H.G. Natke and K. Popp), Mitteilung des Curt-Risch-Institutes der Universität Hannover, CRI-K1/87, pp. 255-272, 1987.

[65] NATKE, H.G. - Anwendung eines versuchsmäßig-rechnerischen Verfahrens zur Ermittlung der Eigenschwingungsgrößen eines elastomechanischen Systems bei einer Erregerkonfiguration, Z. Flugwiss, 18, pp. 290-303, 1970.

RBCM - J. of the Braz.Soc.Mech.Sc.
Vol. XI - nº 4 - pp. 307-321 - 1989

ISSN 0100-7386
Impresso no Brasil

DECOMPOSITION SCHEME FOR A CLASS OF DESIGN OPTIMIZATION PROBLEMS

SISTEMÁTICA DE DECOMPOSIÇÃO PARA UMA CLASSE DE PROBLEMAS DE OTIMIZAÇÃO DE PROJETO

Bernardo Horowitz
UFPE - Departamento de Engenharia Civil
C.P. 7801
Recife, PE - Brasil - CEP 50.730

ABSTRACT

Some structural optimization problems have two distinct classes of design variables. A scheme is proposed to decompose these problems into two subproblems. In each subproblem the objective function is minimized with respect to only one of the groups of design variables. The scheme is particularly effective when the lower level subproblem is a linear programming problem involving most of the design variables. The example of the optimization of concrete columns of general shape is presented in detail. The solution time is reduced to less than half of the original undecomposed problem.

Keywords: Structural Optimization ▪ Linear Programming ▪ Numerical Algorithms ▪ Nondiferentiable Optimization

SUMÁRIO

Alguns problemas de otimização estrutural apresentam dois grupos distintos de variáveis de projeto. Uma estratégia é apresentada para decompor estes problemas em dois subproblemas. Em cada subproblema a função objetiva é minimizada em relação a apenas um dos grupos de variáveis. A estratégia é particularmente eficaz quando o subproblema de nível inferior é de programação linear envolvendo a maioria das variáveis de projeto. É apresentado em detalhe o exemplo de otimização de pilares de concreto de seção qualquer. O tempo de solução é reduzido a menos da metade do problema não decomposto original.

Palavras-chave: Otimização Estrutural ▪ Programação Linear ▪ Algoritmos Numéricos ▪ Problemas Não-Diferenciáveis

Submetido em Maio/89 Aceito em Novembro/89

INTRODUCTION

In structural design optimization some problems have design variables which can be subdivided into two very distinct groups. The case of variables describing cross sectional sizes and variables describing the overall geometry of the structure is a typical example. In these cases it is natural to decompose the problem into two subproblems. A lower level problem is defined in which one group of variables is held fixed while the objective function is minimized with respect to the other group of variables. In the higher level problem the optimal values of the group of variables held fixed in the lower level problem are sought in order to obtain a local minimum of the objective function with respect to all variables. The advantages of this decomposition are multiple. The dimension of each problem is decreased, the nature of the variables is more uniform so that the curvatures of the Lagrangian function are also more uniform, and the complexity of at least one of the problems can be dramatically reduced.

On the other hand this decomposition has to be dealt with due care since in general the higher level problem is not continuously differentiable. As the solution can be a point of nondifferentiability the usual optimization algorithms, designed for smooth functions, may not converge. Difficulties attributable to this problem can be found in the literature [1].

A systematic procedure is proposed to treat the above decomposition. It is shown that the gradient of the objective function of the higher level problem can be computed from the Khun-Tucker pair of the lower level problem. The procedure is then applied to the optimization of reinforced concrete columns of general shape. In this example the decomposition scheme is particularly effective because the lower level problem is a linear programming problem involving the majority of the variables. The resulting higher level problem is nondifferentiable and a reduced subgradient algorithm is proposed for its solution. Finally examples are presented to demonstrate the numerical efficiency of the decomposition scheme.

PROBLEM FORMULATION

Consider the problem (P) below:

$$(P) \qquad \underset{r,s}{\text{Minimize}} \quad F(r,s)$$

$$\text{subject to:} \quad h_i(r) \le 0\,, \quad i = 1, \ldots, nh$$
$$g_j(r,s) \le 0\,, \quad j = 1, \ldots, ng$$

where $r \in \mathbf{R}^{nr}$ and $s \in \mathbf{R}^{ns}$.

This problem can be solved by first fixing $r = \bar{r}$ and minimizing the objective function with respect to s:

$$\text{(P1)} \quad \underset{s}{\text{Minimize}} \quad F(\bar{r}, s)$$

$$\text{subject to:} \quad g(\bar{r}, s) \leq 0$$

Let s^* be the solution to problem (P1). We can then define a new objective function:

$$f(\bar{r}) = F(\bar{r}, s^*) \tag{1}$$

Now the solution to problem (P) can be found by solving:

$$\text{(P2)} \quad \underset{r}{\text{Minimize}} \quad f(r)$$

$$\text{subject to:} \quad h(r) \leq 0$$

We call (P1) the lower level problem and (P2) the higher level problem. As shown below the gradient of the new objective function ∇f is readily obtained from the Lagrange multipliers of (P1).

Computation of ∇f. Consider the following modification of problem (P1):

$$\text{(P1')} \quad \underset{r,s}{\text{Minimize}} \quad F(r, s)$$

$$\text{subject to:} \quad r - \bar{r} = 0$$
$$g(r, s) \leq 0$$

Obviously (P1') is equivalent to (P1). Through the application of the sensivity theorem [2] it can be shown that the sought gradient ∇f is the negative of the Lagrange multipliers associated with the equality constraints of (P1'). Applying the Khun-Tucker first order conditions [2] to (P1') we get:

$$\begin{Bmatrix} \nabla_r F \\ \nabla_s F \end{Bmatrix} + \begin{bmatrix} 1 \\ 0 \end{bmatrix} \lambda + \begin{bmatrix} \nabla_r g \\ \nabla_s g \end{bmatrix} \mu = 0 \tag{2}$$

where $\lambda \in \mathbf{R}^{nr}$, and $\mu \in \mathbf{R}^{ng}$ are the Lagrange multipliers of (P1'). The last row gives:

$$\nabla_s F + \nabla_s g \cdot \mu = 0 \tag{3}$$

this shows that μ is the vector of Lagrange multipliers of the original problem (P1). The first row yields:

$$\nabla f = -\lambda = \nabla_r F + \nabla_r g \cdot \mu \tag{4}$$

It can be concluded therefore that the gradient ∇f can be computed with negligible additional numerical effort once (P1) is solved.

OPTIMIZATION OF CONCRETE COLUMNS

The design of reinforced concrete columns of general shape is frequently encountered in the structural engineering practice. This problem can be formulated as a nonlinear programming problem [3]. Consider the cross section of Figure 1. The concrete geometry is defined by the coordinates of its NVC vertices. Also indicated are locations of the NTS possible reinforcing bars, each of area A_b. The loading is specified by the three factored stress resultants N_{Sd}, M_{Sxd}, and M_{Syd}. Compression and moments causing compression of the first quadrant are considered positive. Let the strain at any point be given by:

$$\varepsilon = \varepsilon_a + y \cdot \varphi_x + x \cdot \varphi_y \tag{5}$$

with corresponding resisting stress resultants given by:

$$N_{Rd} = \int\int \sigma \, dA \; ; \quad M_{Rxd} = \int\int \sigma y \, dA \; ; \quad M_{Ryd} = \int\int \sigma x \, dA \tag{6}$$

The problem is which of the possible NTS bar locations should be actually filled with bars so that the section can resist the external loading with the minimum amount of steel. In [3] this problem is formulated as follows:

$$\text{(PC)} \quad \underset{\substack{A_{s1},\ldots,A_{sNTS} \\ \varepsilon_a, \varphi_x, \varphi_y}}{\text{Minimize}} \quad \sum_{i=1}^{NTS} A_{si}$$

subject to:

$$\begin{aligned}
&\alpha \cdot M_{R1d} - M_{R2d} = 0 \\
&\xi_N \cdot N_{Sd} - \xi_N \cdot N_{Rd} \le 0 \\
&\xi_M \cdot e_{S2} \cdot N_{Rd} - \xi_M \cdot M_{R1d} \le 0 \\
&\varepsilon_{ck} - 3.5 \le 0 , \qquad k = 1, \ldots, NVC \\
&-\varepsilon_{sj} - 10 \le 0 , \qquad j = 1, \ldots, NTS \\
&4 \cdot \varepsilon_{cmax} + 3 \cdot \varepsilon_{cmin} - 14 = 0 \\
&0 \le A_{si} \le A_b , \qquad i = 1, \ldots, NTS
\end{aligned}$$

where:

$|M_{S1d}|$ = max $\{|M_{Sxd}|, |M_{Syd}|\}$, i.e., 1-axis corresponds to that with the largest acting bending moment, while 2-axis is the other axis.

e_{S2} = M_{S1d}/N_{Sd}

α = M_{S2d}/M_{S1d}

ξ_N = *sign* (N_{Sd})

ξ_M = *sign* (M_{S1d})

ε_{ck} = concrete deformation at vertex k (*in* ‰)

ε_{sj} = steel deformation at location j (*in* ‰)

ε_{cmax} = maximum compression strain in the concrete (*in* ‰)

ε_{cmin} = minimum compression strain in the concrete (*in* ‰)

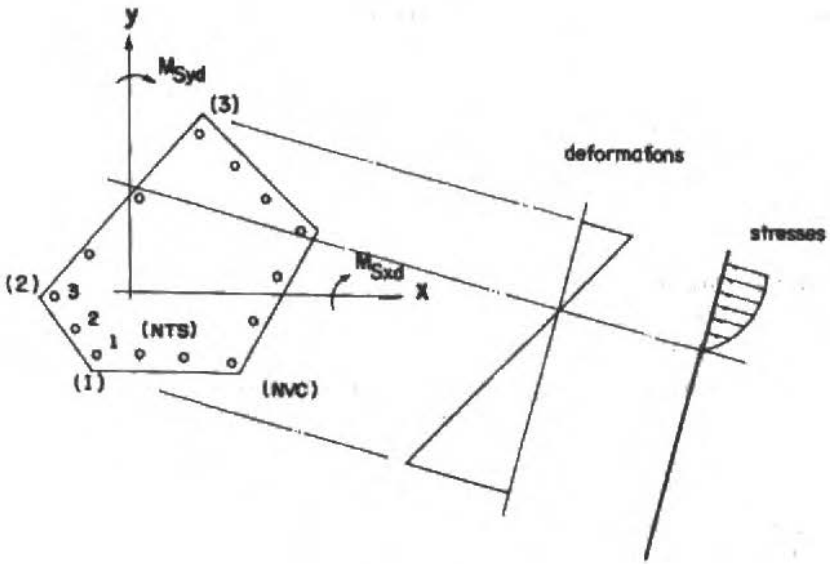

Figure 1. Cross section definition

The first three constraints enforce strength while the next three constraints represent code provisions regarding limiting concrete and steel deformations according to NB-1/78 [4] which are similar to the CEB-Model Code [5]. As done in [3] variables A_{Si} are considered

continuous to simplify the problem.

Decomposition Scheme. Using the procedure described above we can decompose this problem into two subproblems. Given a deformation configuration specified by the values $\bar{\varepsilon}_a, \bar{\varphi}_x, \bar{\varphi}_y$, the lower level problem is:

$$\text{(P1C)} \quad \underset{A_{S1},\ldots,A_{SNTS}}{\text{Minimize}} \quad \sum_{i=1}^{NTS} A_{Si}$$

subject to:

$$\begin{aligned} & \alpha \cdot M_{R1d} + M_{R2d} = 0 \\ & \xi_N \cdot N_{Sd} - \xi_N \cdot N_{Rd} \le 0 \\ & \xi_M \cdot e_{S2} \cdot N_{Rd} - \xi_M \cdot M_{R1d} \le 0 \\ & 0 \le A_{Si} \le A_b, \quad i = 1, \ldots, NTS \end{aligned}$$

and letting A^*_{Si} be the solution to (P1C) we can define the new objective function f as:

$$f(\bar{\varepsilon}_a, \bar{\varphi}_x, \bar{\varphi}_y) = \sum_{i=1}^{NTS} A^*_{Si} \tag{7}$$

The higher level problem is:

$$\text{(P2C)} \quad \underset{\varepsilon_a, \varphi_x, \varphi_y}{\text{Minimize}} \quad f$$

subject to:

$$\begin{aligned} & \varepsilon_{ck} - 3.5 \le 0, \quad k = 1, \ldots, NVC \\ & -\varepsilon_{Sj} - 10 \le 0, \quad j = 1, \ldots, NTS \\ & 4 \cdot \varepsilon_{cmax} + 3 \cdot \varepsilon_{cmin} - 14 \le 0 \end{aligned}$$

The proposed decomposition is actually a generalization of the usual procedure to design rectangular columns subjected to uniaxial bending whereby one fixes the neutral axis and computes the required top and bottom reinforcement applying the equilibrium equations.

The Lower Level Problem. The most significant advantage of the proposed decomposition scheme results from the fact that the lower level problem (P1C) is a linear programming problem. In fact, if the deformation is held fixed the resultant of concrete stresses as well as the steel stresses at bar locations are all fixed. As a consequence the resisting stress resultants

are linear functions of the steel areas:

$$\begin{aligned} N_{Rd} &= N_{Cd} + \Sigma\,(\sigma_{Si}) \cdot A_{Si} \\ M_{Rxd} &= M_{Cxd} + \Sigma\,(\sigma_{Si} \cdot y_i) \cdot A_{Si} \\ M_{Ryd} &= M_{Cyd} + \Sigma\,(\sigma_{Si} \cdot x_i) \cdot A_{Si} \end{aligned} \tag{8}$$

where N_{Cd}, M_{Cxd}, and M_{Cyd} are the concrete stress resultants. These stress resultants as well as their derivatives with respect to ε_a, φ_x, and φ_y are readily computed by the procedure of reference [6]. Notice also that (P1C) usually contains the large majority of the design variables.

In applying (4) to compute the gradient ∇f we observe that the first term vanishes and that the only nonzero columns of the gradients in the second term are those associated with the first three constraints of (P1C). The algorithm of reference [7] is used to solve problem (P1C). The Lagrange multipliers are naturally computed inside the method which has the advantage of using the initial point to decrease the number of iterations.

The Higher Level Problem. Problem (P2C) has only three design variables and all its constraints are linear. It would have been a simple problem to solve if it were not for the fact that f is not continuously differentiable. This happens because the active constraint set of problem (P1C) changes depending on the deformations producing thereby sudden changes of the gradient. Unfortunately this generally happens exactly at the solution rendering the usual optimization algorithms useless.

An important point to keep in mind while one develops an algorithm to handle (P2C) is that one generally knows from the begining the active set at the solution. In fact, this generally amounts to knowing the mostly strained concrete vertex. This can be determined by inspection but can be more reliably done through an initial strength analysis of the section with all bar locations filled. This not only gives a good starting point for the deformation variables but also indicates if the problem is feasible. The next few sections present an algorithm to handle (P2C).

AN ALGORITHM TO SOLVE PROBLEM (P2C)

Only a very brief introduction to the basic tools of nondifferentiable optimization and the schematic algorithm to solve (P2C) are given below. Detailed information can be found in [8-10].

Basic Tools. We shall start the discution with the unconstrained minimization of a piecewise continuously differentiable convex function f defined in $\mathbf{R}^n$. In this case f has

continuous gradients almost everywhere. Vector $g \in \mathbf{R}^n$ is a subgradient of f at $x \in \mathbf{R}^n$ if:

$$f(z) \geq f(x) + \langle g, z - x \rangle \quad , \quad \forall z \in \mathbf{R}^n \tag{9}$$

where $\langle \cdot, \cdot \rangle$ represents scalar products. This can be geometrically interpreted in Figure 2 as a slope that falls below the graph of f.

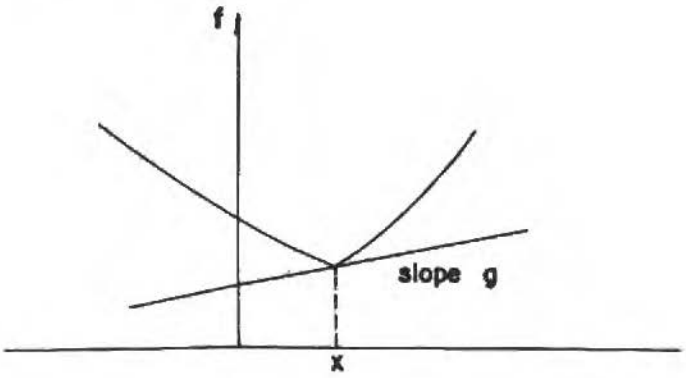

Figure 2. The subgradient

We will call the set of all subgradients of f at x the subdifferential of f at x denoted by $\partial f(x)$. The set $\partial f(x)$ is closed and convex and if the function is continuously differentiable at x it reduces to the usual gradient. It represents the complete behavior of f at x and it can be shown that x^* minimizes f if $0 \in \partial f(x^*)$.

Assuming that we knew how to compute $\partial f(x)$ the probability of it not being only the gradient of f is zero. As a consequence if we use the steepest descent algorithm and we get very close to a point of nondifferentiability it may be impossible to numerically find a usable nonzero move in the direction $-\nabla f$. In which case our method would fail or converge to the wrong solution. This suggest that we need information on f not only at x but also in a neighborhood of x. Convex analysis provides an instrument to solve this problem. Given an $\varepsilon \geq 0$ we define the ε-subdifferential as:

$$\partial_\varepsilon f(x) = \left\{ g \mid f(z) \geq f(x) + \langle g, z - x \rangle - \varepsilon \, , \ \forall z \right\} \tag{10}$$

To be consistent we must also define ε-solutions. Point x^* is an ε-solution to the minimization of f if:

$$f(x) \geq f(x^*) - \varepsilon\,, \quad \forall x \tag{11}$$

Now, let $d = -Nr(\partial_\varepsilon f(x))$, where $Nr(\partial_\varepsilon f(x))$ is the vector with minimum norm in $\partial_\varepsilon f(x)$. It can be shown that d is a kind of steepest descent direction for f at x. Also, if $d = 0$ then x is an ε-solution.

The question that arises in the numerical treatment of these problems is that it is generally impossible to compute the whole set $\partial_\varepsilon f(x)$. What is available in practice is only an element $g \in \partial f(x)$ at every point x. In the so-called "bundle-type" algorithms $\partial_\varepsilon f(x)$ is replaced by an inner approximating politope $G_\varepsilon(x)$ which is constructed as we proceed with the algorithm. Given $x_1, ..., x_k$ with their corresponding subgradients $g_i \in \partial f(x), i = 1, ..., k$, then:

$$G_\varepsilon(x) = \left\{ \sum_{i=1}^{k} \lambda_i g_i \mid \lambda_i \geq 0\,,\ \sum_{i=1}^{k} \lambda_i = 1\,,\ \sum_{i=1}^{k} \lambda_i \cdot \alpha(x, x_i, g_i) \leq \varepsilon \right\} \tag{12}$$

where:

$$\alpha(x, x_i, g_i) = f(x) - f(x_i) - \langle g_i, x - x_i \rangle \tag{13}$$

Notice that $\alpha(x, x_i, g_i)$ is the error at x when f is linearized at x_i with the subgradient g_i. It can be shown that $G_\varepsilon(x) \subseteq \partial_\varepsilon f(x)$.

Reduced Subgradient Algorithm. Let us return to the higher level problem (P2C). It can be writen as:

$$\begin{aligned} &\underset{x}{\text{Minimize}} && f \\ &\text{subject to:} && A \cdot x \leq b \end{aligned}$$

with $x \in \mathbf{R}^n, A \in \mathbf{R}^{m \times n}, b \in \mathbf{R}^m$, and $n = 3$. We can further rewrite the problem above as:

$$\begin{aligned} &\text{(P2C')} \quad \underset{x,y}{\text{Minimize}} && f \\ &\text{subject to:} && A \cdot x + y = \mathbf{A} \cdot \begin{Bmatrix} x \\ y \end{Bmatrix} = b \\ & && y \geq 0 \end{aligned}$$

where $y \in \mathbf{R}^m$, $\mathbf{A} \in \mathbf{R}^{m \times (m+n)}$, with $\mathbf{A} = [A\ I_m]$.

The reduced subgradient algorithm of [11] with a slight modification is used to solve (P2C'). First let us decompose $\mathbf{A}$ into $[B, N]$, where $B \in \mathbf{R}^{m \times m}$ nonsingular, $N \in \mathbf{R}^{m \times n}$. Let us also decompose $(x\ y)$ into $(x_B\ y_B\ x_N\ y_N)$ with $(x_B\ y_B) \in \mathbf{R}^m$ and $(x_N\ y_N) \in \mathbf{R}^n$. Matrix B is called a basis and $(x_B\ y_B)$ is the vector of basic variables. The vector $(x_N\ y_N)$ is the vector of nonbasic variables with $y_N \in \mathbf{R}^{nyN}$.

We can use the m equality constraints of (P2C') basic variables as functions of the n nonbasic variables:

$$\begin{Bmatrix} x_B \\ y_B \end{Bmatrix} = B^{-1} \cdot \left(b - N \cdot \begin{Bmatrix} x_N \\ y_N \end{Bmatrix} \right) \tag{14}$$

Therefore we can write f as a function of the nonbasic variables only: $f(x) = \hat{f}(x_N, y_N)$. We can also rewrite (P2C') as follows:

$$(\hat{\text{P2C}}) \quad \underset{x_N, y_N}{\text{Minimize}} \quad \hat{f}(x_N, y_n)$$

$$\text{subject to:} \quad y_N \geq 0$$
$$y_B(x_N, y_N) \geq 0$$

Problem $(\hat{\text{P2C}})$ is called the reduced problem since it is writen in terms of the nonbasic variables only.

The central idea of the reduced subgradient method is to choose as basic variables those which strictly satisfy their bound constraints. Hence the problem of finding a usable feasible direction for $(\hat{\text{P2C}})$ need only consider the bounds $y_N \geq 0$. Keeping this in mind it can be shown that the Kuhn-Tucker type conditions for $(\hat{\text{P2C}})$ without the bound constraints on y_B are [10,12]:

- let $\varepsilon \geq 0$ and (x_N^*, y_N^*) be feasible. Then (x_N^*, y_N^*) is an ε-solution if and only if there exist scalars ε_0 and v_i, $i = 1, \ldots, nyN$, such that:

$$i)\quad 0 \in \partial_{\varepsilon_0} \hat{f}(x_N^*, y_N^*) - \begin{Bmatrix} 0 \\ v \end{Bmatrix}$$

$$ii)\quad \sum_{i=1}^{nyN} v_i \cdot y_{Ni}^* \leq \varepsilon - \varepsilon_0$$

Therefore, if we are at a point $(\bar{x}, \bar{y})$ and we want to check if it is in fact an ε-solution all we need to do is to find the vector of minimum norm of the set on the right-hand side of

condition (i) above, subjected to condition (ii) as a constraint. Using the bundle approximation and manipulating the problem to remove ε_0, as in [12], we get:

$$\text{(D)} \quad \underset{\substack{\lambda_1,\ldots,\lambda_k \\ v_1,\ldots,v_{myN}}}{\text{Minimize}} \quad \frac{1}{2}\cdot \left|\left|\sum_{i=1}^{k} \lambda_i \cdot \hat{g}_i - \begin{Bmatrix} 0 \\ v \end{Bmatrix}\right|\right|^2$$

$$\text{subject to:} \quad \sum_{i=1}^{k} \lambda_i = 1$$

$$\sum_{i=1}^{k} \lambda_i \cdot \alpha \cdot (\bar{x}, x_i, g_i) + \sum_{j=1}^{myN} v_j \cdot \bar{y}_{Nj} \le \varepsilon$$

$$\lambda \ge 0, \quad v \ge 0$$

where the reduced gradient $\hat{g} = g_N - (B^{-1}\cdot N)^T \cdot g_B$. Let:

$$d_N = \begin{Bmatrix} 0 \\ v^* \end{Bmatrix} - \sum_{i=1}^{k} \lambda_i^* \cdot \hat{g}_i \tag{15}$$

d_N is called the reduced direction of search and is the direction of movement of the nonbasic variables. The corresponding direction of movement of the basic variables is $d_B = -B^{-1}\cdot N \cdot d_N$. Given d_B and d_N we can construct d, the direction of movement of the variables (x, y) of (P2C').

Let u be the Lagrange multiplier associated with the second constraint of problem (D). It can be shown that [10,12]:

i) if $d = 0$ then $\bar{x}$ is an ε-solution

ii) if $d \neq 0$ then d is a feasible direction for (P2C')

iii) if $\partial f(\bar{x}) \subseteq G_0(\bar{x})$, then the directional derivative $f'((\bar{x},\bar{y}), d) \le -\left|\left|d_N\right|\right|^2 - u\cdot\varepsilon$

The Line Search. We will be searching along d. First, we must compute the maximum value of the step length t, such that the bound constraints are not violated:

$$t_{\max} = \min\left\{-\frac{\bar{y}_i}{d_{n+1}} \mid d_{n+1} < 0, T\right\} \tag{16}$$

where T is an arbitrarily large value. We now proceed with the main philosophy of the bundle-type methods. If $G_\varepsilon(\bar{x})$ is a sufficiently good approximation to $\partial_\varepsilon f(\bar{x})$ then, loosely speaking, we will be able to find a new point along d where $<g, d>$ is "large

enough" and f is "small enough". If, on the other hand, $G_e(\bar{x})$ is a bad approximation the line search will not succeed in which case we will stay at the same point but we will enrich the bundle with a new subgradient (null step).

We give next a summary of the line search requirements according to [10]: let $0 < m_2 < m_1 < 1$, $0 < m_3$ and $m_1 + m_3 < 1$, find a stepsize $t \in [0, t_{max}]$ such that at least one of the set of conditions below is satisfied:

i) [Maximum step]: $t = t_{max}$ and
$$f((\bar{x},\bar{y}) + t \cdot d) \le f(\bar{x},\bar{y}) + m_2 \cdot t \cdot a$$

ii) [Serious step]: $t \in]0, t_{max}[$ and
$$<g, d> \ge m_1 \cdot a$$
$$f((\bar{x},\bar{y}) + t \cdot d) \le f(\bar{x},\bar{y}) + m_2 \cdot t \cdot a$$

iii) [Null step]: $t \in]0, t_{max}[$ and
$$<g, d> \ge m_1 \cdot a$$
$$f(\bar{x},\bar{y}) - f((\bar{x},\bar{y}) + t \cdot d) + <g, d> \le \varepsilon \cdot m_3$$

with $a = -||d_N||^2 - u \cdot \varepsilon$, which is an overestimate of the directional derivative as indicated in observation (iii) about problem (D), above.

In the actual implementation we start by bracketing the solution using the procedure in [13]. The first test point is obtained by allowing a maximum change in strain at any vertex between 0.005 and 0.015 %. Infeasible points of (P1C) are treated as having large values of f. The algorithm of [14] is used with the slight modification of forcing, at least, one feasible iteration.

The Algorithm. 0) INITIALIZATION: Given x^1 a feasible point, compute $g_1 \in \partial f(x^1)$ put it in the bundle and select a nondegenerate basis B.

1) DELETION OF SUBGRADIENTS: delete all subgradients in the bundle with $\alpha > 2 \cdot m_3 \cdot \varepsilon$.

2) SEARCH DIRECTION: solve problem (D) and find d_N and d.

3) STOPPING TEST: If $||d_N|| \le TOL$ then stop.

4) LINE SEARCH: perform the line search procedure.

5) UPDATING: add the new subgradient to the bundle. If it is a null step compute the new α and go to (2). Otherwise recompute all α's.

6) BASIS CHANGE: if all basic variables strictly satisfy their bounds go to (1), otherwise select a new basis and go to (1).

Observe that as we have a very good idea of the active set from the begining the basis change in step (6) will rarely be performed. Problem (D) in step (2) is solved using the algorithm of [15].

EXAMPLES

Two examples are given below to demonstrate the numerical efficiency of the proposed decomposition scheme.

Example 1. Consider the cross section shown in Figure 3, where the diameter of all bars is 16mm. Bar locations 1 to 6 are mandatory. The design of Figure 3b was obtained after five iterations of the higher level problem and took 41% of the solution time of the procedure in [3]. The final design is identical in both cases. The values of the parameters used are: $m_1 = 0.2, m_2 = 0.1, m_3 = 0.6, \varepsilon = 2.5 \cdot 10^{-3}, TOL = 2.5 \cdot 10^{-3}$.

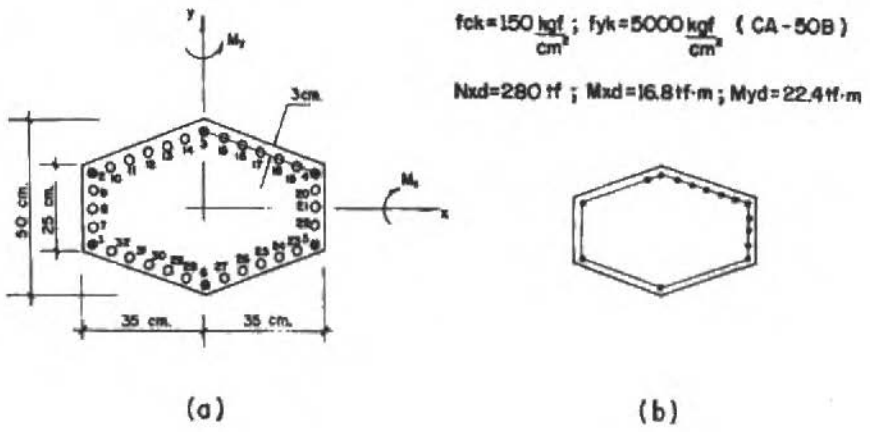

Figure 3. Cross section of example 1

Example 2. In the cross section shown in Figure 4a the diameter of all bars is 16mm and the concrete cover to the center of all bars is 3cm. Locations 1 to 8 are mandatory. The final steel arrangement of Figure 4b was obtained aftersiz iterations of the higher level problem.

The total processing time was slightly less than 50% of the execution time of the procedure in [3]. It interesting to point out that all nonmandatory bars are under compression.

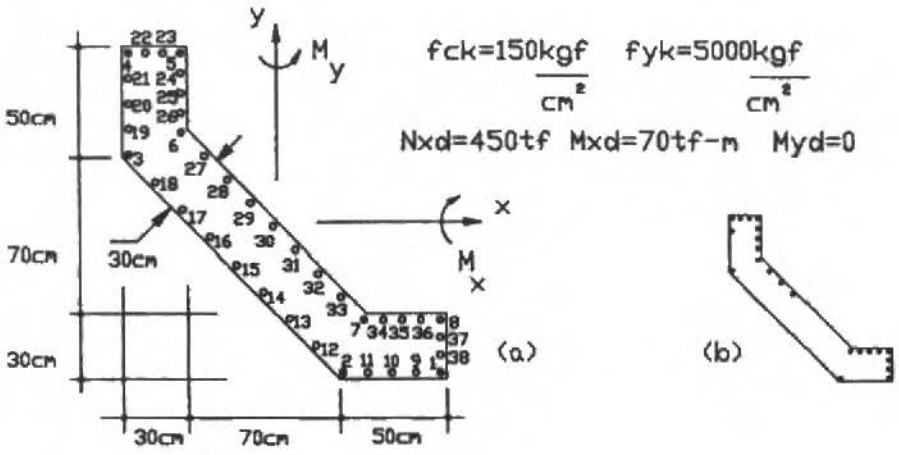

Figure 4. Cross section of example 2

CONCLUSIONS

Some optimization problems have two distinct classes of design variables. A procedure is proposed to decompose such problems into two subproblems. In the lower level problem one group of variables is held fixed while the objective function is minimized with respect to the other group. A new objective function can thus be defined which depends only on the variables held fixed. The higher level problem minimizes this new objective function subjected to those constraints of the original problem involving its variables only. The gradient of the new objective function is readily computed once the lower level problem is solved.

This decomposition scheme is particularly effective in cases where the lower level problem is a linear programming problem involving most of the design variaables. One such case, the optimization of concrete columns of general shape, is treated in detail. A reduced subgradient algorithm is used to solve the higher level problem which is of nonsmooth optimization. For the example presented the solution time of the decomposed problem is less than half of the original undecomposed problem.

REFERENCES

[1] FELIX, J. and VANDERPLAATS, G.N. - Configuration optimization of trusses subject to strength, displacement and frequency constraints, Journal of Mechanisms, Transmissions and Automation in Design, vol. 109, nº 2, pp. 233-241, jun. 1987.

[2] LUENBERGER, D.G. - Linear and nonlinear programming, Second Ed., Addison-Wesley, 1984.

[3] HOROWITZ, B. - Dimensionamento ótimo de pilares de concreto de seção qualquer, Deptº de Eng. Civil, UFPE, 01/88, 1988.

[4] ABNT-Associação Brasileira de Normas Técnicas, NB-1/78 - Cálculo e execução de obras de concreto armado, 1978.

[5] Comite Euro-International du Beton - Model code for concrete structures, Bulletin d'Information 124/125, 1978.

[6] ROTTER, J.M. - Rapid exact inelastic biaxial bending analysis, Journal of Structural Engineering, vol. 111, nº 2, pp. 2659-2674, Dec. 1985.

[7] GILL, P.E. and MURRAY, W. - A numerically stable form of the simplex algorithm, Linear Algebra and its Applications, vol. 7, pp. 99-138, 1973.

[8] LEMARÉCHAL, C.; STRODIOT, J.S. and BIHAIN, A. - On a bundle algorithm for nonsmooth optimization, in Nonlinear Programming 4, Mangasarian, O.L., Meyer, G.L. and Robinson, S.M., Eds., Academic Press, pp. 245-282, 1981.

[9] LEMARÉCHAL, C. - A introduction to the theory of nonsmooth optimization, Optimization, vol. 17, nº 6, pp. 827-858, 1986.

[10] HOROWITZ, B. and SANTOS, M.G. - Application of a reduced subgradient algorithm to solve a class of structural design problems, to appear.

[11] BIHAIN, A.; NGUYEN, V.H.; STRODIOT, J.J. - A reduced subgradient algorithm, Mathematical Programming Study, vol. 30, pp. 127-149, 1987.

[12] STRODIOT, J.J.; NGUYEN, V.H.; HEUKEMES, N. - ε-optimal solutions in nondifferentiable convex programming and some related questions, Mathematical Programming, vol. 25, pp. 307-328, 1983.

[13] VANDERPLAATS, G.N. - Numerical optimization techniques for engineering design with applications, McGraw-Hill, 1984.

[14] MIFFLIN, R. - Stationarity and superlinear convergence of an algorithm for univariate locally Lipschitz constrained minimization, Mathematical Programming, vol. 28, pp. 50-71, 1984.

[15] MIFFLIN, R. - A stable method for solving certain constrained least squares problems, Mathematical Programming, vol. 16, pp. 141-158, 1979.

RBCM - J. of the Braz.Soc.Mech.Sc.
Vol. XI - nº 4 - pp. 323-339 - 1989

ISSN 0100-7386
Impresso no Brasil

MODELOS GEOMÉTRICOS DIRETO E INVERSO NO ESTUDO DE ROBÔS MANIPULADORES

DIRECT AND INVERSE GEOMETRIC MODELS FOR ROBOT MANIPULATORS

João Carlos Mendes Carvalho
Valder Steffen Jr. - Membro da ABCM
Francisco Paulo Lépore Neto - Membro da ABCM
UFU - Departamento de Engenharia Mecânica
Caixa Postal 593 - Campus Santa Mônica
Uberlândia, MG - Brasil - CEP 38.400

RESUMO

É apresentado um método sistemático de obtenção do modelo geométrico direto de um robô manipulador, utilizando rotinas computacionais especiais. Este método pode ser usado na concepção e simulação de robôs manipuladores que podem ter juntas prismáticas e/ou de rotação. O modelo geométrico inverso relaciona as coordenadas generalizadas em função das coordenadas operacionais do robô manipulador. O método apresentado permite obter as expressões analíticas que exprimem o modelo geométrico inverso a partir das matrizes de passagem homogêneas elementares do robô manipulador. As expressões obtidas podem ser facilmente incluídas em um sistema de comando em tempo real.

Palavras-chave: Robótica ▪ Robôs Manipuladores

ABSTRACT

A systematic method to obtain analytically the geometric model of robot manipulator, using special computational routines, is presented. This method can be used in the conception and simulation of robots manipulators, which can have prismatic and/or rotational joints. The inverse geometric model relates the generalized coordinates with respect to operational coordinates of the robot manipulator. An analytical method is presented to obtain the equations that describe the inverse geometric model using homogeneous matrices of the robot manipulator. These equations may be included in a system of real time control.

Keywords: Robotics ▪ Robot Manipulators

Submetido em Maio/89 Aceito em Outubro/89

INTRODUÇÃO

O modelo geométrico direto de um robô manipulador é a função $\{f\}$ que permite obter a posição e a orientação do efetuador em função da configuração do robô manipulador [6,7].

A situação do efetuador isto é, a posição e a orientação, é definida por m coordenadas operacionais $x_1, x_2, ..., x_m$.

A configuração do robô manipulador é definida por n coordenadas generalizadas $q_1, q_2, ..., q_n$.

Se $\{x\}$ representa a matriz das coordenadas operacionais e $\{q\}$ a matriz das coordenadas generalizadas, o modelo geométrico direto do robô manipulador é dado por:

$$\{x\} = \{f(q)\} \tag{1}$$

onde a função $\{f\}$ é geralmente não linear.

Pode-se apresentar o problema do modelo geométrico inverso de um robô manipulador da seguinte forma [5]: quais são as coordenadas generalizadas $\{q\}$ que correspondem às coordenadas operacionais $\{x\}$ dadas? Assim o problema consiste no cálculo de uma função $\{f\}^{-1}$, se ela existe, tal que:

$$\{q\} = \{f(x)\}^{-1} \tag{2}$$

A inversão da função $\{f\}$ é um problema complexo pois ela não é linear. Se são conhecidas as coordenadas generalizadas $\{q^*\}$ correspondentes às coordenadas operacionais $\{x^*\}$ impostas, e a matriz jacobiana possui as condições de regularidade suficientes "no ponto" $\{q^*\}$, pelo teorema das funções implícitas pode-se afirmar a existência da inversa de $\{f\}$ na vizinhança de $\{x^*\}$. Existe aí uma solução local. Por analogia com as soluções dos sistemas lineares, pode-se dizer que, na maioria dos casos e não levando em consideração as restrições físicas, tem-se o seguinte resultado global [2]: - não existe solução quando o número de graus de liberdade n do robô manipulador é inferior ao número de graus de liberdade n_t da tarefa a realizar; existe uma solução ou um número finito de soluções quando n é igual a n_t ; existe uma infinidade de soluções quando n é maior que n_t. Neste caso, o manipulador é dito redundante.

Um dos objetivos desse trabalho é apresentar um método analítico de obtenção do modelo geométrico inverso, lembrando que este método não leva em consideração: a trajetória a ser descrita pelo efetuador; as restrições físicas, seja devido às dimensões dos corpos ou limitações dos movimentos das articulações; consumo mínimo de energia; tempo mínimo de percurso e outros.

Para apresentação do método será utilizado o robô manipulador UFU6R86 como exemplo, facilitando a visualização dos procedimentos utilizados.

DEFINIÇÕES CINEMÁTICAS

Sejam dois sistemas de coordenadas ortogonais R_1 e R_2 e um ponto Q mostrados na Figura 1.

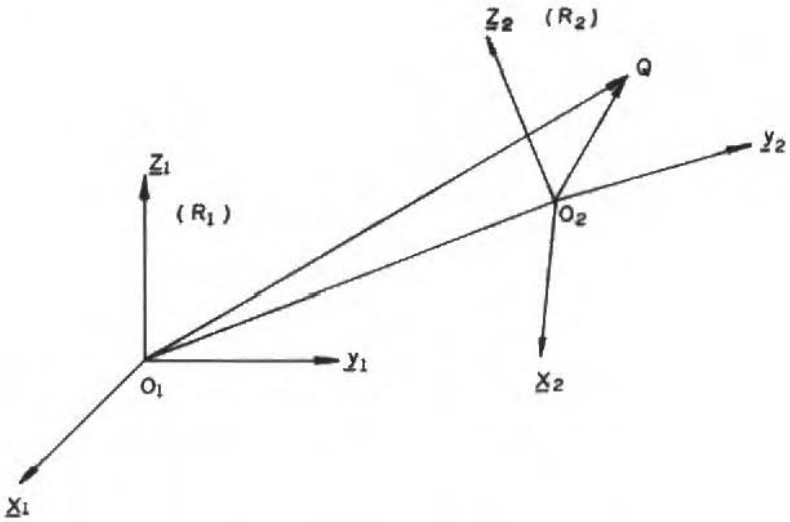

Figura 1. Transformação de coordenadas

A mudança de coordenadas do ponto Q pode ser escrita:

$$\{x_1\} = \{P\} + [R]\{x_2\} \tag{3}$$

e a mudança de referencial dos componentes de um vetor pode ser escrita:

$$\{v_1\} = [R]\{v_2\} \tag{4}$$

onde $\{x_1\}$ e $\{x_2\}$ são as coordenadas do ponto Q no referencial R_1 e R_2 respectivamente, $\{P\}$ são as coordenadas do ponto O_2 no referencial R_1, $[R]$ a matriz de passagem clássica do sistema R_1 ao sistema R_2, $\{v_1\}$ e $\{v_2\}$ são as matrizes dos componentes de um

vetor $\underline{v}$ no referencial R_1 e R_2 respectivamente.

Os componentes homogêneos de um vetor são os três elementos clássicos associados ao valor zero e as coordenadas de um ponto são os quatro escalares obtidos associando o valor 1 as três coordenadas clássicas. Portanto, as Equações (3) e (4) podem ser escritas:

$$\left\{\frac{x_1}{1}\right\} = \begin{bmatrix} R & . & P \\ . & . & . \\ 0 & . & 1 \end{bmatrix} \left\{\frac{x_2}{1}\right\}$$

$$\left\{\frac{v_1}{0}\right\} = \begin{bmatrix} R & . & P \\ . & . & . \\ 0 & . & 1 \end{bmatrix} \left\{\frac{v_2}{0}\right\} \qquad (5)$$

A matriz quadrada que aparece nas duas expressões (5) é denominada matriz de passagem homogênea do referencial R_1 para o referencial R_2 e que será representada por $[T]$ não ortogonal.

$$[T] = \begin{bmatrix} R & . & P \\ . & . & . \\ 0 & . & 1 \end{bmatrix} \qquad (6)$$

As coordenadas operacionais do efetuador são as quantidades escalares que permitem definir sua posição e sua orientação.

Para se determinar a situação do efetuador deve-se considerar dois referenciais ortonormais, um ligado à base do robô manipulador (R_0) e outro ligado ao seu órgão terminal (R_{n+1}).

Seja $\{x_p\}$ a matriz cujos elementos definem a posição da origem O_{n+1} do referencial R_{n+1} em relação ao referencial R_0 e $\{x_R\}$ a matriz que define a orientação desse referencial R_{n+1} em relação ao mesmo referencial R_0. A matriz $\{x\}$ cujos elementos definem a situação do referencial R_{n+1}, fixo ao efetuador em relação ao referencial R_0, fixo à base, é dada por:

$$\{x\} = \left\{\frac{x_p}{x_R}\right\} \qquad (7)$$

A posição do efetuador é definida pela posição do ponto fixo O_{n+1} do referencial R_{n+1} com relação ao referencial R_0. Esta posição pode ser definida através de coordenadas cartesianas, cilíndricas ou esféricas de acordo com a natureza da manipulação a efetuar.

A orientação do referencial R_{n+1}, ligado ao efetuador do robô manipulador, com relação ao referencial R_0 pode ser definida utilizando os parâmetros de Euler (p, q, r, s), os parâmetros de rotação finita (u, v, w), os cosenos diretores entre outros.

A partir da definição da matriz de passagem homogênea, pode-se escrever a matriz de passagem homogênea $[T_{0,n+1}]$ do referencial R_0 ao referencial R_{n+1}.

$$[T_{0,n+1}] = \left[\begin{array}{c|c} R_{0,n+1} & P_{0,n+1} \\ \hline 0 & 1 \end{array}\right] \tag{8}$$

onde, $[R_{0,n+1}]$ é a matriz passagem clássica do referencial R_{n+1} ao referencial R_0 e que permite definir a orientação do referencial R_{n+1} em relação ao referencial R_0. $\{P_{0,n+1}\}$ é a matriz dos componentes do ponto O_{n+1} no referencial R_{n+1} em relação ao referencial R_0. Deve-se observar que as matrizes de passagens homogêneas conservam as mesmas propriedades de multiplicidade das matrizes de passagem clássicas.

Pode-se dizer que, qualquer que seja a escolha das coordenadas operacionais, o modelo geométrico direto se deduz do cálculo dos elementos $t_{ij}\,(i,j = 1,2,3,4)$ da matriz de passagem homogênea $[T_{0,n+1}]$.

As relações entre alguns parâmetros que definem a situação do efetuador e os componentes da matriz de passagem homogênea podem ser encontradas em [1] e [2].

O robô manipulador é constituído de $n+1$ ligações $C_i\,(i = 0,1, ..., n)$, teoricamente rígidos, articulados entre si, através de juntas $L_i\,(i = 1,2, ..., n)$.

Na construção de robôs manipuladores são utilizadas as juntas de rotação (ou rotóides) e as juntas de translação (ou prismáticas) que permitem, respectivamente, um movimento de rotação ou um de translação do corpo C_i em relação ao seu antecedente C_{i-1}. Assim, todo corpo C_i possui um grau de liberdade em relação ao seu antecedente C_{i-1}.

A primeira ligação C_1 da cadeia é articulado sobre uma base C_0, fixa ou móvel. A última ligação C_n da cadeia é o efetuador (Figura 2).

Pode-se definir o coeficiente binário $\sigma_i\,(i = 0,1,2, ..., n)$ que é nulo se C_i gira em relação a C_{i-1} em torno do eixo da ligação L_i e igual a 1 se C_i translada em relação à C_{i-1} ao longo do eixo da ligação L_i. O coeficiente binário conjugado será $\bar{\sigma}_i = 1 - \sigma_i$.

Para a sistematização do cálculo do modelo geométrico direto, define-se um método iterativo para ligar cada ligação C_i um referencial ortonormal R_{n+1} a partir do referencial R_1 ligado à base do robô manipulador. A única restrição que é feita ao referencial R_1 é que o vetor unitário $\underline{z}_1$ esteja na direção do eixo da primeira junta.

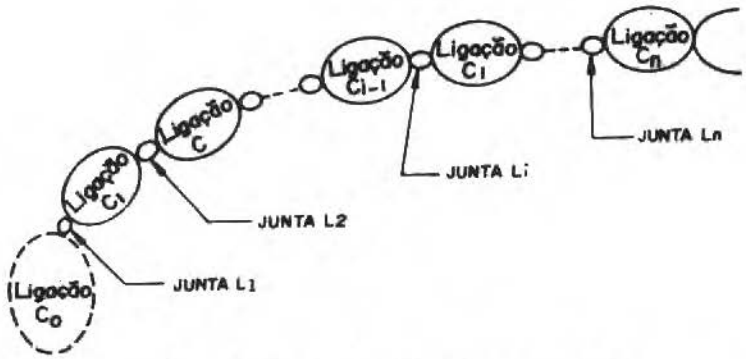

Figura 2. Cadeia cinemática do robô manipulador

O método consta de:

- O_{i+1} é a intersecão da perpendicular comum aos eixos das juntas L_i e L_{i+1}, situado sobre o eixo da junta L_{i+1}.. Se os eixos das duas juntas são paralelos ou coincidentes pode-se escolher arbitrariamente uma perpendicular comum; o ponto O_{i+1} fica assim determinado. Neste caso, considerações de simetria ou de simplicidade permitem uma escolha racional.
- $\underline{x}_{i+1}$ é um vetor unitário desta perpendicular comum orientado do eixo da junta L_i na direção da ligação L_{i+1}. Se os eixos dessas duas juntas são concorrentes ou coincidentes, a orientação é arbitrária. Entretanto, considerações de simetria ou simplicidade permitem uma escolha racional.
- $\underline{z}_{i+1}$ é um vetor unitário do eixo da junta L_{i+1}, orientado arbitrariamente.
- $\underline{y}_{i+1}$ é definido pelo produto vetorial positivo entre $\underline{x}_{i+1}$ e $\underline{z}_{i+1}$.

A posição e a orientação da ligação C_i em relação à ligação C_{i-1} são definidas pelos quatro parâmetros de DENAVIT-HARTENBERG [3] $(ai, \alpha_i, \theta_i, r_i)$ como mostrado na Figura 3.

Tendo em conta a orientação definida para $\underline{x}_{i+1}$, a_i é sempre positivo ou nulo. Os ângulos θ_i e α_i são definidos positivos, aplicando-se a regra da mão direita.

Para este método iterativo é necessário definir uma direção L_{n+1}, sem que exista a junta correspondente. Esta direção deve ser tal que o ponto O_{n+1} esteja situado no centro geométrico do efetuador e os vetores $\underline{x}_{n+1}$, $\underline{y}_{n+1}$ e $\underline{z}_{n+1}$ de preferência segundo as direções de simetria geométrica do mesmo.

de simetria geométrica do mesmo.

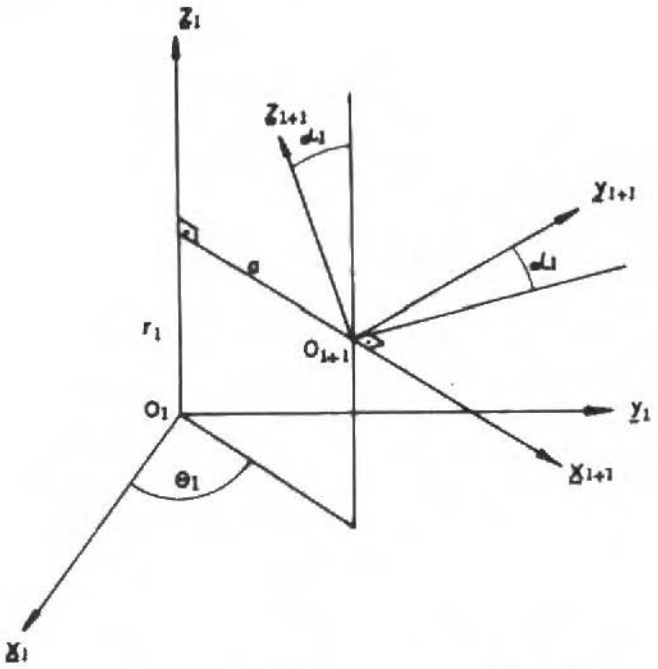

Figura 3. Parâmetros de Denavit-Hartenberg

Deve-se ligar um segundo referencial R_0 à ligação C_0 conforme definido anteriormente. Uma escolha adequada de R_0 permite simplificar as operações de transformação entre R_0 e R_1.

A situação da ligação C_i relação ao corpo C_{i-1} é definida pela matriz de passagem homogênea $[\,_{i,i+1}]$ do referencial R_i (ligado ao corpo C_{i-1}) ao referencial R_{i+1} (ligado à ligação C_i). Em função dos parâmetros de Denavit-Hartenberg $a_i, \alpha_i, \theta_i, r_i$, tem-se:

$$[T_{i,i+1}] = \begin{bmatrix} \cos\theta_i & -\,sen\,\theta_i \cdot \cos\alpha_i & sen\,\theta_i \cdot sen\,\alpha_i & a_i \cdot \cos\theta_i \\ sen\,\theta_i & \cos\theta_i \cdot \cos\alpha_i & -\cos\theta_i \cdot sen\,\alpha_i & a_i \cdot sen\,\theta_i \\ 0 & sen\,\alpha_i & \cos\alpha_i & r_i \\ \cdots & \cdots & \cdots & \cdots \\ 0 & 0 & 0 & 1 \end{bmatrix} \qquad (9)$$

Conforme as definições dadas, pode-se concluir que a i-ésima coordenada generalizada q_i se identifica com θ_i se a junta L_i é de rotação em torno de z_i ou com r_i se L_i é uma de junta de translação ao longo de z_i. Conseqüentemente,

$$q_i = \sigma_i \theta_i + \sigma_i r_i \quad (10)$$

Do ponto de vista prático, pode-se representar os referenciais ligados às diferentes ligações robô manipulador para uma configuração genérica. Entretanto, deve-se procurar representá-lo numa configuração particular a mais simples possível, onde os parâmetros de Denavit-Hartenberg são mais fáceis de visualizar.

MODELO GEOMÉTRICO DIRETO

Pode-se verificar que a matriz $[T_{i,i+1}]$ é função da i-ésima coordenada generalizada q_i, portanto $[T_{i,i+1}] = [T_{i,i+1}(q_i)]$ lembrando que $[T_{0,1}]$ é constante com o tempo quando C_0 é fixo. Assim, pode-se escrever:

$$[T_{0,n+1}(q_1, q_2, \ldots, q_n)] = [T_{0,1}] \cdot [T_{1,2}(q_1)] \ldots [T_{n,n+1}(q_n)] \quad (11)$$

O cálculo dos elementos t_{ij} da matriz de passagem homogênea $[T_{0,n+1}]$ permite determinar o modelo geométrico direto do robô manipulador em função das coordenadas operacionais escolhidas.

A sistematização do cálculo do modelo geométrico direto, permite a utilização de rotinas computacionais para sua determinação, evitando erros nas expressões analíticas e erros numéricos de cálculo. Através dessa rotina computacional conversacional onde o usuário define os dados literais dos parâmetros de Denavit-Hartenberg, o número de G.D.L. e o tipo de ligação, obtém-se as expressões analíticas dos elementos da matriz de passagem homogênea $[T_{0,n+1}]$, bem como das matrizes de passagem homogêneas intermediárias. O fluxograma é apresentado na Figura 4.

Para exemplificar o método é apresentado o cálculo da matriz de passagem homogênea $[T_{0,n+1}]$ para o robô manipulador UFU6R86 representado numa posição particular simples conforme a Figura 5.

A Figura 6 mostra os referenciais ligados às diferentes ligações do UFU6R86 e a Tabela 1 apresenta os valores dos parâmetros de Denavit-Hartenberg.

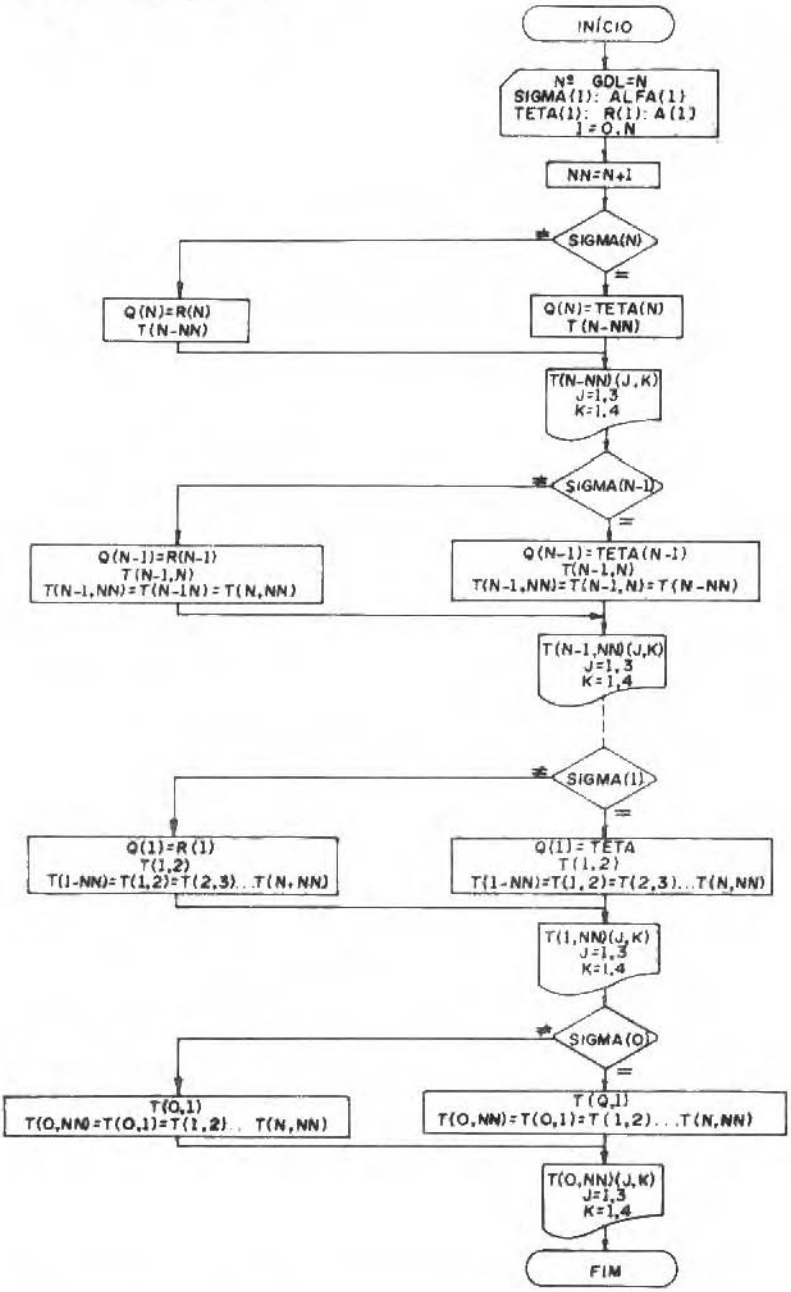

Figura 4. Fluxograma da rotina computacional para obtenção analítica do modelo geométrico direto

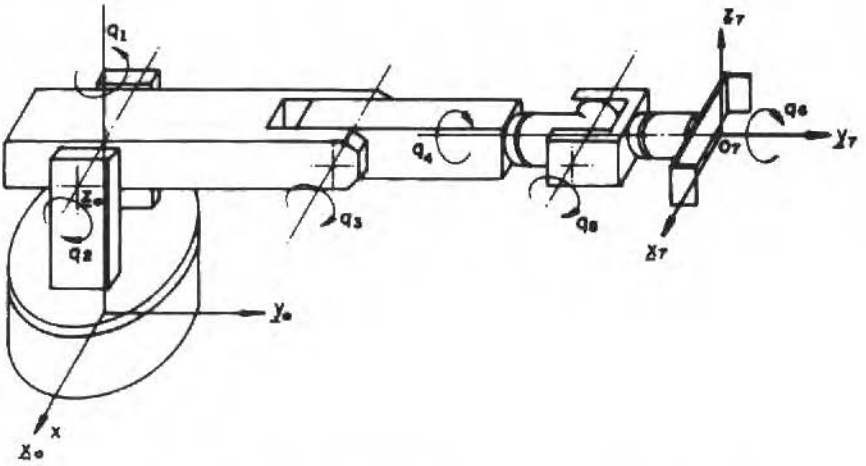

Figura 5. Robô manipulador UFU 6R86 e suas coordenadas generalizadas

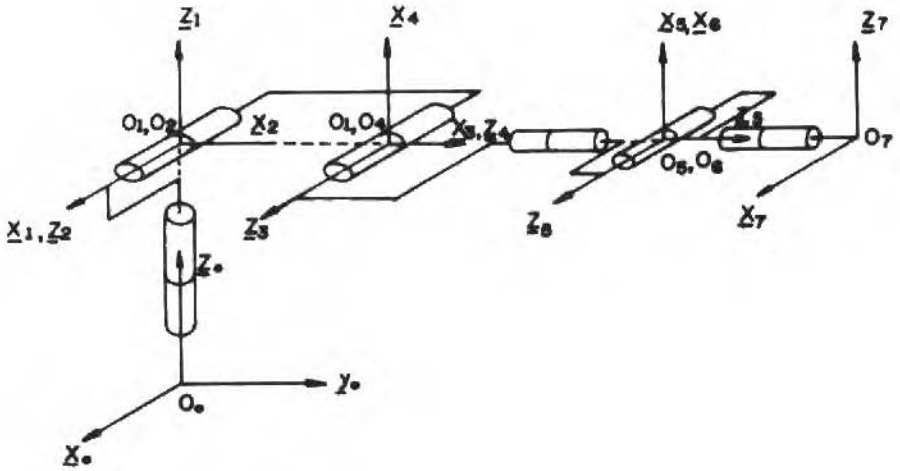

Figura 6. Referenciais ligados às diferentes ligações do robô manipulador UFU 6R86

Fazendo $c = \cos\theta_i$, $s_i = sen\ \theta_j$, $c_{i+j} = \cos(\theta_i + \theta_j)$ e $s_{i+j} = sen(\theta_i + \theta_j)$ e utilizando a rotina computacional obtém-se elementos t_{ij} (i = 1,2,3 e j = 1,2,3,4) da matriz de passagem homogênea $[T_{07}]$.

Tabela 1. Valores dos parâmetros de Denavit-Hartenberg para o robô manipulador UFU 6R86

Parâm. i	0	1	2	3	4	5	6
σ_i	-	0	0	0	0	0	0
α_i	0	$\pi/2$	0	$\pi/2$	$-\pi/2$	$\pi/2$	$\pi/2$
a_i	0	0	a_2	0	0	0	0
θ_i	0	q_1	q_2	q_3	q_4	q_5	q_6
r_i	r_0	0	0	0	r_4	0	r_6

$$t_{11} = c_1 \cdot c_2 \cdot c_3 (c_4 \cdot c_5 \cdot c_6 - s_4 \cdot s_6) - s_3 \cdot s_5 \cdot c_6 - s_2 \cdot s_3 (c_4 \cdot c_5 \cdot c_6 - - s_4 \cdot s_6) + c_3 \cdot s_5 \cdot c_6 + s_1 (s_4 \cdot c_5 \cdot c_6 + c_4 \cdot s_6)$$

$$t_{12} = c_1 \cdot c_2 (c_3 \cdot c_4 \cdot s_5 + s_3 \cdot c_5) - s_2 (s_3 \cdot c_4 \cdot s_5 - c_3 \cdot c_5) + s_1 \cdot s_4 \cdot s_5$$

$$t_{13} = c_1 \cdot c_2 \cdot c_3 (c_4 \cdot s_6 \cdot c_5 + s_4 \cdot c_6) - s_3 \cdot s_5 \cdot s_6 - - s_2 \cdot s_3 (c_4 \cdot c_5 s_6 + s_4 \cdot c_6) + c_3 \cdot s_5 \cdot s_6 + s_1 (s_4 \cdot s_6 \cdot c_5 - c_4 \cdot c_6)$$

$$t_{14} = c_1 \cdot c_2 \cdot c_3 \cdot c_4 \cdot s_5 \cdot r_6 + s_3 (c_5 \cdot r_6 + r_4) - s_2 \cdot s_3 c_4 \cdot s_5 \cdot r_6 - - c_3 (c_5 \cdot r_6 + r_4) + a_2 \cdot c_2 + s_1 \cdot s_4 \cdot s_5 \cdot r_6$$

$$t_{21} = s_1 \cdot c_2 \cdot c_3 (c_4 \cdot c_5 \cdot c_6 - s_4 \cdot s_6) - {}_3 \cdot s_5 \cdot c_6 - - s_2 \cdot s_3 (c_4 \cdot c_5 \cdot c_6 - s_4 \cdot s_6) + c_3 \cdot s_5 \cdot c_6 - c_1 (s_6 \cdot c_5 \cdot c_6 + c_4 \cdot s_6)$$

$$t_{22} = s_1 [c_2 (c_3 \cdot c_4 \cdot s_5 + s_3 \cdot c_5) - s_2 (s_3 \cdot c_4 \cdot s_5 - c_3 \cdot c_5)] - c_1 \cdot s_4 \cdot s_5$$

$$t_{23} = s_1 \cdot c_2 \cdot c_3 (c_4 \cdot c_5 \cdot s_6 + s_4 \cdot c_6) - s_3 \cdot s_5 \cdot s_6 - - s_2 \cdot s_3 (c_4 \cdot c_5 \cdot s_6 + s_4 \cdot c_6) + c_3 \cdot s_5 \cdot s_6 - c_1 (s_4 \cdot c_5 s_6 - c_4 \cdot c_6)$$

$$t_{24} = s_1 \cdot c_2 c_3 \cdot s_5 \cdot r_6 + s_3 (c_5 \cdot r_6 + r_4) - s_2 \cdot s_3 \cdot c_4 \cdot s_5 \cdot r_6 - - c_3 (c_5 \cdot r_6 + r_4) + s_2 \cdot c_2 - c_1 \cdot s_4 \cdot s_5 \cdot r_6$$

$$t_{31} = c_1 \cdot c_2 (c_3 \cdot c_4 \cdot s_5 + s_3 \cdot c_5) - s_2 (s_3 \cdot c_4 \cdot s_5 - c_3 \cdot c_5) + s_1 \cdot s_4 \cdot s_5$$

$$t_{32} = s_2 (c_3 \cdot c_4 \cdot s_5 + s_3 \cdot c_5) + c_2 (s_3 \cdot c_4 \cdot s_5 - c_3 \cdot c_5)$$

$$t_{33} = s_2 \cdot c_3 (c_4 \cdot c_5 \cdot s_6 + s_4 \cdot c_6) - s_3 \cdot s_5 \cdot s_6 + \\ + c_2 \cdot s_3 (c_4 \cdot c_5 \cdot s_6 + s_4 \cdot c_6) + c_3 \cdot s_5 \cdot s_6$$

$$t_{34} = s_2 \cdot c_3 \cdot c_4 \cdot s_5 \cdot r_6 + s_3 (c_5 \cdot r_6 + r_4) + c_2 \cdot s_3 \cdot c_4 \cdot s_5 \cdot r_6 - \\ - c_3 (c_5 \cdot r_6 + r_4) + a_2 \cdot s_2 + r_0$$

MODELO GEOMÉTRICO INVERSO

Para obter as n coordenadas generalizadas $\{q^*\}$ correspondentes à situação imposta $\{x^*\}$ é possível utilizar métodos analíticos ou métodos numéricos iterativos. Os métodos analíticos permitem obter todos os modelos geométricos inversos sob forma literal. Entretanto, eles se aplicam apenas aos robôs manipuladores mais simples, isto é, aqueles que possuem um grande número de parâmetros de Denavit-Hartenberg nulos, como os que são utilizados atualmente na indústria. Apesar da dificuldade de obtenção analítica do modelo inverso, pode-se calcular numericamente, através de um pequeno número de operações, as coordenadas generalizadas $\{q^*\}$ correspondentes à situação imposta $\{x^*\}$, utilizando-se das expressões analíticas obtidas. Estes cálculos podem ser facilmente incluídos em um sistema de comando em tempo real.

Os métodos numéricos iterativos são de caráter geral, mas necessitam um grande número de operações e possuem delicados problemas de convergência.

O método que será apresentado utiliza as matrizes de passagem homogêneas $[T_{i,n+1}]$ e $[T_{i,i+1}]$ $(i = 0,1,2, ..., n)$ que podem ser obtidas através do modelo geométrico direto. A cada passo i $(i = 0,1,2, ..., n)$ são determinadas as matrizes $[T_{i+1,i}] = [T_{i,i+1}]^{-1}$ e $[T^*_{i+1,n+1}] = [T_{i+1,i}] \times [T^*_{i,n+1}]$. Da igualdade das matrizes $[T_{i+1,n+1}]$ e $[T^*_{i+1,n+1}]$ obtém-se doze equações que são funções de q_i que, escolhidas adequadamente, permitem obter com maior facilidade a equação literal que expressa a coordenada generalizada q_i. A matriz de passagem $[T^*_{0,n+1}]$ corresponde à situação desejada do efetuador com relação à base do robô manipulador e pode ser obtida em função dos parâmetros adotados, ou seja: parâmetros de Euler, cosenos diretores, etc.

Se o robô manipulador termina com juntas de rotação concorrentes num ponto 0, o que ocorre com os "punhos" clássicos, torna-se interessante utilizar um referencial adicional R_{n+1} com eixos paralelos ao referencial R_{n+1} e de origem em 0. Este procedimento facilita

as operações de obtenção analítica de $\{f\}^{-1}$. A matriz de passagem $[T_{i,n+1}]$ se deduz facilmente de $[T_{i,n+1}]$ desde que seja conhecido o vetor $\underline{O_{n+1}O}$ no referencial R_{n+1}. Do mesmo modo pode-se obter a matriz de passagem $[T^*_{i,n+1}]$ a partir da matriz $[T^*_{i,n+1}]$.

A Figura 7 apresenta o robô manipulador UFU 6R86 com os referenciais ortonormais ligados às diferentes ligações. Por possuir um "punho" clássico é utilizado o referencial auxiliar $\overline{R}_{n+1} \equiv R_7$. Portanto, o referencial $\overline{R}_7$ é obtido de R_7 pela translação do vetor $\underline{O_7O_5} = \underline{O_7O_6}$.

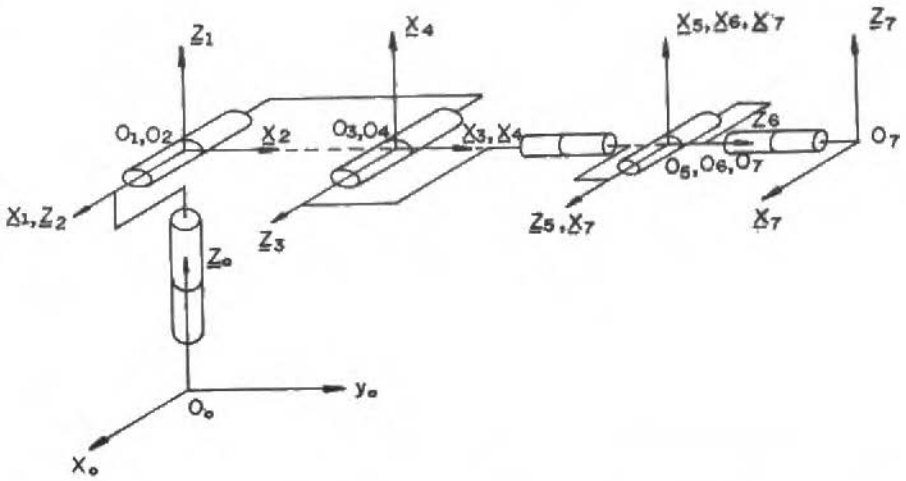

Figura 7. Referenciais ligados às diferentes ligações do robô manipulador UFU 6R86

Os parâmetros de Denavit-Hartenberg já foram apresentados na Tabela 1.

A situação desejada $\{x^*\}$ pode ser definida pela matriz $[T^*_{07}]$, ou seja:

$$[T^*_{07}] = \begin{bmatrix} t^*_{11} & t^*_{12} & t^*_{13} & \vdots & t^*_{14} \\ t^*_{21} & t^*_{22} & t^*_{23} & \vdots & t^*_{24} \\ t^*_{31} & t^*_{32} & t^*_{33} & \vdots & t^*_{34} \\ \cdots & \cdots & \cdots & \vdots & \cdots \\ 0 & 0 & 0 & \vdots & 1 \end{bmatrix} \tag{12}$$

Fazendo a translação para o referencial $\overline{R}^*_{i,n+1}$, tem-se:

- q_4 e q_5 podem ser calculados desde que $m_{12}^2 + m_{22}^2 \neq 0$, o que significa que $q_5 \neq 0$ ou $q_5 \neq \pm\pi$.
- Pode-se determinar q_3 independentemente da posição desejada do efetuador.

As posições para as quais não é possível o cálculo das coordenadas generalizadas correspondem às singularidades do robô manipulador.

CONCLUSÕES

A utilização do método sistemático para obtenção do modelo geométrico direto através da rotina computacional apresentada, possui uma grande vantagem, por ser conversacional, podendo ser utilizada por pessoas não especializadas em robótica e/ou computação representando uma ajuda preciosa na concepção e construção de novos robôs manipuladores permitindo sua simulação.

A rotina computacional permite a minimização das operações de adição, subtração e multiplicação que intervém no cálculo, reduzindo consideravelmente o tempo de processamento e obtenção dos elementos da matriz $[T_{0,n+1}]$, melhorando o comando em tempo real.

A obtenção analítica do modelo geométrico direto permite resolver analiticamente o modelo geométrico inverso, determinar analiticamente a matriz jacobiana do robô manipulador, que é necessária para o estudo do modelo dinâmico e ao seu controle além da obtenção analítica de suas configurações singulares.

O processo de obtenção analítica do modelo geométrico inverso apresentado pode ser utilizado separadamente para cada caso particular de robô manipulador de cadeia simples e permite sua inclusão em sistemas de comando em tempo real utilizando-se as expressões literais obtidas que definem as coordenadas generalizadas $\{q^*\}$ em função da situação imposta $\{x^*\}$.

REFERÊNCIAS

[1] CARVALHO, J.C.M.; STEFFEN JR., V. e LÉPORE N., F.P. - Modelo geométrico direto de um robô manipulador, Anais do IX Congresso Brasileiro de Engenharia Mecânica - COBEM 87, Florianópolis, SC, pp. 975-978, Dez. 1987.

[2] GORLA, B. et RENAUD, M. - Modèles des robots manipulateurs, application à leur commande, Toulouse, Cepadues - Editions, 200p., 1984.

[3] DENAVIT, J. and HARTENBERG, R.S. - A kinematic notation for lower-pair mechanisms based on matrices, J. of Applied Mechanics, 22, pp. 215-221, June 1955.

[4] RENAUD, M. - Contribuition à la modelisation et à la commande dynamique des robots manipulateurs, Tese de Docteur d'Etat, Université Paul Sabatier de Toulouse (Sciences), Toulouse, 187p., 1980.

[5] CARVALHO, J.C.M.; STEFFEN Jr., V. e LÉPORE N., F.P. - Modelo geométrico inverso de um robô manipulador, Anais do IX Congresso Brasileiro de Engenharia Mecânica - COBEM 87, Florianópolis, SC, pp. 971-973, Dez. 1987.

[6] CRAIG, J.J. - Introduction to robotics, mechanics and control, Addison-Wesley Publ. Company - Reading, Massachusetts, Don Mills, Ontario, Wokinghan, England.

[7] RIVIN, E.I. - Mechanical design of robots, McGraw-Hill Book Company, 1988.

RBCM - J. of the Braz.Soc.Mech.Sc.
Vol. XI - nº 4 - pp. 341-378 - 1989

ISSN 0100-7386
Impresso no Brasil

ON THE BEHAVIOUR OF ADHESIVE JOINTS VIA HEMIVARIATIONAL INEQUALITIES. NECESSARY AND SUFFICIENT CONDITIONS

SOBRE O COMPORTAMENTO DE CONEXÕES ADESIVAS VIA DESIGUALDADES HEMIVARIACIONAIS. CONDIÇÕES NECESSÁRIAS E SUFICIENTES

P.D. Panagiotopoulos
Aristotle University - Dept. of Civil Engineering
GR 54006 Thessaloniki and Faculty of Mathematics and Physics
RWTH - D-51 Aachen

ABSTRACT

In the present paper the debonding effect of interfaces is formulated and studied. The non-monotone, possibly multivalued stress-strain laws simulating the interface behaviour are expressed by nonconvex superpotentials leading to hemivariational inequalities and to sub-stationarity problems. The arising hemivariational inequalities are studied concerning the existence and the approximation of their solutions. Necessary conditions as well as sufficient conditions are derived. Finally the unloading problem is considered.

Keywords: Hemivariational Inequalities ▪ Adhesion ▪ Debonding ▪ Nonconvex Analysis

RESUMO

No presente artigo, formula-se e estuda-se o efeito de descolamento de interfaces. Expressa-se as leis tensão-deformação, não-monótononas e possivelmente a valores múltiplos, simulando-se o comportamento de interface através de superpotenciais não-convexos que levam a desigualdades hemivariacionais e a problemas sub-estacionários. Estuda-se as desigualdades hemivariacionais obtidas quanto à existência e à aproximação de suas soluções. Estabelece-se as condições necessárias, assim como as suficientes. Finalmente, considera-se o problema de descarregamento.

Palavras-chave: Desigualdades Hemivariacionais ▪ Adesão ▪ Descolamento ▪ Análise Não-Convexa

Submetido em Março/89 Aceito em Agosto/89

INTRODUCTION

The debonding between connected bodies through an adhesive material can be described by nonmonotone stress-strain laws which may include vertical complete jumps, i.e. they are multivalued. Nonmonotone, possibly multivalued laws can be expressed in terms of nonconvex superpotentials and lead to a new type of variational inequality expressions, the so-called hemivariational inequalities, which express the principle of virtual work or power in inequality form.

We recall here that the study of variational inequalities begun in 1963 with the works of FICHERA [1], [2] and LIONS-STAMPACCHIA [3]. In 1968 MOREAU [4] introduced the notion of convex superpotential in order to describe monotone possibly multivalued mechanical laws, and proved the relation of this new notion with the theory of variational inequalities. Moreau's superpotential permitted the study and the correct solution of large classes, of yet unsolved, problems in Mechanics and Engineering.

Until 1981 all the inequality problems studied were expressed in terms of variational inequalities and included convex superpotentials describing monotone mechanical relations. In order to overcome the constraint of monotonicity the author of the present paper introduced and studies [5]-[9] the notion of nonconvex superpotential by using a new mathematical tool, the generalized gradient of Clarke. Thus a new type of variational inequality expression emerges the hemivariational inequality. Moreover the static hemivariational inequalities lead to substationarity "principles" for the potential and the complementary energy, instead of the minimum "principles" as happens in the case of convex superpotentials. For the study of the variational inequalities we refer the reader to [2], [7], [10]-[14] and for the hemivariational inequalities to [7]-[9] both for the mechanical and the mathematical aspects of the theory. In the present paper we study the debonding problem of adhesively connected deformable bodies.

After the formulation of the corresponding hemivariational inequalities, we study a semicoercive hemivariational inequality and we derive necessary and sufficient conditions for the existence of its solution. The problems studied here and the proofs given are general and may be repeated for all types of hemivariational inequalities.

The theory of hemivariational inequalities is a part of Nonsmooth Mechanics [7]-[9]. At this point we would like to emphasize the great differences between "Smooth Mechanics" based on the notion of classical potentials and "Nonsmooth Mechanics" involving nonsmooth, convex or nonconvex superpotentials. For the reader's convenience we give further some definitions and notations from Nonsmooth Analysis ([15]-[17]).

MATHEMATICAL NOTIONS AND DEFINITIONS. NONCONVEX SUPERPOTENTIALS

Let X be a locally convex Hausdorff topological vector space, X' its dual space and $<x',x>$ the duality pairing. The reader who is not familiar with this terminology could consider X as a classical Hilbert space (then $X = X'$ and $<x',x>$ is the scalar product of the Hilbert space), or more simply as the classical n-dimensional Euclidean space $\mathbf{R}^n$ (then $<x',x> = x'_i x_i, i = 1,2,...,n$). A functional $f: X \to (-\infty, +\infty]$ with $f \not\equiv \infty$ is called proper. Moreover f is lower semicontinuous (1.s.c) on X if and only if the set $epif = \{(x,\lambda) \mid f(x) \leq \lambda, \lambda \in \mathbf{R}\}$ is closed in $X \times \mathbf{R}$. Functional f is locally Lipschitz at x if a neighborhood U of x exists on which f is finite and

$$| f(x_1) - f(x_2) | \leq cp(x_1 - x_2) , \qquad \forall x_1, x_2 \in U \tag{1}$$

where c is a positive constant depending on U and p is a continuous seminorm on X. If (1) holds at every $x \in A \subset X$ then f is called (locally) Lipschitzian on A. Note that f is Lipschitzian at x, if it is continously differentiable at x, or convex (resp. concave) and finite at x or a linear combination of Lipschitzian functions at x.. We denote by $f^0(x,y)$ the directional differential in the sense of F.H. Clarke at x in the direction y. It is defined for f Lipschitzian at x by the expression:

$$f^0(x,y) = \limsup_{\substack{\lambda \to 0 \\ h \to 0}} \frac{f(x+h+\lambda y) - f(x+h)}{\lambda} \tag{2}$$

Then the generalized gradient of f at x is by definition:

$$\bar{\partial} f(x) = \left\{ x' \in X' \mid f^0(x, x_1 - x) \geq <x', x_1 - x> \ \forall x_1 \in X \right\} . \tag{3}$$

It should be noted that if f is convex then $\bar{\partial} f(x)$ coincides with the subdifferential $\partial f(x)$ defined as:

$$\partial f(x) = \left\{ x' \in X' \mid f(x_1) - f(x) \geq <x', x_1 - x> \ \forall x_1 \in X \right\} . \tag{4}$$

For f continuously differentiable at x, $\bar{\partial} f(x) = \{grad f(x)\}$. Note that the generalized gradient can be defined for any functional $f: X \to [-\infty, +\infty]$. In this case $f^0(x,y)$ has to be replaced in (3) by the more sophisticated notion of the upper subdifferential of R.T. ROCKAFELLAR [14] $f^\dagger(x,y)$. Then:

$$\bar{\partial} f(x) = \left\{ x' \in X' \mid f^{\uparrow}(x, x_1 - x) \geq \langle x', x_1 - x \rangle \ \forall x_1 \in X \right\} . \tag{5}$$

Moreover $\bar{\partial} f(x) = \emptyset$ if $f^{\uparrow}(x, 0) = -\infty$, otherwise $\bar{\partial} f(x) \neq \emptyset$. It is worth noting that $\bar{\partial} f(x)$ is never empty, if f attains a local minimum at x, or if f is Lipschitzian at x. A point x_0 is called a substationarity point of f, if x_0 satisfies the multivalued equation:

$$0 \in \bar{\partial} f(x) . \tag{6}$$

Every local minimum and every saddle point is a substationarity point. Also a local maximum x_0 is a substationarity point if f is Lipschitzian around x_0.

A functional $f : X \to [-\infty, +\infty]$ is called $\bar{\partial}$-regular if:

$$f^{\uparrow}(x, y) = f'(x, y) \ \forall y \in X \text{ where } f'(x, y) = \lim_{\lambda \to 0^+} \frac{f(x + \lambda y) - f(x)}{\lambda} . \tag{7}$$

If f is convex or a maximum type function, then f is $\bar{\partial}$-regular. Let now Σ be a mechanical system, let $f \in F$ and $u \in U$ be the corresponding generalized force vector and the generalized velocity vector. Here F and U are vector spaces being in (separating) duality through the bilinear form $\langle u, f \rangle$ which expresses the work produced by f due to u. We denote by $\Phi : U \to [-\infty, +\infty]$ a generally nonconvex and nondifferentiable function and we assume that between f and u a relation of the form:

$$-f \in \bar{\partial} \Phi(u) \quad \text{in} \quad \Sigma \tag{8}$$

holds. By definition, (7) is equivalent to the relation:

$$\Phi^{\uparrow}(u, v - u) \geq \langle f, v - u \rangle \qquad \forall v \in U . \tag{8a}$$

Inequality (8) is called a hemivariational inequality and Φ is a nonconvex superpotential.

i) Let Φ be the indicator I_C of a closed set $C \subset U = \mathbf{R}^n$, i.e. $\Phi(u) = I_C(u) = \left\{ 0 \text{ if } u \in C, \infty \text{ if } u \notin C \right\}$ and let $u = \left\{ u_1, \ldots, u_n \right\}$. Then $\bar{\partial} \Phi(u) = N_C(u)$, where $N_C(u)$ denotes the normal cone to C at the point u [15].

ii) Let Φ be a maximum type function, i.e. $u \to \Phi(u) = \max_i \left\{ \varphi_i(u) \right\}, i = 1, \ldots, m$, where $u = \left\{ u_1, \ldots, u_n \right\}$ and $\varphi_1(.)$ are smooth functions. We introduce the sets $A_i = \left\{ u \mid \Phi(u) = \varphi_1(u) \right\}$. Then [17]:

$$\bar{\partial}\Phi(u) = \{grad\,\varphi_i(u)\}, \quad \text{if} \quad u \in A_i \tag{9}$$

$$\bar{\partial}\Phi(u) = co\,\{grad\,\varphi_i(u), grad\,\varphi_j(u)\}, \quad \text{if} \quad u \in A_i \cap A_j \tag{10}$$

$$\bar{\partial}\Phi(u) = co\,\{grad\,\varphi_i(u), grad\,\varphi_j(u), grad\,\varphi_k(u)\}, \quad \text{if} \quad u \in A_i \cap A_j \cap A_k\,. \tag{11}$$

Here co is the convex hull. Therefore in (10) (resp. (11)) $\bar{\partial}\Phi(u)$ is the line segment (resp. the triangle) connecting the ends of two (resp. the three) gradients.

iii) Suppose now that in (i) $C = \{u \in \mathbf{R}^n \mid \varphi_i(u) \le 0, i = 1, ..., m\}$ where the functions φ_i are smooth. Then we can show by means of u (cf. [7], p. 146) that:

$$N_C(u) = \{f \in F = \mathbf{R}^n \mid f = \sum_{i=1}^{m} \lambda_i\, grad\,\varphi_i(u),\ \lambda_i \ge 0,\ \varphi_i \le 0,\ \lambda_i \varphi_i = 0\} \tag{12}$$

on the assumption that if $u \in$ (boundary of C) a vector y exists such that:

$$\langle y, grad\,\varphi_i(u)\rangle < 0 \tag{12a}$$

for every i corresponding to an active constraint $\varphi_1(u) = 0$ at u (multiplier type formula).

SUPERPOTENTIAL LAWS FOR ADHESIVELY CONNECTED INTERFACES

We consider a deformable body Ω and let Γ be its boundary. Ω is referred to a fixed orthogonal Cartesian system $Ox_1x_2x_3$. On Γ we can distinguish three types of boundary conditions on the disjoint parts Γ_F, Γ_U and Γ_S. On Γ_U the displacements $u = \{u_i\}$ are prescribed and on Γ_F the boundary forces $S = \{S_i\}$ are given where $S_i = \sigma_{ij} n_j$ ($i, j = 1, 2, 3$-summation convention), $\sigma = \{\sigma_{ij}\}$ is the stress tensor and $n = \{n_j\}$ is the outward unit normal vector to Γ. On Γ_S we consider that the body is adhesively connected with the support in the normal direction. In order to describe this type of boundary conditions we decompose on Γ_S u (resp. S) into normal and tangential components u_N and u_T (resp. S_N and S_T). The adhesive contact condition is described by a nonmonotone relation between $-S_N$ and u_N (see Figure 1a). The adhesive material can sustain large compressive forces and very small tensile forces for a monotonic loading beginning from zero. (The case of unloading will be examined at the end of the present

paper). Thus we may write that:

$$\begin{aligned} &\text{if } u_N > u_{N_0} \quad \text{then} \quad S_N + k(u_N) = 0 \\ &\text{if } u_N = u_{N_0} \quad \text{then} \quad 0 \le S_N \le k(u_{N_0}) \\ &\text{if } u_N < u_{N_0} \quad \text{then} \quad S_N = 0 \quad \text{(debonding)} \end{aligned} \tag{13}$$

The dotted line in Figure 1a is more realistic, since we avoid the ideally brittle behaviour. Function k is generally nonmonotone and may include vertical jumps corresponding to local locking and crushing phenomena (stick-"slip" in the normal direction). Note that if $u_{N_0} = 0$ then (13) describes the unilateral contact (Figure 1a) with a granular support (rock, concrete etc.). The boundary condition (13) may be called a nonmonotone multivalued Winkler law. It must be combined in the tangential direction with another law as, e.g. the simple assumption of given tangential displacements or forces on Γ_S. The relation (13) can be put in the form:

$$-S_N \in \bar{\partial} j_N(u_N) \tag{14}$$

where

$$j_N(\xi) = \int_0^{\xi^+} k(t)\,dt\,, \quad \xi_+ = sup\,(0, \xi)\,. \tag{15}$$

In the tangential direction the normal laws may be combined with a general tangential nonmonotone relation of the form:

$$-S_T \in \bar{\partial} j_T(u_T) \tag{16}$$

in order to describe frictional phenomena or the adhesive debonding and gradual slipping. For $S_N = C_N$, given, Figure 1c depicts the friction law of Coulomb. In Figure 1d to Figure 1f and for $\Omega, \Omega \subset \mathbf{R}^2$ some other friction laws or stick-slip laws are depicted expressing the evolution of the tangential debonding. In case $\Omega \subset \mathbf{R}^3$ the additional assumption that the vectors $-S_T$ and u_T are collinear has to be made. The graphs of $(-S_T, u_T)$ diagrams may include vertical jumps describing local cracking and crushing of the contact surface asperities in the case of friction or stick-slip phenomena in the case of adhesive connection. Note also the analogy between Scanlon's diagram [18] for reinforced concrete in tension (Figure 1g) and the sawtooth debonding or friction diagrams describing the change of the

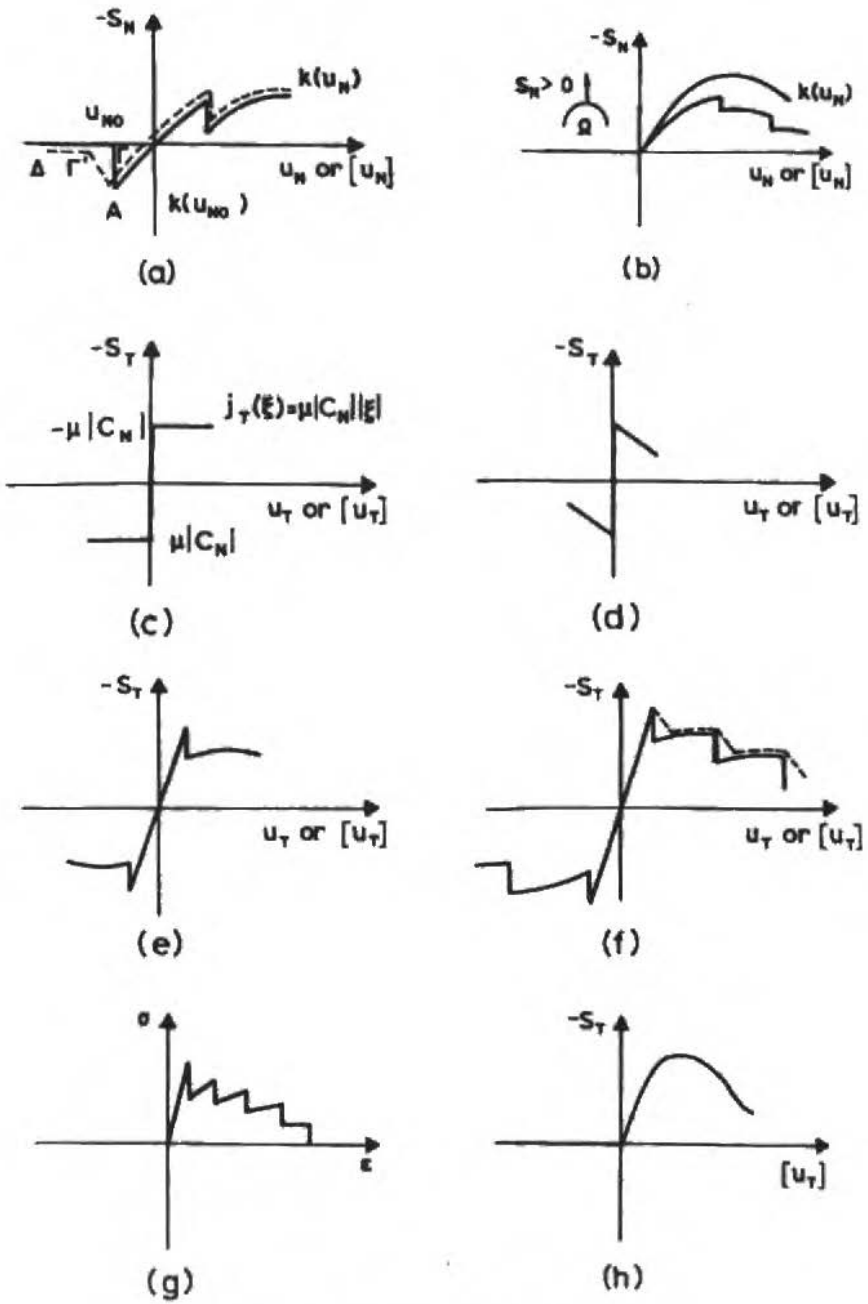

Figure 1. Superpotential Interface Laws

mechanical properties of the contact surface due to increasing loading. Finally we give in Figure 1h the friction diagram between fiber and matrix in fiber-reinforced materials or between reinforcement and concrete. Here $[u_T]$ denotes the relative tangential displacement between the two structural elements in contact. In [19] we have shown that the anisotropic or orthotropic friction is a special case of (16) and we have derived multidimensional nonmonotone friction laws.

Let us now assume that in Ω there is an interface A along which debonding and slip is possible. The surface A may be a rock joint, a fault, or an interface between different structural components, e.g. between the adjacent laminae in a laminated structure. We assume that the interface can be simulated by fictitious elements having two strain components, the normal strain ε_N and the shearing strain ε_T, with σ_N the corresponding stresses. Then the same laws as those of Figure 1, can be assumed between σ_N and ε_N, and between σ_T and ε_T, where, now, $-S_N$ and $-S_T$ are replaced by σ_N and σ_T respectively. This consideration assumes that the interface A is a part of Ω with different behaviour. Especially for laminated structures another approach is suitable. Each side of the interface is considered to belong to a different body. Then we introduce relations of the form:

$$-S_N \in \bar{\partial} j_N([u_N]), \qquad -S_T \in \bar{\partial} j_T([u_T]) \tag{17}$$

on the interface, where $[u_N]$ and $[u_T]$ denote the relative normal and tangential displacements of the two bodies, and j_N and j_T are nonconvex superpotentials (cf. (14)). Of course relations (17) hold if the normal action can be decoupled from the tangential one. If this is not the case (17) has to be replaced by a general relation of the form $-S \in \bar{\partial} j([u])$.

We shall further give two examples of the above interface laws.

a) **Massonry structures**: In these structures cracks appear due to tension, compression or shear usually in the weak positions of the structure i.e. in the joints, where the mortar fractures between the stones, due to exceeding of the mortar strength normally or tangentially to the joint (Figure 2a). In the case of brick structures, another weak position in the middle of a brick is possible (Figure 2b). In order to study this problem we assume that on the interfaces the superpotential relations (17) hold.

b) **The delamination effect**: Let us consider a composite plate consisting for the shake of simplicity of two plates connected with an adhesive material (Figure 3). Each plate is assumed to be elastic and is referred to an orthogonal Cartesian coordinate system $Ox_1x_2x_3$. The two plates have thicknesses h_1 and h_2, which are constant, and the middle surface of each plate coincides with the Ox_1x_2-plane of the coordinate system. Let Ω_1 and Ω_2 be two open, bounded and connected subsets of $\mathbf{R}^2$ and let Γ_1, Γ_2 be their

undeformed state. The plates are connected together on $\Omega' \subset \Omega_1 \cap \Omega_2$ so as to act as an integral structural element. (Here Ω_1 are the projections of the plates onto the interface plane). Further we denote by $\zeta_i(x)$ the deflection of the point $x = \{x_1, x_2, x_3\}$. Let $f_i = (0, 0, f_{3i})$ be the distributed load for the i-th plate per unit area of its middle surface. For $i = 1$ (resp. 2) we have the upper (resp. the lower) plate Ω_1 (resp. Ω_2). In order to study the delamination effect we notice that the interlaminar normal stress σ_{33} is responsible for the delamination effect in all types of composite plates, i.e. in layered plates, sandwich plates, or laminated plates (cf. e.g. [20], p. 220).

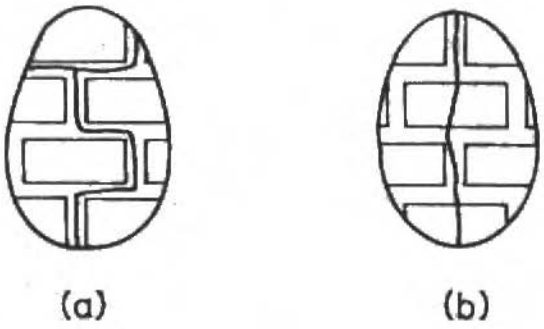

Figure 2. Interfaces in massonry structures

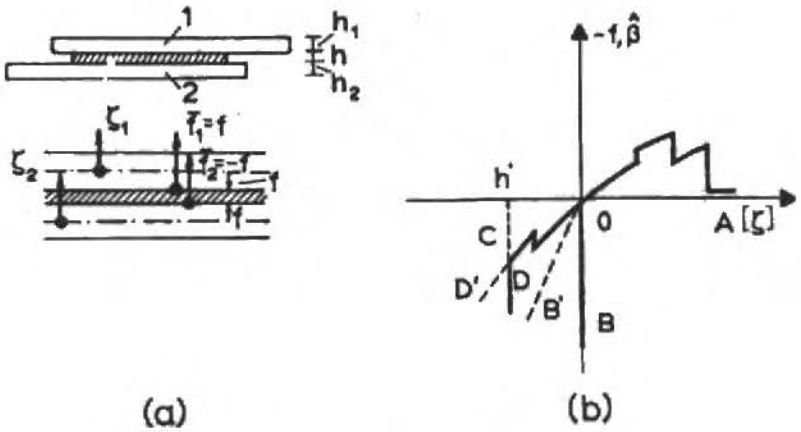

Figure 3. On the delamination effect of composite plates

Thus we split f_i into $\bar{\bar{f}}_i$ which is the given loading of the i-th plate, and into $\bar{f}_i$, which describes the interaction of the two plates due to the binding material, i.e.:

$$f_i = \bar{\bar{f}}_i + \bar{f}_i \quad \text{in } \Omega_i, \quad i = 1, 2 \tag{18}$$

assuming that $\bar{f}_i$ is a nonmonotone multivalued function b of the relative displacement $[\zeta] = \zeta_1 - \zeta_2$ of the two plates. We have that (Figure 3):

$$-\bar{f}_1 \in \hat{b}(\zeta_1 - \zeta_2) \text{ and } +\bar{f}_2 \in \hat{b}(\zeta_1 - \zeta_2) \text{ on } \Omega' \subset \Omega_1 \cap \Omega_2 , \tag{19}$$

where $\bar{f}_1 = -\bar{f}_2 = f$ and

$$\bar{f}_1 = 0 \quad \text{on} \quad \Omega_1 - \Omega', \quad \bar{f}_2 = 0 \quad \text{on} \quad \Omega_2 - \Omega' \tag{20}$$

The graph of the multifunction b results from a function $b \in L^{\infty}_{loc}(\mathbf{R})$ by "filling in" the gaps (see Sec. 5 and Figure 4). If $b(\xi_{\pm 0})$ exists for every $\xi \in \mathbf{R}$ then, according to CHANG [21] a locally Lipschitz function $j : \mathbf{R} \to \mathbf{R}$ can be determined (up to an additive constant) such that:

$$\hat{b}(\xi) = \bar{\partial} j(\xi) \quad \text{where } j(\xi) = \int_0^{\xi} b(t)\, dt \tag{21}$$

Thus (19) is put in the form:

$$-f \in \bar{\partial} j([\zeta]) \quad \text{on } \Omega' \tag{22}$$

The diagram AOB of Figure 3b describes phenomenologically the plate debonding and takes into account stick-slip possibilities for the adhesive in the normal direction. This graph describes the adhesive contact of two plates with adhesive material with negligible thickness at the interface. The branch OB is vertical (nonpenetrability condition) due to the incompressibility of each lamina in the Ox_3-direction according to the assumptions of plate theory. Here, however, we assume that the line OB has a small slope, i.e. we consider the diagram AOB', in order to take into account the possibility of small elastic deformations of the plates in the Ox_3-direction. Analogously the graphs of the forms $AOCD$ or $AOCD'$ correspond to an adhesive with thickness $h > h'$. See in this context [22]-[26].

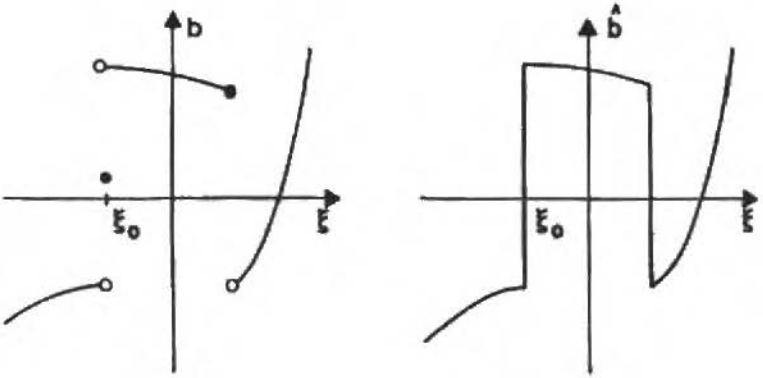

Figure 4. On the definition of b and $\hat{b}$

DERIVATION OF HEMIVARIATIONAL INEQUALITIES

In order to show the method for derivation of hemivariational inequalities we study a specific mechanical problem, the problem of equilibrium of elastic bodies with adhesive contacts for a given external loading. Note that this is a free boundary problem. Indeed, assuming that the adhesive material has the behaviour depicted in Figure 1a, it is not a priori known at which points of the interface the debonding takes place.

Let $\Omega_m, m = 1, 2, ..., 1$ be open bounded, connected, subsets of R^2 representing a set of deformable bodies each with different elasticity properties. The boundaries $\Gamma_m, m = 1, 2, ..., l$, are assumed to be appropriately regular. Ω_m's are referred to a fixed Cartesian orthogonal coordinate system $Ox_1x_2x_3$. Let now $x = \{x_1\}, i = 1, 2, 3$ be a point of $\mathbf{R}^3$ and let $\sigma^{(m)} = \sigma_{ij}^{(m)}$ and $\varepsilon^{(m)} = \varepsilon_{ij}^{(m)}, i, j = 1, 2, 3$, be the stress and strain tensors of the m-body. We denote by $f^{(m)} = \{f_i^{(m)}\}$ and $u^{(m)} = \{u_i^{(m)}\}$ the volume force and the displacement vector in each body. If $n^{(m)} = \{n_i^{(m)}\}$ is the outward unit normal vector to $\Gamma^{(m)}$, the boundary force on $\Gamma^{(m)}$ is $S_i^{(m)} = \sigma_{ij}^{(m)} n_{ij}^{(m)}$ (summation convention) with $S_T^{(m)}$ and $S_T^{(m)}$ the normal and tangential components, of it. The corresponding displacement components are $u_N^{(m)}$ and $u_T^{(m)}$. The boundary $\Gamma^{(m)}$ is divided into three non-overlaping parts $\Gamma_U^{(m)}$, $\Gamma_F^{(m)}$ and $\Gamma_S^{(m)}$. On $\Gamma_U^{(m)}$ the displacements and on $\Gamma_F^{(m)}$ the forces are prescribed, i.e.:

$$u_i^{(m)} = U_i^{(m)} \quad \text{on} \quad \Gamma_U^{(m)} \tag{23}$$

$$S_i^{(m)} = F_i^{(m)} \quad \text{on} \quad \Gamma_F^{(m)} \ . \tag{24}$$

On $\Gamma_S^{(m)}$ - which is the interface of the body m with all the other bodies - nonmonotone interface conditions hold describing slip and delamination effects. We write the interface conditions in the form:

$$-S_N^{(m)} \in \bar{\partial} j_{N(m)}([u_N^{(m)}]) \tag{25}$$

$$-S_T^{(m)} \in \bar{\partial} j_{T(m)}([u_T^{(m)}]) \tag{26}$$

in the normal and in the tangential direction to the interface. The superpotentials j_N and j_T are assumed to be locally Lipschitz functions of the interlayer gap $[u_N]$ and slip $[u_T]$ respectively. Then (25), (26) are equivalent to the inequalities:

$$j^0_{N(m)}([u_N^{(m)}], v - [u_N^{(m)}]) \geq -S_N^{(m)}(v - [u_N^{(m)}]) \quad \forall v \in \mathbf{R} \tag{27}$$

$$j^0_{T(m)}([u_T^{(m)}], v - [u_T^{(m)}]) \geq -S_{T_i}^{(m)}(v_i - [u_T^{(m)}]) \quad \forall v_i \in \mathbf{R}\ ,\ i = 1,2,3\ . \tag{28}$$

The m bodies connected with the adhesive material constitute a body Ω. In Ω we denote the joints by Γ_q, $q = 1, 2, ..., k$, where k is the total number of joints (Figure 5).

Assuming small strains and linear elastic behaviour for $\Omega^{(m)}$, $m = 1, 2, ..., l$ we can write the relations:

$$\sigma_{ij,j}^{(m)} + f_i^{(m)} = 0 \tag{29}$$

$$\varepsilon_{ij}^{(m)} = \frac{1}{2}(u_{i,j}^{(m)} + u_{j,i}^{(m)}) = \varepsilon_{ij}(u^{(m)})\ , \tag{30}$$

$$\sigma_{ij}^{(m)} = C_{ijhk}^{(m)} \varepsilon_{hk}^{(m)}\ . \tag{31}$$

The comma denotes the differentiation and $C^{(m)} = \left\{C^{(m)}_{ijhk}\right\}$ is Hooke's tensor. Then the principle of virtual work for every body $\Omega^{(m)}$ takes the form:

$$\int_{\Omega^{(m)}} \sigma^{(m)}_{ij}\, \varepsilon^{(m)}_{ij}\,(v^{(m)} - u^{(m)})\, d\Omega = \int_{\Omega^{(m)}} f^{(m)}_i\,(v^{(m)}_i - u^{(m)}_i)\, d\Omega +$$

$$+ \int_{\Gamma^{(m)}_F} F^{(m)}_i\,(v^{(m)}_i - u^{(m)}_i)\, d\Gamma + \int_{\Gamma^{(m)}_S} [S^{(m)}_N\,(v^{(m)}_N - u^{(m)}_N) +$$

$$+ S^{(m)}_{T_i}\,(v^{(m)}_{T_i} - u^{(m)}_{T_i})]\, d\Gamma \qquad \forall v \in U^{(m)}_{ad}\,. \tag{32}$$

Here $U^{(m)}_{ad}$ is the kinematically admissible set of $\Omega^{(m)}$:

$$U^{(m)}_{ad} = \left\{v^{(m)} \mid v^{(m)} = v^{(m)}_i,\, v^{(m)}_i \in U(\Omega^{(m)}),\, v^{(m)}_i = U^{(m)}_i \text{ on } \Gamma^{(m)}_U\right\}. \tag{33}$$

We denote by $U(\Omega^{(m)})$ a space of functions defined on $\Omega^{(m)}$. Now we add with respect to m all the expressions (32) and we take into account the interconnection of the bodies. This yields a relation of the form:

$$\sum_{m=1}^{l} \int_{\Omega^{(m)}} \sigma^{(m)}_{ij}\, \varepsilon_{ij}\,(v^{(m)} - u^{(m)})\, d\Omega = \sum_{m=1}^{l} [\int_{\Omega^{(m)}} f^{(m)}_i\,(v^{(m)}_i - u^{(m)}_i)\, d\Omega +$$

$$+ \int_{\Gamma^{(m)}_F} F^{(m)}_i\,(v^{(m)}_i - u^{(m)}_i)\, d\Gamma] + \sum_{q=1}^{k} [\int_{\Gamma^{(q)}} S^{(q)}_N\,([v^{(q)}_N] -$$

$$- [u^{(q)}_N]\, d\Gamma) + \int_{\Gamma^{(q)}} S^{(q)}_{T_i}\,([v^{(q)}_{T_i}] - [u^{(q)}_{T_i}]\, d\Gamma) \quad \forall v \in U_{ad}\,, \tag{34}$$

where $U_{ad} = \bigcup_{m=0}^{l} U^{(m)}_{ad}$.

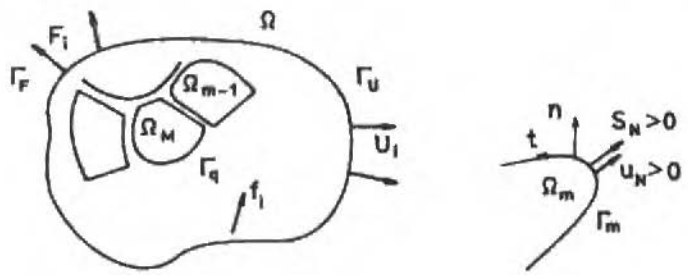

Figure 5. On the interface problem

In (34) we introduce now the integrals along the joints Γ_q, $q = 1, ..., k$. The new numbering of the $\Gamma_S^{(m)}$-boundaries has the advantage that finally the energy of each joint appears. Further the elastic energy of the m-structure is introduced:

$$a(u^{(m)}, v^{(m)}) = \int_{\Omega^{(m)}} C_{ijhk}^{(m)} \varepsilon_{ij}(u^{(m)}) \varepsilon_{hk}(v^{(m)}) \, d\Omega \ . \tag{35}$$

Now combining (26), (28), (35) with (34) we obtain the following hemivariational inequality:

Find $u \in U_{ad}$ such as satisfy:

$$\sum_{m=1}^{l} a(u^{(m)}, v^{(m)} - u^{(m)}) + \sum_{q=1}^{k} \Big[\int_{\Gamma^{(q)}} \big[j^0_{N(q)}([u_N^{(q)}], [v_N^{(q)}] - [u_N^{(q)}]) +$$

$$+ j^0_{T(q)}([u_T^{(q)}], [v_T^{(q)}] - [u_T^{(q)}]) \geq$$

$$\geq \sum_{m=1}^{l} \Big[\int_{\Omega^{(m)}} f_i^{(m)}(v_i^{(m)} - u_i^{(m)}) \, d\Omega +$$

$$+ \int_{\Gamma_F^{(m)}} F_i^{(m)}(v_i^{(m)} - u_i^{(m)}) \, d\Gamma \Big] \quad \forall v \in U_{ad} \ . \tag{36}$$

This hemivariational inequality is the expression of the principle of virtual work in its inequality form for the considered problem. Let us check now in which sense a solution of

(36) satisfies (29), the boundary conditions on $\Gamma_F^{(m)}$ and the interface relations on $\Gamma_S^{(m)}$, $m = 1, ..., l$. To this end the functional setting of the problem will be made more precise: We assume that $f_i^{(m)} \in L^2(\Omega^{(m)})$, $F^{(m)} \in L^2(\Gamma_F^{(m)})$, $C_{ijhk}^{(m)} \in L^\infty(\Omega^{(m)})$, $u_i^{(m)}, v_i^{(m)} \in H^1(\Omega^{(m)})$ (classical Sobolev space).

Then $u_N^{(m)}, u_{T_i}^{(m)} \in H^{1/2}(\Gamma^{(m)})$ and $S_N^{(m)}, S_{T_i}^{(m)} \in H^{-1/2}(\Gamma^{(m)})$. We set in (36) $v_i^{(m)} - u_i^{(m)} = \pm \varphi_i^{(m)}$ where $\varphi_i^{(m)}$ belongs to the space of infinitely differentiable functions with compact support in $\Omega^{(m)}$, $\mathbf{D}(\Omega^{(m)})$. Then (36) implies by setting $v_i^{(m)} - u_i^{(m)} = \pm \varphi_i^{(m)}$ for $m = n$ and $v_i^{(m)} - u_i^{(m)} = 0$ for $m \neq n$ that:

$$a\left(u^{(n)}, \varphi^{(n)}\right) = \int_{\Omega^{(n)}} f_i^{(n)} \varphi_i^{(n)} \, d\Omega \tag{37}$$

since $\varphi_i^{(n)} = 0$ on $\Gamma^{(n)}$. From (37) using the notations (30) and (31) we find that (29) holds on $\Omega^{(n)}$ in the sense of distributions over $\Omega^{(n)}$. This procedure is repeated for $n = 1, 2, ..., l$. Now applying the Green-Gauss theorem to each body we obtain the equality:

$$\begin{aligned} a\left(u^{(m)}, v^{(m)} - u^{(m)}\right) = & \int_{\Omega^{(m)}} f_i^{(m)} \left(v_i^{(m)} - u_i^{(m)}\right) d\Omega + \\ & + \langle S_i^{(m)}, v_i^{(m)} - u_i^{(m)} \rangle_{\Gamma - \Gamma_s} + \langle S_N^{(m)}, v_N^{(m)} - u_N^{(m)} \rangle_{\Gamma_s} + \\ & + \langle S_{T_i}^{(m)}, v_{T_i}^{(m)} - u_{T_i}^{(m)} \rangle_{\Gamma_s} \end{aligned} \tag{38}$$

where $\langle \cdot, \cdot \rangle$ is the duality pairing between $H^{1/2}(\Gamma)$ and $H^{-1/2}(\Gamma)$. From (38) and (36) we derive the inequality:

$$\sum_{q=1}^{k}\Big[\int_{\Gamma_q}\Big[j^0_{N(q)}\Big(\big[u_N^{(q)}\big],\big[v_N^{(q)}\big]-\big[u_N^{(q)}\big]\Big)+j^0_{T(q)}\Big(\big[u_T^{(q)}\big],\big[v_T^{(q)}\big]-$$

$$-\big[u_T^{(q)}\big]\Big)\Big]d\Gamma+\sum_{m=1}^{l}<S_i^{(m)}-F_i^{(m)},v_i^{(m)}-u_i^{(m)}>_{\Gamma_F^{(m)}}+\sum_{q=1}^{k}\Big\{<S_N^{(q)},\big[v_N^{(q)}\big]-$$

$$-\big[u_N^{(q)}\big]>_{\Gamma_q}+<S_{T_i}^{(q)},\big[v_{T_i}^{(q)}\big]-\big[u_{T_i}^{(q)}\big]>_{\Gamma_q}\Big\}\geq 0\quad\forall v\in U_{ad}\ . \tag{39}$$

If in (39) we take that on $\Gamma_F^{(m)}$, $v_i^{(m)}-u_i^{(m)}=-r_i^{(m)}\in H^{1/2}(\Gamma^{(m)})$ for $m=n$, and that $v_i^{(m)}-u_i^{(m)}=0$ for $m\neq n$ on $\Gamma_F^{(m)}$ and on Γ_q for every q, we obtain $S_i^{(n)}=F_i^{(n)}$ as an equality in $H^{-1/2}(\Gamma^{(m)})$; this can be shown for every n. From (39) by setting $[v_N^{(q)}]-[u_N^{(q)}]=r_N^{(q)}$ on Γ_q for $q=n$ and the same difference $=0$ for $q\neq n$, and setting $[v_T^{(q)}]-[u_T^{(q)}]=0$ on Γ_q for every q we obtain:

$$\int_{\Gamma_n}j^0_{N(n)}\Big(\big[u_N^{(n)}\big],r_N^{(n)}\Big)d\Gamma\geq-<S_N^{(n)},r_N^{(n)}>_{\Gamma_n}\quad\forall r_N^{(n)}\in H^{1/2}(\Gamma) \tag{40}$$

which is a "weak" formulation of (25) on $H^{-1/2}(\Gamma)\times H^{1/2}(\Gamma)$. Analogously from (39) a weak form of (26) is botained. Let us now consider the following substationarity problem: Find $u\in U_{ad}$ such that the potential energy of the structure:

$$\Pi(v)=\frac{1}{2}\sum_{m=1}^{l}a\big(v^{(m)},v^{(m)}\big)+\sum_{q=1}^{k}\int_{\Gamma_q}\Big[j_{N_{(q)}}\Big(\big[v_N^{(q)}\big]\Big)+j_{T_{(q)}}\Big(\big[v_T^{(q)}\big]\Big)\Big]d\Gamma-$$

$$-\sum_{m=1}^{l}\int_{\Omega^{(m)}}f_i^{(m)}v_i^{(m)}d\Omega-\sum_{m=1}^{l}\int_{\Gamma^{(m)}}F_i^{(m)}v_i^{(m)}d\Gamma \tag{41}$$

is substationary at $v=u$, where $v\in U_{ad}$. The following proposition holds.

Proposition 1. If $\xi\to j_{N(m)}(\xi)$ and $\xi\to j_{T(m)}(\xi)$ are locally Lipschitz and $\bar{\partial}$-regular for $m=1,...,l$, then every solution of the substationarity problem is a solution of the

hemivariational inequality (36) and conversely.

The proof is similar to the one given in [9], p. 108 and it is omitted here.

Suppose now that the substructures $\Omega^{(m)}$, $m = 1, ..., I$ obey a general nonmonotone law of the form $\sigma^{(m)} \in \partial w_{(m)}(\varepsilon)$, where $w_{(m)}$ is an extended realvalued function, nonconvex and noneverywhere differentiable. This law holds e.g. for a fiber reinforced composite material in order to describe the sawtooth form of the stress-strain law. For three-dimensional generalizations of Figure 1g cf. [9]. Then the variational expression of the problem is the same as (36) with the difference that now the term $\sum_{m=1}^{I} a(u^{(m)}, v^{(m)} - u^{(m)})$ is replaced by $\sum_{m=1}^{I} \int_{\Omega^{(m)}} w^{\uparrow}_{(m)}(\varepsilon(u^{(m)}), \varepsilon(v^{(m)} - u^{(m)}))\, d\Omega$. If the $w_{(m)}$'s are convex superpotentials, i.e. they are convex, l.s.c. and proper functionals, then let:

$$W_{(m)}(\varepsilon) = \begin{cases} \int_{\Omega^{(m)}} w_{(m)}(\varepsilon)\, d\Omega & \text{if } w_m(\cdot) \in L^1(\Omega^{(m)}) \\ \infty & \text{otherwise} \end{cases} \tag{42}$$

In this case we obtain a variational formulation analogous to (36) where the elastic energy variation $a(\cdot, \cdot)$ is replaced by the difference $\sum_{m=1}^{I} [W_m(\varepsilon(v^{(m)})) - W_m(\varepsilon(u^{(m)}))]$. This is a variational-hemivariational inequality [8], [9] and is the expression of the principle of virtual work for the considered problem.

If the interface superpotential is not a Lipschitz continuous function, then Clarke's directional differentials $j_N^0(\cdot, \cdot)$ and $T_T^0(\cdot, \cdot)$ must be replaced in the previous hemivariational inequalities by $j_N^{\uparrow}(\cdot, \cdot)$ and $j_T^{\uparrow}(\cdot, \cdot)$. Analogous is the treatment of dynamic problems on the assumption of small displacements. Then $f_i^{(m)}$ has to be replaced by $f_i^{(m)} - \rho^{(m)} \frac{\partial^2 u_i^{(m)}}{\partial t^2}$, where $\rho^{(m)}$ is the density of the m-body; also initial conditions for the displacements $u_i^{(m)}$ and the velocities $\partial u_i^{(m)}/\partial t$ must be given. The resulting hemivariational inequality expresses the d'Alembert principle in inequality form. Note that in the dynamic case the holonomic interface relations (25) and (26) may be replaced by the relations:

$$-S_N^{(m)} \in \bar{\partial} j_{N(m)}\left[\frac{\partial u_N^{(m)}}{\partial t}\right], \tag{43}$$

$$-S_T^{(m)} \in \bar{\partial} j_{T(m)}\left[\frac{\partial u_T^{(m)}}{\partial t}\right]. \tag{44}$$

In this case we formulate again (32) by considering instead of displacement variations, velocity variations. Thus a hemivariational inequality similar to (36) is derived having instead of $v^{(m)} - u^{(m)}$ and $[v_N^{(m)}] - [u_N^{(m)}]$ the following variations:

$$v^{(m)} - \frac{\partial u^{(m)}}{\partial t} \quad \text{and} \quad [v_N^{(m)}] - \left[\frac{\partial u_N^{(m)}}{\partial t}\right].$$

STUDY OF A SEMICOERCIVE HEMIVARIATIONAL INEQUALITY. NECESSARY AND SUFFICIENT CONDITIONS

In this section we shall study a hemivariational inequality similar to (36) and we shall develop a general method which permits to prove the existence of the solution. Moreover the proof indicates a method for the approximation of the solution. Let us consider for $u_i, v_i \in V_i$, $i = 1, 2, ..., r$ where V_i is a real Hilbert space defined on Ω_i, a symmetric continuous bilinear form $a_i(\cdot, \cdot)$: $V_i \times V_i \to R$. Here index i enumerates the "deformable bodies" and not the vector components as is the previous sections. Let V_i' be the dual space of V_i and assume that for Ω_i open and bounded subset of R^n:

$$V_i \subset L^2(\Omega_i) \subset V_i', \qquad i = 1, ..., r, \tag{45}$$

where the injections are continuous. We denote by $(\cdot, \cdot)_i$ the L^2-product and the duality pairing, the norm of V_i by $\|\cdot\|_i$ and the norm of $L^2(\Omega_i)$ by $|\cdot|$. We shall omit index i if no ambiguity occurs. We recall here that the linear form $(\cdot, \cdot)_i$ extends uniquely [27] from $V_i \times L^2(\Omega_i)$ to $V_i \times V_i'$. Further let us assume that for each i:

$$V_i \subset L^2(\Gamma_i) \quad \text{is compact}, \tag{46a}$$

where Γ_i is the boundary of Ω_i assumed to be Lipschitz and that:

$$V_i \cap L^\infty(\Gamma_i) \text{ is dense in } V_i \text{ for the } ||\cdot||_i\text{-norm} . \tag{46b}$$

The bilinear forms are assumed to have a nonzero kernel, i.e.:

$$ker a_i(u_i, u_i) = \{q_i \mid a_i(q_i, q_i) = 0\} \neq \{0\} , \tag{47}$$

and let:

$$ker a_i \text{ be finite dimensional, } i = 1, ..., r . \tag{48}$$

The norm $||v||_i$ on V_i is assumed to be equivalent to $|||v|||_i = p_i(\tilde{v}) + |q|_i$ where $v = \tilde{v} + q$, $q \in ker a_i$, $\tilde{v} \in ker a_i$ (i.e. $(\tilde{v}, q)_i = 0, \forall q \in ker a_i$ $p(\tilde{v})$ is a seminorm on V_i such that $p_i(v) = p(v + q), \forall v \in V_i, q \in ker a_i$ and let:

$$a_i(v, v) \geq c\,(p_i(v))^2 , \quad \forall v \in V_i , \; c\ const > . \tag{49}$$

Now let $\beta_i \in L^\infty_{loc}(\mathbf{R}), j = 1, ..., \rho$, and let us define for any $\mu > 0$ and $\xi_1 R$ the functions:

$$\underline{\beta}_{j\mu}(\xi) = \operatorname*{ess\,inf}_{|\xi - \xi_1| < \mu} \beta_j(\xi) \quad \text{and} \quad \overline{\beta}_{j\mu}(\xi) = \operatorname*{ess\,sup}_{|\xi - \xi_1| < \mu} \beta_j(\xi) \tag{50}$$

Since $\mu \to \underline{\beta}_{j\mu}$ and $\mu \to \overline{\beta}_{j\mu}$ are monotonically decreasing and increasing functions respectivelly, their limits as $\mu \to 0$ exist (they may be also $\pm \infty$) and let:

$$\underline{\beta}_j(\xi) = \lim_{\mu \to 0} \underline{\beta}_{j\mu}(\xi) \quad \text{and} \quad \overline{\beta}_j(\xi) = \lim_{\mu \to 0} \overline{\beta}_{j\mu}(\xi) . \tag{51}$$

Now the multivalued function:

$$\xi \to \hat{\beta}_j(\xi) = [\underline{\beta}_j(\xi), \overline{\beta}_j(\xi)] \tag{52}$$

is defined. The graph $\{\xi, \hat{\beta}_i(\xi)\}$ is the same as $\{\xi, \beta_i(\xi)\}$, the only difference being that it contains the vertical segments at the points of discontinuity of β_i (cf. Figure 4).

From β_i a locally Lipschitz function $J_i : \mathbf{R} \to \mathbf{R}$ is defined up to an additive constant by the relation:

$$J_j(\xi) = \int_0^{\xi} \beta_j(\xi_1)\, d\xi_1 \ . \tag{53}$$

It satisfies the inclusion $\partial J_j(\xi) \subset \hat{\beta}_j(\xi)$ and if $\beta_j(\xi_\pm)$ exists for every $\xi \in \mathbf{R}$, the equality:

$$\partial J_j(\xi) = \hat{\beta}_j(\xi) \ , \quad j = 1, ..., \rho \tag{54}$$

holds according to [21]. Now the following problem is formulated for $f_i \in L^2(\Omega_i)$, $i = 1, ..., r$.

Problem P. Find $u_i \in V_i, i = 1, ..., r$ so as to satisfy the hemivariational inequality:

$$\sum_{i=1}^{r} a_i(u_i, v_i - u_i) + \sum_{j=1}^{\rho} \int_{\Gamma_j'} Jj^0([u]_i, [v]_j - [u]_j)\, d\Gamma \geq$$

$$\geq \sum_{i=1}^{r} (f_i, v_i - u_i) \quad \forall v_i \in V_i \ . \tag{55}$$

Here $[u]_j$ is the relative boundary displacement of the two Ω's separated by the interface Γ_j'. Analogous is the meaning of $[q]_j$. The following proposition gives a necessary and sufficient condition for the existence of the solution. We introduce the notations.

$$\beta_j(-\infty) = \lim_{\xi \to -\infty} sup\, \beta_j(\xi) \quad \text{and} \quad \beta_j(\infty) = \lim_{\xi \to \infty} inf\, \beta_j(\xi) \tag{56}$$

for $j = 1, 2, ..., \rho$. Moreover $[q]$ is the relative "rigid" displacement with respect to Γ_j' and $[q]_+$ (resp. $[q]_-$) denotes the positive (resp. negative) part of $[q]$:

$$\text{i.e.} \quad [q]_+ = \frac{[q] + |[q]|}{2} \ , \qquad [q]_- = \frac{|[q]| - [q]}{2} \ .$$

Proposition 2. Let:

$$\beta_j(-\infty) \leq \beta_j(\xi) \leq \beta_j(\infty) \quad \forall \xi \in \mathbf{R} \ ; \quad j = 1, ..., \rho \ . \tag{57}$$

Then a necessary condition for the existence of a solution $u_i \in V_i, i = 1, ..., r$ of problem P is the inequality:

$$\sum_{j=1}^{\rho}\Big(\int_{\Gamma_j'}(\beta_j(-\infty)\,[q]_{j+}-\beta_j(\infty)\,[q]_{j-})\,d\Gamma\Big)\le\sum_{i=1}^{r}\overset{=}{(f_i,q_i)}\le$$

$$\le\sum_{j=1}^{\rho}\Big(\int_{\Gamma_j'}(\beta_j(\infty)\,[q]_{j+}-\beta_j(-\infty)\,[q]_{j-})\,d\Gamma\Big)\quad\forall q_i\in kera_i,\quad i=1,\ldots,r\ .\tag{58}$$

If at least one inequality in (57) holds strictly (with $<$ instead of $\le$) the same holds for (58).

Proof. Let us set in (55) $v_i-u_i=\pm q\in Kera_i$. We obtain:

$$\sum_{j=1}^{\rho}\int_{\Gamma_j'}f_j^0([u]_j,\pm[q]_j)\,d\Gamma\ge\sum_{i=1}^{r}\overset{=}{(f_i,\pm q_i)}\quad\forall q_i\in Kera_i,\ q_i\neq 0,\ i=1,\ldots,r,\tag{59}$$

which implies due to the fact that $q\to f^0(\xi,q)$ is positively homogeneous that:

$$\sum_{j=1}^{\rho}\int_{\Gamma_j'}f_j^0([u]_j,[q]_j)\,d\Gamma\ge\sum_{i=1}^{r}\overset{=}{(f_i,q_i)}\ge$$

$$\ge-\sum_{j=1}^{\rho}\int_{\Gamma_j'}f_j^0([u]_j,[q]_j)\,d\Gamma\quad\forall q_i\in Kera_i,\ q_i\neq 0,\ i=1,\ldots,r\ .\tag{60}$$

From the definition of J_i and J_j^0 for $j=1,\ldots,\rho$ and from (57) we obtain that:

$$\int_{\Gamma_j'}f_j^0([u]_j,[q]_j)\,d\Gamma=\int_{\Gamma_j'}\Big(\limsup_{\substack{\lambda\to 0\\ h\to 0^+}}\frac{1}{\lambda}\int_{[u]_j+h}^{[u]_j+h+\lambda[q]_j}\beta_j(t)\,dt\,d\Gamma\Big)=$$

$$=\int_{[q]_j>0}\ldots d\Gamma+\int_{[q]_j>0}\ldots d\Gamma\ge\int_{[q]_j>0}\beta_j(\infty)\,[q]_j\,d\Gamma+$$

$$=\int_{[q]_j>0}\beta_j(-\infty)\,[q]_j\,d\Gamma=\int_{\Gamma_j'}(\beta_j(\infty)\,[q]_{j+}-\beta_j(-\infty)\,[q]_{j-})\,d\Gamma\ .\tag{61}$$

Accordingly:

$$\sum_{i=1}^{r} \overset{=}{(f_i, q_i)} \leq \sum_{j=1}^{\rho} \left(\int_{\Gamma_j'} (\beta_j(\infty)[q]_{j+} - \beta_j(-\infty)[q]_{j-}) \, d\Gamma \right.$$

$$\forall q_i \in Kera_i \,, \; q_i \neq 0 \,, \; i = 1, ..., r \tag{62}$$

and analogously for $-\int f_j^0 [u]_j \,, [q]_j) \, d\Omega$. Thus (58) is proved.

The proof of the rest of the proposition is trivial, q.e.d. Further a sufficient condition will be derived. To this end the regularized Problem P_ε is defined:

Let p be a mollifier ($p \in C_c^\infty(-1.+1), p \geq 0$ with $\int_{-\infty}^{+\infty} p(\xi)\, d\xi = 1$), and let:

$$\beta_{\varepsilon j} = p_\varepsilon * \beta_j \,, \quad \varepsilon > 0 \,, \quad j = 1, ..., \rho \tag{63}$$

Here $p_\varepsilon(\xi) = (1/\varepsilon) p(\xi/\varepsilon)$ and $*$ denotes the convolution product. The regularized problem P_ε reads:

Problem P_ε. Find $u_{\varepsilon i} \in V_i, i = 1, ..., r$, such as to satisfy the variational equality:

$$\sum_{i=1}^{r} a_i(u_{\varepsilon i}, v_i) + \sum_{j=1}^{\rho} \int_{\Gamma_j'} \beta_{\varepsilon j}([u_\varepsilon]_j)[v]_j \, d\Gamma =$$

$$= \sum_{i=1}^{r} \overset{=}{(f_i, v_i)} \,, \quad \forall v_i \in V_i \tag{64}$$

Further a Galerkin bais is introduced for each one of the spaces $V_i \cap L^\infty(\Gamma_i), i = 1, ..., r$, let V_{in} denote the corresponding n-dimensional subspace of $V_i \cap L^\infty(\Gamma_i)$. Then Problem $P_{\varepsilon n}$ results.

Problem $P_{\varepsilon n}$. Find $u_{\varepsilon ni} \in V_{in}, i = 1, 2, ..., r$ such:

$$\sum_{i=1}^{r} a_i(u_{\varepsilon ni}, v_i) + \sum_{j=1}^{\rho} \int_{\Gamma_j'} \beta_{\varepsilon j}([u_{\varepsilon n}]_j)[v]_j \, d\Gamma =$$

$$= \sum_{i=1}^{r} \overset{=}{(f_i, v_i)} \,, \quad {}^n v_i \in V_{in} \,, \quad i = 1, ..., r \,. \tag{65}$$

Proposition 3. Let:

$$\beta_j(-\infty) < \beta_j(\infty) \ , \quad j = 1, ..., \rho \tag{66}$$

Then if,

$$\sum_{j=1}^{\rho} \Big(\int_{\Gamma_j'} (\beta_j(-\infty)[q]_{j+} - \beta_j(\infty)[q]_{j-}) \, d\Gamma \Big) < \sum_{i=1}^{r} (\bar{f}_i, q_i) <$$

$$< \sum_{j=1}^{\rho} \Big(\int_{\Gamma_j'} (\beta_j(\infty)[q]_{j+} - \beta_j(-\infty)[q]_{j-} \Big) \, d\Omega \ ,$$

$$\forall q_i \in Kera_i \ , \ q_i \neq 0 \ , \ i = 1, ..., r \tag{67}$$

problem P has at least one solution:

Proof. (66) implies that for some $\xi \in \mathbf{R}$:

$$\sup_{(-\infty, -\xi)} \beta_{\varepsilon j}(\xi) \leq \inf_{(\xi, \infty)} \beta_{\varepsilon j}(\xi) \ . \tag{68}$$

Thus we may determine for every j two numbers $\rho_{1j} > 0$ and $\rho_{2j} > 0$ such that $\beta_{\varepsilon j}(\xi) \geq 0$:

$$\text{if } \ \xi > \rho_{1j} \ , \ \beta_{\varepsilon j}(\xi) \leq 0 \ \text{ if } \ \xi < -\rho_{1j} \ \text{ and } \ |\beta_{\varepsilon j}(\tilde{\xi})| \leq \rho_{2j} \ \text{ if } \ |\xi| \leq \rho_{1j}$$

and thus,

$$\int_{\Gamma_j'} \beta_{\varepsilon j}([u_{\varepsilon n}]_j)\,[u_{\varepsilon n}]_j \, d\Gamma = \int_{|[u_{\varepsilon n}]_j| > \rho_{1j}} \ldots \, d\Gamma + \int_{|[u_{\varepsilon n}]_j| \leq \rho_{1j}} \ldots \, d\Gamma \geq$$

$$\geq 0 - \rho_{1j}\rho_{2j} \, mes \, \Gamma_j' \tag{69}$$

This estimate which was applied to the coercive problem [7] will now be improved for the semicoercive problem. First (65) is written in the form:

$$< \Lambda(\bar{u}_{\varepsilon n}'), \bar{v}' > = 0 \ , \ \text{ for } \bar{v}' = \{v_i\} \ , \ \forall v_i \in V_{in} \ , \ i = 1, 2, ..., r \ . \tag{70}$$

From (70), (69) and (49) we find that:

$$<\Lambda(\bar{u}_{\varepsilon n}'),\bar{u}_{\varepsilon n}'> \geq c\sum_{i=1}^{r}\left[p_i(\tilde{u}_{\varepsilon ni})\right]^2 - c\sum_{i=1}^{r}|||u_{\varepsilon ni}||| -$$

$$-\sum_{j=1}^{\rho}\rho_{1j}\rho_{2j}\,mes\,\Gamma_j' \,, \quad c\ const > 0 \,. \tag{71}$$

Now using Brouwer's theorem we shall show that (70) has at least one solution $\bar{u}_{\varepsilon n}$ and that $\{|||u_{\varepsilon ni}|||\}$ is bounded for every i. Accordingly to this theorem (cf. [28], p. 53) it suffices to show that there exists a number $M > 0$ such that:

$$|||u_{\varepsilon ni}||| > M \,, \quad i = 1,...,r \quad \text{implies} \quad (\Lambda(\bar{u}_{\varepsilon n}'),\bar{u}_{\varepsilon n}') > 0 \tag{72}$$

For the proof of (72) it is sufficient to prove that:

$$(\Lambda(\bar{u}_{\varepsilon n}'),\bar{u}_{\varepsilon n}') \leq 0 \quad \text{implies} \quad |||u_{\varepsilon ni}||| \leq c \,, \quad i = 1,...,r \,. \tag{73}$$

Due to (71) we deduce that, if $(\Lambda(\bar{u}_{\varepsilon n}'),\bar{u}_{\varepsilon n}') \leq 0$, then a constant $c > 0$ exists such that:

$$\Big(\sum_{i=1}^{r}p_i(\tilde{u}_{\varepsilon ni})\Big)^2 \leq c\sum_{i=1}^{r}|q_{\varepsilon ni}|_2 + c \tag{74}$$

where $u_{\varepsilon ni} = \tilde{u}_{\varepsilon ni} + q_{\varepsilon ni}$. Accordingly it is sufficient to prove that $<\Lambda(\bar{u}_{\varepsilon n}'),\bar{u}_{\varepsilon n}'> \leq 0$ implies $|q_{\varepsilon ni}|_2 \leq c, i = 1,...,r$ or equivalently, that a number $R > 0$ can be determined such that:

$$|q_{\varepsilon ni}|_2 > R \,, \ i = 1,...,r \ \text{and (74)} \Rightarrow <\Lambda(\bar{u}_{\varepsilon n}'),\bar{u}_{\varepsilon n}'> > 0 \,. \tag{75}$$

This last relation will now be proved. From the definition of $\beta_{\varepsilon j}$ we prove that:

$$\beta_{\varepsilon j}(\infty) = \lim_{\xi\to\infty}\beta_{\varepsilon j}(\xi) = \lim_{\xi\to\infty}\int_{-\varepsilon}^{+\varepsilon}\beta_j(\xi - t)\,p_\varepsilon(t)\,dt \geq$$

$$\geq \lim_{\xi\to\infty}\ ess\ inf_{|x-\xi|\leq\varepsilon}\ \beta_j(x) \geq \lim_{\xi\to\infty}\ ess\ inf_{\xi-\varepsilon\leq x<\infty}\ \beta_j(x) =$$

$$= \lim_{x\to\infty}\ inf\ \beta_j(x) = \beta_j(\infty) \,. \tag{76}$$

Similarly we show that $\beta_{ej}(-\infty) \le \beta_j(-\infty)$. Thus (67) implies that:

$$\sum_{j=1}^{\rho} \Big(\int_{\Gamma_j'} (\beta_{ej}(-\infty)\,[q]_{j+} - \beta_{ej}(\infty)\,[q]_{j-})\,d\Gamma < \sum_{i=1}^{r} \overset{=}{(f_i, q_i)} <$$

$$< \sum_{j=1}^{\rho} \Big(\int_{\Gamma_j'} (\beta_{ej}(\infty)\,[q]_{j+} - \beta_{ej}(-\infty)\,[q]_{j-})\,d\Gamma \Big),$$

$$\forall q_i \in Kera_i\,,\ q_i \neq 0\,,\ i = 1, \ldots, r\,. \tag{77}$$

Due to (66) numbers $\bar{M}_j > \rho_{1j}$ (cf. (69)) can be chosen such that for functions $\bar{u}_i \in V_i$ with $[\bar{u}(x)]_j > \bar{M}_j$ and sign $[\bar{u}(x)]_j = sign\,[q(x)]_j$ for almost every $x \in \Gamma_j'$, we have from (77) that for $[q]_j > 0$, $[q]_j = [q]_{j+}$ and $[\bar{u}(x)]_j > M_j$, $j = 1, \ldots, \rho$ sufficiently large,

$$\sum_{j=1}^{\rho} \int_{\{x \,|\, [q(x)]_j > 0\}} \beta_{ej}([\bar{u}(x)]_j)\,[q(x)]_j\,d\Gamma - \sum_{i=1}^{r} \overset{=}{(f_i, q_i)} > 0\,, \tag{78}$$

$$\sum_{j=1}^{\rho} \int_{\{x \,|\, [q(x)]_j > 0\}} \beta_{ej}(-[\bar{u}(x)]_j)\,[q(x)]_j\,d\Gamma + \sum_{i=1}^{r} \overset{=}{(f_i, q_i)} > 0\,. \tag{79}$$

For $[q]_j < 0$ we have $[q]_j = -[q]_{-j}$ and for $[\bar{u}(x)]_j < -M_j$ we obtain from (77):

$$\sum_{j=1}^{\rho} \int_{\{x \,|\, [q(x)]_j < 0\}} \beta_{ej}([\bar{u}(x)]_j)\,[q(x)]_j\,d\Gamma - \sum_{i=1}^{r} \overset{=}{(f_i, q_i)} > 0 \tag{80}$$

$$\sum_{j=1}^{\rho} -\int_{\{x \,|\, [q(x)]_j < 0\}} \beta_{ej}(-[\bar{u}(x)]_j)\,[q(x)]_j\,d\Gamma + \sum_{i=1}^{r} \overset{=}{(f_i, q_i)} > 0\,. \tag{81}$$

By an appropriate choice of the numbers $\delta_j \in (0, 1]$, $N_j > 1$, $\eta > 0$, and $\alpha_j > 0$, and by taking into account that $\beta_{ej}([\bar{u}(x)]_j) \cdot [\bar{u}(x)]_j \ge 0$ and that sign $[\bar{u}(x)]_j = sign\,[q(x)]_j$, $j = 1, \ldots, \rho$, these inequalities imply for every $[\bar{u}]_j$ as above, the relations:

$$\sum_{j=1}^{\rho}\left(1-\frac{1}{N_j}\right)\int_{\left\{x\,|\,|[q(x)]_j|>\delta_j\alpha_j\right\}}\beta_{ej}\left([\tilde{u}(x)]_j\right)[q(x)]_j\,d\Gamma-$$

$$-\sum_{i=1}^{r}(f_i,q_i)>\sum_{i=1}^{r}\eta\,|q_i|_2 \tag{82}$$

$$\sum_{j=1}^{\rho}-\left(1-\frac{1}{N_j}\right)\int_{\left\{x\,|\,|[q(x)]_j|>\delta\alpha_j\right\}}\beta_{ej}\left(-[\tilde{u}(x)]_j\right)[q(x)]_j\,d\Gamma+$$

$$+\sum_{i=1}^{r}(f_i,q_i)>\sum_{i=1}^{r}\eta|q_i|_2 \tag{83}$$

as is obvious by taking $\delta_j\to 0$. We take now $u_{eni}=\tilde{u}_{eni}+q_{eni}$. Then for N_j as in (82), (83) and for $\alpha_j>\alpha_{0j}=\bar{M}_j\delta_j^{-1}\left(1-\frac{1}{N_j}\right)^{-1}$ for $j=1,\ldots,\rho$ we have (we omit the index (j) in (84)-(87) for the sake of simplicity).

$$\int_{\Gamma_j'}\beta_e([u_{en}])\,[u_{en}]\,d\Gamma=\int_{\substack{|[\tilde{u}_{en}(x)]|<\frac{\delta\alpha}{N}\\ |[q_{en}(x)]|>\delta\alpha}}\ldots+\int_{\substack{|[\tilde{u}_{en}(x)]|=>\frac{\delta\alpha}{N}\\ |[q_{en}(x)]|>\delta\alpha}}\ldots+\int_{|[q_{en}(x)]|\le\delta\alpha}\ldots\geq$$

$$\geq\int_{\substack{|[\tilde{u}_{en}(x)]|<\frac{\delta\alpha}{N}\\ |[q_{en}(x)]|>\delta\alpha}}\beta_e([u_{en}])\,[u_{en}]\,d\Gamma-\rho_1\rho_2\,mes\,\Gamma_j'\geq$$

$$\geq\left(1-\frac{1}{N}\right)\int_{\substack{|[\tilde{u}_{en}(x)]|<\frac{\delta\alpha}{N}\\ |[q_{en}(x)]|>\delta\alpha}}[q_{en}]\,\beta_e([u_{en}]\,d\Omega-\rho_1\rho_2\,mes\,\Gamma_j' \tag{84}$$

Indeed for $|[\tilde{u}_{en}(x)]|<\delta\alpha/N$ and $|[q_{en}(x)]|>\delta\alpha$ we have that for $\alpha>\alpha_0$:

$$|[u_{en}]|=|[\tilde{u}_{en}+q_{en}]|>\left(1-\frac{1}{N}\right)\delta\alpha>\bar{M} \tag{85}$$

and thus $\beta_e([u_{en}])\cdot[u_{en}]\geq 0$, and $\beta_e([u_{en}])\cdot[q_{en}]\geq 0$. Further it can be verified that for $[q_{en}(x)]>\delta\alpha$:

$$[u_{en}(x)] = [\tilde{u}_{en}(x)] + [q_{en}(x)] > -\frac{\delta\alpha}{N} + [q_{en}(x)] > [q_{en}(x)]\left(1 - \frac{1}{N}\right) \tag{86}$$

and therefore:

$$\beta_e[u_{en}][u_{en}] \geq \left(1 - \frac{1}{N}\right)[q_{en}]\beta_e([u_{en}]) \ . \tag{87}$$

Similarly for $[q_{en}(x)] < -\delta\alpha$. Accordingly (65) implies the inequality:

$$<\Lambda(\tilde{u}_{en}'), \tilde{u}_{en}'> \geq \sum_{j=1}^{p}\left(1 - \frac{1}{N_j}\right) \int\limits_{\substack{|[\tilde{u}_{en}(x)]_j| < \frac{\delta_j \alpha_j}{N_j} \\ |[q_{en}(x)]_j| > \delta_j \alpha_j}} [q_{en}]_j \beta_{ej}([u_{en}]_j)\, d\Gamma_j' -$$

$$- \sum_{j=1}^{p} \rho_{1j}\rho_{2j}\, mes\, \Gamma_j' - \sum_{i=1}^{r} \overset{=}{(f_i, q_{eni})} - \sum_{i=1}^{r} \overset{=}{(f_i, \tilde{u}_{eni})} . \tag{88}$$

By taking into (82) and (83) we obtain from (88) for $\alpha_j > \alpha_{0j}$ sufficiently large, that:

$$<\Lambda(\tilde{u}_{en}'), \tilde{u}_{en}'> > \sum_{i=1}^{r} \eta\, |q_{eni}|_2 - \sum_{j=1}^{p} \rho_{1j}\rho_{2j}\, mes\, \Gamma_j' -$$

$$- \sum_{i=1}^{r} \overset{=}{(f_i, \tilde{u}_{eni})} \geq \sum_{i=1}^{r} \eta\, |q_{eni}|_2 - c_1 - c_2 \sum_{i=1}^{r} ||\tilde{u}_{eni}|| \geq$$

$$\geq \sum_{i=1}^{r} \eta\, |q_{eni}|_2 - c_1 - c_2' \sum_{i=1}^{r} ||\tilde{u}_{eni}|| \geq$$

$$\geq \sum_{i=1}^{r} \eta\, |q_{eni}|_2 - c_1 - c_2' \sum_{i=1}^{r} |||\tilde{u}_{eni}||| =$$

$$= \sum_{i=1}^{r} \eta\, |q_{eni}|_2 - c_1 - c_2' \sum_{i=1}^{r} p(\tilde{u}_{eni}) , \quad c_1, c_2, c_2' \ const > 0 \tag{89}$$

From (89) we obtain due to (74) the final estimate:

$$<\Lambda(\bar{u}_{en}'),\bar{u}_{en}'> \geq \sum_{i=1}^{r} \eta\,|q_{eni}|_2 - c_1 - c\sqrt{\sum_{i=1}^{r}|q_{eni}|_2 + c}\ ,$$

$$c, c_1 \ const > 0 \tag{90}$$

The right-hand side of (90) is positive for $|q_{eni}|_2 > R$, $i = 1, ..., r$, where R is an appropriately large number. Thus (75) has been shown. Thus due to Brouwer's fixed point theorem, problem P_{en} has a solution u_{eni} with $||u_{eni}|| < c$, $i = 1, ..., r$. Now we may determine subsequences, again denoted by $\{u_{eni}\}$, $i = 1, ..., r$, such that for $\varepsilon \to 0, n \to \infty$:

$$u_{eni} \to u_i \quad \text{weakly in} \quad V_i\,, \quad i = 1, ..., r\ , \tag{91}$$

and because of the compact imbeddings in (46a) and considering the correspondence of Ω_i's with the interfaces Γ_j' we have:

$$u_{eni} \to u_i \quad \text{strongly in} \quad L^2(\Gamma_j')\,, \quad i = 1, ..., r\ . \tag{92}$$

Accordingly:

$$u_{eni} \to u_i \quad \text{a.e. in} \quad \Gamma_j'\,, \quad i = 1, ..., r\ . \tag{93}$$

Further we may omit the indices (i) and (j) if no ambiguity occurs. Now we shall prove that $\beta_{ej}([u_{en}]_j)$ is weakly precompact in $L^1(\Gamma_j')$, $j = 1, ..., \rho$ [29]. Applying the Dunford-Pettis theorem (e.g. [30], p. 239) we show that for each $\mu_j > 0$ and $\delta_j > 0$ can be determined such that for $\omega_j \subset \Gamma_j'$ with $mes\,\omega_j < \delta_j$:

$$\int_{\omega_j} |\beta_{ej}([u_{en}]_j)|\,d\Gamma_j' < \mu\ . \tag{94}$$

From the inequality:

$$\xi_0\,|\beta_e(\xi)| \leq |\beta_e(\xi)\,\xi| + \xi_0 \sup_{|\xi| \leq \xi_0} |\beta_e(\xi)| \tag{95}$$

we obtain (we omit the index j):

$$\int |\beta_\varepsilon([u_{\varepsilon n}])|\, d\Gamma' \le \frac{1}{\xi_0}\int_\omega |\beta_\varepsilon([u_{\varepsilon n}])\,[u_{\varepsilon n}]|\, d\Gamma' +$$

$$+ \int_\omega \sup_{|[u_{\varepsilon n}(x)]| \le \xi_0} |\beta_\varepsilon([u_{\varepsilon n}])|\, d\Gamma' \tag{96}$$

But:

$$\int_{\Gamma_j'} |\beta_\varepsilon([u_{\varepsilon n}])\,[u_{\varepsilon n}]|\, d\Gamma' = \int_{|[u_{\varepsilon n}(x)]|>\rho_1} |\ldots|\, d\Gamma' + \int_{|[u_{\varepsilon n}(x)]|\le\rho_1} |\ldots|\, d\Gamma' =$$

$$= \int_{|[u_{\varepsilon n}(x)]|>\rho_1} |\ldots|\, d\Gamma' - \int_{|[u_{\varepsilon n}(x)]|\le\rho_1} |\ldots|\, d\Gamma' = 2\int_{|[u_{\varepsilon n}(x)]|\le\rho_1} |\ldots|\, d\Gamma' \le$$

$$\le \int_{|[u_{\varepsilon n}(x)]|>\rho_1} |\ldots|\, d\Gamma' + \int_{|[u_{\varepsilon n}(x)]|\le\rho_1} |\ldots|\, d\Gamma' + 2\int_{|[u_{\varepsilon n}(x)]|\le\rho_1} |\ldots|\, d\Gamma' =$$

$$= \int_{\Gamma_j'} \beta_\varepsilon([u_{\varepsilon n}])\,[u_{\varepsilon n}]\, d\Gamma' + 2\int_{|[u_{\varepsilon n}(x)]|\le\rho_1} |\beta_\varepsilon([u_{\varepsilon n}])\,[u_{\varepsilon n}]|\, d\Gamma' . \tag{97}$$

Now we choose in (65) appropriate variations which make all the terms but one of the sum $\sum_{j=1}^{\rho} \ldots$ disappear. This is possible by setting e.g. $v_1 = \tilde{v}_1 \in V_{1n}$, $v_2 = \tilde{v}_2 \in V_{2n}$, ..., $v_r = \tilde{v}_r \in V_{rn}$ such that $[v]_j \neq 0$ on Γ_j' and $[v]_k = 0$ on Γ_k' for $k = 1, 2, \ldots, j-1, j+1, \ldots, \rho$. Then we take that $[v]_j = [u_{\varepsilon n}]_j$ on Γ_j' and we have from (97) that generally for $1 < \tilde{r} \le r$:

$$\int_{\Gamma_j'} |\beta_{\varepsilon j}([u_{\varepsilon n}])\,[u_\varepsilon n])_j|\, d\Gamma \le \sum_{i=1}^{\tilde{r}} (f, u_{\varepsilon ni}) - \sum_{i=1}^{\tilde{r}} a_i(u_{\varepsilon ni}, u_{\varepsilon ni}) +$$

$$+ 2\int_{|[u_{\varepsilon n}(x)]_j|\le\rho_{1j}} |\beta_{\varepsilon j}([u_{\varepsilon n}]_j)\,[u_{\varepsilon n}]_j|\, d\Gamma \le$$

$$\le c + 2\rho_{1j}\rho_{2j}\, mes\, \Gamma_j' \qquad \forall j = 1, \ldots, \rho \tag{98}$$

From the definition of the mollifier and from (63) we prove easily the estimate:

$$\sup_{|\xi| \le \xi_0} |\beta_{\varepsilon j}(\xi)| \le \operatorname{ess\,sup}_{|\xi| \le \xi_0 + 1} |\beta_j(\xi)| \tag{99}$$

Choosing ξ_0, such that for all ε and n:

$$\frac{1}{\xi_0} \int_{\omega_j} |\beta_{\varepsilon j}([u_{\varepsilon n}]_j)\,[u_{\varepsilon n}]_j|\, d\Gamma_j' \le \frac{1}{\xi_0}(c + 2\rho\gamma_j 2\rho\gamma_j \, mes\, \Gamma_j') \le \frac{\mu_j}{2} \tag{100}$$

and δ_j such that for $mes\, \omega_j < \delta_j$:

$$\operatorname{ess\,sup}_{|\xi| \le \xi_0 + 1} |\beta_j(\xi)| \le \frac{\mu_j}{2\delta_j} \tag{101}$$

we obtain that:

$$\int_{\omega_j} \sup_{|[u_{\varepsilon n}(x)]_j| \le \xi_0} |\beta_{\varepsilon j}([u_{\varepsilon n}]_j)|\, d\Gamma_j' \le$$

$$\le \operatorname*{ess\,sup}_{|[u_{\varepsilon n}(x)]_j| \le \xi_0 + 1} |\beta_j([u_{\varepsilon n}]|\, mes\, \omega_j \le \frac{\mu_j}{2} \tag{102}$$

From (96), (98), (100), (102) and (94) the weak precompactness of $\beta_{\varepsilon j}([u_{\varepsilon n}]_j)$, $j = 1, 2, ..., \rho$ in $L^1(\Gamma_j')$ results. Thus, as $\varepsilon \to 0$ and $n \to \infty$, a subsequence again denoted by $\{\beta_{\varepsilon j}([u_{\varepsilon n}]_j)\}$ can be determined such that:

$$\beta_{\varepsilon j}([u_{\varepsilon n}]_j) \to \chi_j \quad \text{weakly in } L^1(\Gamma_j'),\ j = 1, 2, ..., \rho \tag{103}$$

From (91) and (103) passing to the limit $n \to \infty$, $\varepsilon \to 0$ we obtain from (65) that:

$$\sum_{i=1}^{r} a_i(u_i, v_i) + \sum_{j=1}^{\rho} \int_{\Gamma_j'} \chi_j [v]_j\, d\Gamma_j' =$$

$$= \sum_{i=1}^{r} \overset{=}{(f_i, v_i)},\quad \forall v_i \in V_i,\quad i = 1, 2, ..., r, \tag{104}$$

where we have used (46b). Note that $V_i \cap L^\infty(\Gamma_j')$ where Γ_j' is any subset of Γ_i (on which Ω_i is connected with neighboring body) is also dense in V_i for the V_i-norm.

To complete the proof we have to prove that:

$$\chi_j \in \hat{\beta}_j([u]_j), \quad j = 1, 2, ..., \rho \tag{105}$$

To show (105) we follow a method developed by RAUCH [29]: (93) implies by Egoroff's theorem, that for every $\alpha > 0$, we can determine $\omega_j, j = 1, ..., \rho$ with $mes\,\omega_j < \alpha$ such that:

$$u_{\varepsilon nj} \to u_j \quad \text{uniformly in} \quad \Gamma_j' - \omega_j, \quad j = 1, 2, ..., \rho \tag{106}$$

with $u_j \in L^\infty(\Gamma_j' - \omega_j)$. Due to this uniform convergence, for every $\alpha > 0$ a ω_j with $mes\,\omega_j < \alpha$ can be found such that for any $\mu > 0$, and for $\varepsilon < \varepsilon_0 < \mu/2$ and $n > n_0 > 2/\mu$:

$$|[u_{\varepsilon n}] - [u]| < \frac{\mu}{2}, \quad \forall x \in \Gamma_j' - \omega_j \tag{107}$$

From (55) we derive easily the inequality:

$$\beta_{\varepsilon_i}(\xi) = (p_\varepsilon * \beta_j)(\xi) = \int_{-\varepsilon}^{+\varepsilon} \beta_j(\xi - t)\, p_\varepsilon(t)\, dt \le \operatorname*{ess\,sup}_{|t| \le \varepsilon} \beta_j(\xi - t) \tag{108}$$

and analogously,

$$\operatorname*{ess\,inf}_{|t| \le \varepsilon} \beta_j(\xi - t) \le \beta_{\varepsilon j}(\xi)\,. \tag{109}$$

From (107) and (108, 109) we obtain that:

$$\beta_{\varepsilon j}([u_{\varepsilon n}]) \le \operatorname*{ess\,sup}_{|[u_{\varepsilon n}] - \xi| \le \varepsilon} \beta_j(\xi) \le \operatorname*{ess\,sup}_{|[u_{\varepsilon n}] - \xi| < \mu/2} \beta_j(\xi) \le$$

$$\le \operatorname*{ess\,sup}_{|[u] - \xi| < \mu} \beta_j(\xi) = \bar{\beta}_{j\mu}([u]) \tag{110}$$

and

$$\beta_{j\mu}([u]) \le \operatorname*{ess\,inf}_{|[u] - \xi| < \mu} \beta_j(\xi) \le \beta_{\varepsilon j}([u_{\varepsilon n}])\,, \tag{111}$$

respectively. Due to (110), (111) we obtain for any $e \ge 0$ a.e. in $\Gamma_j' - \omega_j$ with $e \in L^\infty(\Gamma_j' - \omega_j)$ that:

$$\int_{\Gamma_j'-\omega_j} \underline{\beta}_{j\mu}([u])\, e\, d\Gamma \le \int_{\Gamma_j'-\omega_j} \beta_{ej}([u_{en}])\, e\, d\Gamma \le \int_{\Gamma_j'-\omega_j} \overline{\beta}_{j\mu}([u])\, e\, d\Gamma \tag{112}$$

which as $e \to 0$ and $n \to \infty$ becomes:

$$\int_{\Gamma_j'-\omega_j} \underline{\beta}_{j\mu}([u])\, e\, d\Gamma \le \int_{\Gamma_j'-\omega_j} \chi_j\, e\, d\Gamma \le \int_{\Gamma_j'-\omega_j} \overline{\beta}_{j\mu}([u])\, e\, d\Gamma \tag{113}$$

Passing to the limit $u \to 0$ we have using Lebesque's theorem that:

$$\int_{\Gamma_j'-\omega_j} \underline{\beta}_j([u])\, e\, d\Gamma \le \int_{\Gamma_j'-\omega_j} \chi\, e\, d\Gamma \le \int_{\Gamma_j'-\omega_j} \overline{\beta}_j([u])\, e\, d\Gamma \tag{114}$$

Since $e \ge 0$ is arbitrary, (114) implies that:

$$\chi_j \in \hat{\beta}_j([u]) \quad \text{a.e. in } \Gamma_j' - \omega_j\,, \quad j = 1, ..., \rho$$

Taking α as small as possible, implies (105) q.e.d.

Remark 1. If the interfaces are not on the boundaries of the bodies Ω_i but on $\Omega_i' \subset \Omega_i$, as e.g. happens in the case of composite plates, then in (46a,b) $L^2(\Gamma_i), L^\infty(\Gamma_j)$ have to be replaced by $L^2(\Omega_i'), L^\infty(\Omega_i')$ respectively. However for plates the compact imbedding $V_i = H^2(\Omega_i) \subset C^0(\overline{\Omega_i})$ implies that $H^2(\Omega_i) \subset L^\infty(\Omega_i)$ and therefore (46b) is superfluous.

ON THE UNLOADING AND THE NUMERICAL SOLUTION OF HEMIVARIATIONAL INEQUALITIES

Here we shall consider the case of unloading in the interface relations which we have introduced. All these relations are generally multivalued and nonmonotone. We recall that in [31] a method was given for the calculation of a structure for a given unloading path; the method was called "method of macroincrements". Here a more general method taking into account all the possibilities of loading and/or unloading (not only along a given unloading path), is presented. This becomes possible by using appropriately defined multifunctions involving $\varepsilon, \sigma, \dot{\varepsilon}$ and $\dot{\sigma}$. Here the dot means the time partial derivatives (assumptions of small strains and displacements). We assume that the unloading is linear and that the modulus of elasticity changes with the strain. The onedimensional case or an equivalent

modulus of elasticity changes with the strain. The onedimensional case or an equivalent stress-strain uniaxial law, is depicted in Figure 6. At each point along the softening branch AB the question arises whether $\dot{e} = \{\dot{e}_{ij}\}$ is positive, i.e. that one must remain on AB, or negative and then the elastic unloading paths $AC, A'C'$ etc. should be realized. If at the end of a load increment the stress-strain of an interface element is on OAB, then within the next load increment we can write that:

$$\sigma_N \in \bar{\partial}\varphi(\varepsilon_N) \quad \text{if} \quad \varepsilon_N < \varepsilon_0, \text{ or if } \varepsilon_N \geq \varepsilon_0 \text{ and } \dot{\varepsilon}_N \geq 0 \tag{115}$$

$$\sigma_N = C(\varepsilon_N)\,\varepsilon_N \quad \text{if} \quad \varepsilon_N \geq \varepsilon_0 \text{ and } \dot{\varepsilon}_N < 0\,. \tag{116}$$

If the stress and strain of an interface element are, e.g., on $A'C'$ then:

$$\sigma_N = C(\varepsilon_{N'})\,\varepsilon_N \tag{117}$$

where $\varepsilon_{N'}$ denotes the strain at A'. We may easily conclude that (115-117) can be written as:

$$\sigma_N \in \bar{\partial}\varphi(\varepsilon_N)\cdot\psi(\varepsilon_N) + [\bar{\partial}\varphi(\varepsilon_N)\chi_+ + C(\varepsilon_N)\cdot(\varepsilon_N)\cdot\chi_-]\,q(\varepsilon_N,\sigma_N)(1-\psi(\varepsilon_N)) +$$

$$+ C(\varepsilon_{N'})\cdot(\varepsilon_N)\cdot(1-q(\varepsilon_N,\sigma_N))\cdot(1-\psi(\varepsilon_N))\,, \tag{118}$$

where $\psi(\varepsilon_N) = \{1 \text{ for } \varepsilon_N < \varepsilon_0, 0 \text{ for } \varepsilon_N \geq \varepsilon_0\}$ and ε_0 is the strain for which irreversible strains appear, $\chi = \dfrac{\dot{\varepsilon}_N}{|\dot{\varepsilon}_N|}$ and χ_+ and χ_- are the positive and the negative parts of χ respectively, $q(\varepsilon_N,\sigma_N) = \{1 \text{ if } (\varepsilon_N,\sigma_N) \in E, 0 \text{ otherwise}\}$ with $E = \{(\varepsilon_N,\sigma_N) \mid \sigma_N \in \bar{\partial}\varphi(\varepsilon_N)\}$. In (118) $C(\varepsilon_{N'})$ is assumed as known and corresponds to $(\varepsilon_N, \sigma_N) \notin E$. The aforementioned thoughts hold for any type of nonmonotone stress-strain law with unloading. The general form of the above law is a differential inclusion of the form:

$$0 \in F(\varepsilon_N, \sigma_N, \dot{\varepsilon}_N) \tag{119}$$

where F is an appropriately defined multifunction. Note that the classical elastoplastic law is a special case of (119). Usually we know σ_N and ε_N for a given load p and let a new load $\dot{p}\delta t$ be imposed. For the total load $p + \dot{p}\delta t$ be imposed. For the total load $p + \dot{p}\delta t$ the stresses and strains become $\sigma_N + \dot{\sigma}_N\delta t$ and $\varepsilon_N + \dot{\varepsilon}_N\delta t$ and thus for the whole process an incremental relation of the form:

$$\dot{\sigma}_N \in F_1(\varepsilon N, \sigma_N, \dot{\varepsilon}_N) \tag{120}$$

can be written. Thus in the framework of the interface problem of Section 4 we can formulate now the following dynamic problem on the assumption of small strains and small displacements.

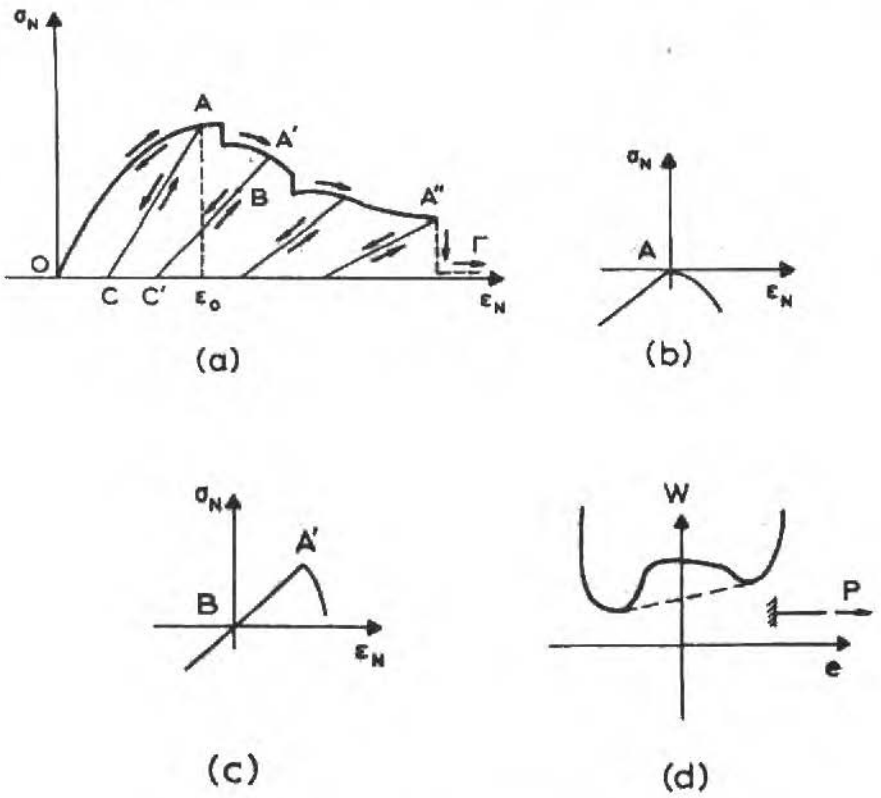

Figure 6. On the unloading problem

Find on $\Omega^{(m)} \times (OT)$, $m = 1, 2, ..., I$, displacement fields $u^{(m)}$ which satisfy:

$$\rho^{(m)} \ddot{u}_i^{(m)} = \sigma_{ij,j}^{(m)} + f_i^{(m)}, \quad \varepsilon_{ij}^{(m)} = \frac{1}{2}(u_{i,j}^{(m)} + u_{j,i}^{(m)}), \quad \sigma_{ij}^{(m)} = C_{ijhk}\varepsilon_{hk}^{(m)} \tag{121}$$

the boundary conditions (23) and (24), the initial conditions $u^{(m)} = u_0^{(m)}$, $\dot{u}^{(m)} = u_1^{(m)}$, $\sigma_{ij}^{(m)} = \sigma_{ij0}^{(m)}$, and the interface conditions:

$$0 \in F_N(S_N^{(m)}, u_N^{(m)}, \dot{u}_N^{(m)}; S_T^{(m)}), \quad 0 \in F_T(S_T^{(m)}, u_T^{(m)}, \dot{u}_T^{(m)}; S_N^{(m)}) \tag{122}$$

where F_N and F_T are appropriately defined multifunctions.

Note that the application of a classical incremental iterative method for the numerical treatment of the loading-unloading law of Figure 6 leads naturally to hemivariational inequalities and actually to eigenvalue problems for hemivariational inequalities. In order to explain it let us consider an interface whose behaviour is simulated by interface elements obeying the law of Figure 6a. Suppose that at the end of a load increment some interface elements have stress and strain on the loading branch of the diagram, say at A, and some on an unloading branch, say at B. Then for the next load increment Δp we have to solve a problem where the interface elements at A obey the law of Figure 6b and the interface elements at B the law of Figure 6c. Obviously a hemivariational inequality characterizes the new position(s) of equilibrium. Of course we may consider the loading $\lambda \Delta p$, where λ is unknown and to solve a "parametric hemivariational inequality" in order to find the value of the load increment for which the loading-unloading mode remains the same, i.e. the laws of Figure 6b,c hold at the interface. Note that an appropriate approximation of the curved parts of the diagrams by line segments leads to nonconvex linear complementarity problems (cf. [12]). It is worth mentioning that the diagrams of Figure 6b and 6c contain a "decision" problem concerning the branch to be followed. A classical incremental iterative procedure uses only a part of the "information" contained into the aforementioned linear complementarity problem.

Concerning the numerical treatment of hemivariational inequalities there are many open questions. Note first that a convexification of the energy eliminates certain important positions of equilibrium (cf. Figure 6d). Let us now consider a static problem: The total load p is given and we have to find all possible positions of equilibrium. The problem leads to a substationarity problem and every local minimum of the potential energy corresponds to an equilibrium configuration. Usually there are huge numerical difficulties concerning the determination of all local minima of a general nonconvex and nondifferentiable function. We mention here as a possible algorithm the bundle method of LEMAREGHAL-STRODIOT [32] which is now at the stage of experimentation. Analogously to the case of classical trial and error methods, one could make some combinatorial attempts to find on which part of a nonmonotone interface law, (cf. e.g. Figure 1f) the solution can appear. But the substationarity property of the solution gives the answer, exactly as in the case of convex contact problems the minimum property of the solution. Another method related to the previous one is the regularization method whose convergence has been already discussed in the previous Section. By means of the discretization and regularization (Problem $P_{\varepsilon h}$) we obtain a system of semilinear algebraic equations depending on ε. The solution of this system "tends" as $\varepsilon \to 0$ to the solution of the initial problem. This system of algebraic equations has the general form:

$$Ku + B_\varepsilon(Tu) = p \tag{123}$$

where u (resp. p) is the otal displacement (resp. load) vector, K is the stiffness matrix, T is a transformation matrix such that Tu gives the appropriate relative displacements and $B_\varepsilon(\cdot)$ is the vector of the nonlinear terms. Noteworthy is the sparsity of the nonlinear terms which in some cases only slightly influences the monotonicity of the problem. In this case the classical Newton-Raphson algorithm gives good results. At this point we would like to remark that a structure with interfaces may have an overall equilibrium position in which one or some elements simulating the interface may be in unstable equilibrium. For further information on the numerical techniques for hemivariational inequalities and on the arising questions we refer the reader to [9].

ACKNOWLEDGEMENTS

Parts of the present paper were presented at PUC, RJ during the months September and October 1987. This period the author was visiting Professor at the Department of Mechanical Engineering of PUC, RJ. The author would like to thank Professor Rubens Sampaio for the invitation and for stimulating discussions during his stay at PUC. This research work was partially supported by the Scientific Division of NATO (Scientific cooperation grant nº 86/0694).

REFERENCES

[1] FICHERA, G. - Problemi elastostatici con vincoli unilaterali: il problema di Signorini con ambigue condizioni al contorno, Mem. Accad. Naz. Lincei, VIII 7, pp. 91-140, 1964.

[2] FICHERA, G. - Existence theorems in elasticity. In: Encyclopedia of Physics (ed. by S. Flügge), vol. VIa/2, Springer-Verlag, Berlin, 1972.

[3] LIONS, J.L. and STAMPACCHIA, G. - Variational inequalities, Comm. Pure and Applied Math., XX, pp. 493-519, 1967.

[4] MOREAU, J.L. - La notion de sur-potentiel et les liaisons unilatérales en élastostatique, C.R. Acad. Sc. Paris, 267A, pp. 954-957, 1968.

[5] PANAGIOTOPOULOS, P.D. - Non-convex superpotentials in the sense of F.H. Clarke and applications, Mech. Res. Comm., 8, pp. 335-340, 1981.

[6] PANAGIOTOPOULOS, P.D. - Nonconvex energy functions. Hemivariational inequalities and substationarity principles, Acta Mechanica, 42, pp. 160-183, 1983.

[7] PANAGIOTOPOULOS, P.D. - Inequality problems in mechanics and applications. Convex and nonconvex energy functions, Birkhäuser Verlag, Boston-Basel 1985 (Rus. Transl. MIR Pub., Moscow 1989).

[8] PANAGIOTOPOULOS, P.D. - Hemivariational inequalities and their applications, In: J.J. Moreau, R.D. Panagiotopoulos, G. Strang (eds), Topicsin Nonsmooth Mechanics, Birkäuser Verlag, Basel, Boston, 1988.

[9] PANAGIOTOPOULOS, P.D. - Nonconvex superpotentials and hemivariational inequalities. Quasidifferentiability in Mechanics in "Nonsmooth Mechanics and Applications", CISM Lect. Notes, vol. 302 (ed. by J.J. Moreau, P.D. Panagiotopoulos), Springer Verlag, Wien 1988.

[10] DUVAUT, G. and LIONS, J.L. - Les inéquations en mécanique et en physique, Dunod, Paris, 1972.

[11] BAIOCCHI, C. and CAPELO, A. - Variational and quasivariational inequalities, J. Wiley, New York, 1984.

[12] KINDERLEHRER, D. and STAMPACCHIA, G. - An introduction to variational inequalities and their applications, Academic Press, New York, 1980.

[13] FRIEDMAN, A. - Variational principles and free boundary problems, J. Wiley, New York, 1982.

[14] RODRIGUEZ, J.F. - Obstacle problems in mathematical physics, North Holland, Amsterdam, 1987.

[15] CLARKE, F.H. - Optimization and nonsmooth analysis, J. Wiley, New York, 1983.

[16] ROCKAFELLAR, R.T. - Generalized directional derivatives and subgradients of non-convex functions, Can. J. Math., XXXII, pp. 257-280, 1980.

[17] ROCKAFELLAR, R.T. - La théorie des sous-gradients et ses applications à l'optimization. Fonctions convexes et non-convexes, Les Presses de l'Université de Montréal, Montréal, 1979.

[18] FLOEGL, H. and MANG, H.A. - Tension stiffening concept based on bond slip, ASCE, ST 12, 108, pp. 2681-2701, 1982.

[19] PANAGIOTOPOULOS, P.D. - Hemivariational inequalities in frictional contact problems and applications, In: Mech. of Material Interfaces (ed. by A.P.S. Selvadurai, G.Z. Voyatzis), Elsevier Sc. Publ., Amsterdam, 1986.

[20] JONES, R. - Mechanics of composite materials, McGraw Hill, New York, 1975.

[21] CHANG, K.C. - Variational methods for non-differentiable functionals and their applications to partial differential equations, J.Math.An.Ap. ,80, pp.102-129, 1981.

[22] STAVROULAKIS, G. and PANAGIOTOPOULOS, P.D. - Laminated orthotropic plates under subdifferential boundary conditions. A Hemivariational inequality approach, ZAMM, 68, pp. 213-224, 1988.

[23] PANAGIOTOPOULOS, P.D. and STAVROULAKIS, G. - A hemivariational inequality approach to the delamination effect in the theory of layered plates, Archives of Mechanics, 39, pp. 497-512, 1987.

[24] NANIEWICZ, Z. and WOZNIAK, C.Z. - On the quasi-stationary models of debonding processes in layered composites, Ing. Archiv. (to appear).

[25] NANIEWICZ, Z. - On some nonmonotone subdifferential boundary conditions in elastostatics, J. Eng. Math., (to appear).

[26] NANIEWICZ, Z. - On some nonconvex variational problems related to hemivariational inequalities. Nonlinear analysis and applications, (to appear).

[27] AUBIN, J.P. - Applied functional analysis, J. Wiley, New York, 1979.

[28] LIONS, J.L. - quelques méthodes de résolution des problèmes aux limites non linéaires, Dunod/Gauthier-Villars, Paris, 1969.

[29] RAUCH, J. - Discontinuous semilinear differential equations and multiple valued maps, Proc. A.M.S. 64, pp. 277-282, 1977.

[30] EKELAND, I. and TEMAM, R. - Convex analysis and variational problems, North-Holland, Amsterdam and American Elsevier, New York, 1976.

[31] PANAGIOTOPOULOS, P.D. - Dynamic and incremental variational inequality principles, differential inclusions and their applications to co-existent phases problems, Acta Mechanica, 40, pp. 85-107, 1981.

[32] STRODIOT, J.J. and NGUYEN, V.H. - On the numerical treatment of the inclusion $0 \in \partial f(x)$, In: Topics in Nonsmooth Mechanics (ed. by J.J. Moreau, P.D. Panagiotopoulos, G. Strang), Birkhäuser Verlag, Basel, 1988.

RBCM - J. of the Braz.Soc.Mech.Sc.
Vol. XI - nº 4 - pp. 379-399 - 1989

ISSN 0100-7386
Impresso no Brasil

PARAMETRIC IDENTIFICATION OF CONSERVATIVE SELF ADJOINT STRUCTURES

IDENTIFICAÇÃO PARAMÉTRICA DE ESTRUTURAS AUTO ADJUNTAS CONSERVATIVAS

G. Lallement
J. Piranda
A. Hamrani
Laboratoire de Mécanique Appliquée, Associé au CNRS
UFR Sciences et Techniques
25.030 Besancon Cedex - France

ABSTRACT

This paper examines the parametric correction of the symmetric mass and stiffness matrices representing the linear elastodynamic behavior of the associated conservative structure to a real dissipative structure. The initial estimations of these matrices are considered to have been constructed by a finite element discretization. The parametric correction is based on the minimization of the distance between the eigensolutions of the model to be corrected and the identified eigensolutions of the physical structure.

Keywords: Dynamics of Structures ▪ Finite Element Model Updating ▪ Modal Tests

RESUMO

Este trabalho examina a correção paramétrica de matrizes de massa de rigidez simétricas que representam o comportamento elastodinâmico linear da estrutura conservativa associada a uma estrutura real dissipativa. As estimativas iniciais destas matrizes são supostas construídas através de uma discretização por elementos finitos. A correção paramétrica é baseada na minimização da distância entre as auto soluções de modelos a ser correlacionado com as auto soluções identificadas a partir da estrutura física.

Palavras-chave: Dinâmica de Estruturas ▪ Validação de Modelos de Elementos Finitos ▪ Testes Modais

Apresentado no 3º DINAME, Águas de S. Pedro, Agosto/89.

INTRODUCTION

This article deals with the dynamics of linear elastic structures. The objective is to construct knowledge models allowing the following predictive calculations to be performed with increased precision:

- free or forced (transitory or steady state) behavior,
- parametric sensitivity and parametric optimization,
- active or semi-active control.

In order to accomplish this objective, the results of calculations deriving from finite element (F.E.) models are combined with the results of prototype tests. The design variables of the F.E. model are then corrected in such a way as to converge its behavior toward the observed behavior of the prototype. The corrected F.E. model can then, observing certain precautions, lead to an improved precision in the three kinds of predictive calculations cited above.

A physical approach to this problem of parametric adjustment (identification) consists first of all in understanding why differences are observed between the behavior of the real structure and its initial mathematical model (initial estimation), then to remedy the situation by correction of the parameters:

- responsable for three differences,
- respecting the configuration (connectivity) of the F.E. model,
- maintaining a clear physical (or energetic) meaning.

The proposed method proceeds by a preliminary phase of localization of the regions of the F.E. model presenting dominant errors. The parameters characterizing these errors are physical parameters such as: elastic coefficients; density; cross-sections; second order moments of inertia (beams); thicknesses (plates); ... associated to the groups of F.E. regrouped into macro-elements. This regrouping allows, on the one hand, to take into account the physical reality of the structure, and on the other hand, to reduce the number of parameters in such a way as to deal with overdetermined systems, which are less sensitive to the non-systematic errors present in the measured data.

ADJUSTMENT DATA

In the formulations which follow, the dynamic behaviors taken into account for the parametric adjustment are the eigensolutions (eigenvalues and sub-eigenvectors) of the F.E. model and of the structure. The eigensolutions of the structure are assumed to be identified

by a technique of modal identification allowing, in addition, the generalized masses to be identified (see for example [1]).

The adjustment is performed using the following known quantities:

- $K^e, M^e \in R^{C,C}$ stiffness and mass matrices of the F.E. model, symmetric, positive definite
- $\lambda_\nu^e, y_\nu^e \in R^{C,1}, \nu = 1, ..., N$ eigenvalues and eigenvectors of the F.E. problem: $[K^e - \lambda_\nu^e M^e] y_\nu^e = 0$, normalized such that: ${}^T y_\nu^e M^e y_\nu^e = 1$.

Let:

$$\Lambda^e = diag\,(\lambda_\nu^e) \in R^{N,N} \quad ; \quad Y^e = [.. y_\nu^e ..] \in R^{C,N}$$

These matrices satisfy the orthonormality relations:

$${}^T Y^e \cdot M^e Y^e = I_N \ , \qquad {}^T Y^e K^e Y^e = \Lambda^e \ .$$

- $\lambda_\nu^m, z_\nu^m \in R^{c,1}, \nu = 1, ..., n$ eigenvalues and normalized sub-eigenvectors identified on the structure at c instrumented degrees of freedom (dof). z_ν^m is a sub-vector of $y_\nu^m \in R^{C,1}$, solution of the F.E. problem: $[K^m - \lambda_\nu^m M^m] y_\nu^m = 0$, where $K^m, M^m \in R^{C,C}$ are the unknown (and to be identified) mass and stifness matrices of the structure.

Let:

$$Z^m = [.. z_\nu^m ..] \in R^{c,n} \ ; \quad Z^e = [.. z_\nu^e ..] \in R^{c,N}$$

where $z_\nu^e \in R^{C,1}$ is the sub-vector of y_ν^e associated with the c instrumented dof.

CHARACTERIZATION OF THE "DISTANCE" BETWEEN THE STRUCTURE AND ITS FINITE ELEMENT MODEL

The distance is evaluated by calculating the difference between homologous eigenvalues and eigenvectors:

$$\Delta\lambda_\nu = \lambda_\nu^m - \lambda_\nu^e \ , \quad \nu = 1, ..., n \ ; \quad \Delta z_\nu = z_\nu^m - z_\nu^e \ , \quad \nu = 1, ..., n \ , \in R^{c,1} \ .$$

This yields $c \cdot n + n$ equations. In practice, these differences are in fact utilized in the form of dimensionless quantities, which have not been introduced here in order to simplify the notation.

The evaluation of this distance makes sense only if the eigensolutions have been matched, that is to say, if it is possible to associate an identified eigenmode with its homologous F.E. mode (in eigenshape and in sign). With this purpose, the matching matrice A is formed, whose elements are calculation from:

$$A_{sv} = \frac{T_{z_s^e} z_v^m}{||z_s^e|| \; ||z_v^m||}$$

The matrice A is equal to the unit matrice when the identified and calculated modes are identical. In practice, two modes are considered to be homologous when, in a column of A, the largest element has an absolute value $A_{sv} > .7$. The s^{th} F.E. mode is then the homologue of the v^{th} measured mode. If this condition is not respected, it will be seen that it is still possible to use the equations relative to these modes by employing an appropriate technique.

PRINCIPLES OF THE LOCALIZATION BY A SENSITIVITY METHOD. DETERMINISTIC GAUSS-NEWTON APPROACH

Parameterization of the Macro-Elements. Having defined the "distance" between the structure and its F.E. model by: $\Delta\lambda_v$; Δz_v, $v = 1, ..., n$, it is then natural to use a sensivity method to express the evolution of the eigenvalue and sub-eigenvectors as a function of the variations of the design parameters intervening in the F.E. model. These $2r \cdot$ macro-element parameters are assumed to intervene linearly in the stiffness and mass matrices:

$$K^e = \sum_{i=1}^{r} s_i K_i^e \quad ; \quad M^e = \sum_{i=1}^{r} m_i M_i^e \tag{1}$$

where r is the number of macro-elements, K_i^e, M_i^e are the stiffness and mass matrices of the i^{th} macro-element; s_i, m_i the stiffness and mass modification parameters of the i^{th} macro-element. It is possible that several mass and stiffness parameters may be defined for the same macro-element (corresponding for example, for the stiffness of a beam, to the longitudinal, torsion and bending energies) in such a way as to act independently on the different types of kinetic and strain energies.

Calculation of the Sensitivity Matrix. The vector z_ν^m is expressed as a function of z_ν^e by performing a first order Taylor series expansion:

$$z_\nu^m = z_\nu^e + \sum_{i=1}^{r} \frac{\partial z_\nu^e}{\partial s_i} ds_i + \sum_{i=1}^{r} \frac{\partial z_\nu^e}{\partial m_i} dm_i \ ,$$

$$\Delta z_\nu = z_\nu^m - z_\nu^e = S_\nu{}' \ \Delta p \ , \qquad \text{with:}$$

$$S_\nu{}' \cdot \Delta p = \left[\frac{\partial z_\nu^e}{\partial s_1} \ .. \ \frac{\partial z_\nu^e}{\partial s_r} \ \middle| \ \frac{\partial z_\nu^e}{\partial m_1} \ .. \ \frac{\partial z_\nu^e}{\partial m_r} \right] \begin{bmatrix} ds_1 \\ . \\ ds_r \\ \hline dm_1 \\ . \\ dm_r \end{bmatrix} \ , \quad \nu = 1, ..., n \tag{2}$$

An analogous definition can be made for the eigenvalues:

$$\Delta\lambda_\nu = \lambda_\nu^m - \lambda_\nu^e = S_\nu{}'' \cdot \Delta p \ , \qquad \text{with:}$$

$$S_\nu{}'' \cdot \Delta p = \left[\frac{\partial \lambda_\nu^e}{\partial s_1} \ .. \ \frac{\partial \lambda_\nu^e}{\partial s_r} \ \middle| \ \frac{\partial \lambda_\nu^e}{\partial m_1} \ .. \ \frac{\partial \lambda_\nu^e}{\partial m_r} \right] \begin{bmatrix} ds_1 \\ . \\ ds_r \\ \hline dm_1 \\ . \\ dm_r \end{bmatrix} \ , \quad \nu = 1, ..., n \tag{3}$$

Regrouping equations (2) and (3) yields:

$$\begin{bmatrix} \Delta z_1 \\ \Delta z_n \\ \Delta \lambda_1 \end{bmatrix} = \left[\begin{array}{ccc|ccc} \frac{\partial z_1}{\partial s_1} & \cdots & \frac{\partial z_1}{\partial s_r} & \frac{\partial z_1}{\partial m_1} & \cdots & \frac{\partial z_1}{\partial m_r} \\ \cdot & & \cdot & \cdot & & \cdot \\ \cdot & & \cdot & \cdot & & \cdot \\ \frac{\partial z_n}{\partial s_1} & \cdots & \frac{\partial z_n}{\partial s_r} & \frac{\partial z_n}{\partial m_1} & \cdots & \frac{\partial z_n}{\partial m_r} \\ \frac{\partial \lambda_1}{\partial s_1} & \cdots & & \cdots & & \frac{\partial \lambda_1}{\partial m_r} \end{array}\right] \begin{bmatrix} ds_1 \\ \cdot \\ \cdot \\ ds_r \\ dm_1 \\ \cdot \\ \cdot \\ dm_r \end{bmatrix} \tag{4}$$

$$d = S \cdot \Delta p \qquad \text{where } d \in R^{cn+n,1}$$

The calculation of the terms of the sensitivity matrix is well known. The only hypothesis made is that the derivatives of the eigenvectors can be expressed on the extended basis of N $(N \geq n)$ F.E. eigenvectors:

$$\frac{\partial y_v^e}{\partial s_i} = Y^e t_v^i \; ; \qquad \frac{\partial y_v^e}{\partial m_i} = Y^e a_v^i \tag{5}$$

It can easily be shown from the derivation of the equilibrium equations and from the orthonormality relations that:

$$\frac{\partial y_v^e}{\partial s_i} = Y^e t_v^i \; ; \; t_{sv}^i = \frac{d_{sv}^{s_i}}{\lambda_s^e - \lambda_v^e} \; ; \; t_{vv}^i = 0 \; ; \; d_s^{s_i} = -{}^T Y^e K_i^e y_v^e \tag{6}$$

$$\frac{\partial y_v^e}{\partial m_i} = Y^e a_v^i \; ; \; a_{sv}^i = \frac{d_{sv}^{m_i}}{\lambda_s^e - \lambda_v^e} \; ; \; a_{vv}^i = -\frac{1}{2}({}^T y_v^e M_i^m y_v^e) \; ; \; d_v^i = \lambda_v^e {}^T Y^e M_i^e y_v^e$$

$$\frac{\partial \lambda_v^e}{\partial s_i} = -d_{vv}^{s_i} \; ; \; \frac{\partial \lambda_v^e}{\partial m_i} = -d_{vv}^{m_i} \tag{6 bis}$$

From the expressions (6), it is apparent that the sensitivity matrix depends essentially on the eigenvalues calculated by F.E. and on the matrices ${}^T Y^e K_i^e Y^e$ and ${}^T Y^e M_i^e Y^e$.

In order to transcend the particular type of F.E. code used, the assembly of the elementary matrices M_i^e, K_i^e of the macro-elements and the preceeding products are performed in an independent program. The results are stored in a standard file. This preliminary work being done, the sensitivity matrix S can be evaluated without having to re-read the matrices

M^e; K^e, which are often of very large size.

The expressions (6) show that the terms of the sensitivity matrix depend in the denominator on the differences $(\lambda_s^e - \lambda_v^e)$, which can provoke numerical instabilities (or lead to a non-convergent series expansion) when the F.E. model possesses quasi-multiple eigenvalues. A method has been proposed [2] allowing these eigenvalues to be artificially separated in the calculation model by modifying the stiffness matrix by the addition of a sum of singular matrices of rank 1. The measured data are also corrected in order to account for the introduction of these matrices. The problem posed by the quasi-multiple frequencies for the calculation of the sensitivity matrix is then surmounted under to condition that, after the introduction of these modifications, the matching between calculated and measured modes remains possible.

If this matching is no longer possible, it is proposed to replace the equations corresponding to the differences between the eigenvalues of homologous modes by the sensitivity relations relative to the products and sums of the neighboring eigenvalues [3].

Exploitation of the Sensitivity Matrix for the Localization of the Dominant Errors. Before the construction of the sensitivity matrix, a first step consists in selecting the macro-elements. It is required that all the elements belonging to the same macro-element be related to a common set of mass and stiffness parameters, and that the columns of the sensitivity matrix corresponding to these parameters have a significative importance.

The first partitioning into macro-elements is generally performed as a function of the geometry of the structure. Certain elements of the sensitivity matrix depend on the quadratic forms ${}^T y_v^e M_i^e y_v^e$ and ${}^T y_v^e K_i^e y_v^e$ which represent the kinetic and potential energies of the i^{th} macro-element at the mode v. It would be all together illusory to seek to select parameters in region having weak energies. The parameters associated with the macro-elements whose energies are negligeable relative to the global energy of the structure are thus eliminated a priori (or regrouped with others).

This elimination being made, the problem takes on the following form:

$$d = S_R \cdot \Delta\rho_R \ , \tag{7}$$

where S_R represents the sensitivity matrix with a certain number of columns suppressed (or regrouped); $\Delta\rho_R$ is the vector of parameters to be localized.

In (7), $n \cdot c$ equations are relative to the eigenvectors, n relative to the eigenvalues. In order to manipulate lines and columns having equations of the same dimensions, (7) is modified in such a way that the vectors d and $\Delta\rho_R$ contain the relative variations of the eigenvalues, eigenvectors and parameters. Finally, to account for the fact that the identification of the

eigenvalues is much more accurate than that of the eigenvectors, these n equations are weighted by a coefficient of the order of c. This leads then to the relation:

$$d' = S_R' \cdot \Delta p_R' \quad . \tag{8}$$

It is a matter of qualitatively exploiting (8) in order to find which parameters allow the best representation of the vector d' expressing the distance between the structure and its mathematical model. A first solution consists in resolving (8) in the least squares sense:

$$\Delta p_R' = [{}^T S_R' \, S_R']^{-1} \, {}^T S_R' \, d' \tag{9}$$

Experience shows that this solution is not the best. In effect, it tends to give a global solution in which the components corresponding to the weakly sensitive regions are too important. A phenomena of compensation can also be observed where the augmentation of parameters in one region is compensated for by the diminution of the parameters in a neighboring region (problems of linear quasi-dependence).

As an alternative, the relation (8) can be exploited in the following fashion: Among the columns of S_R', the single column is sought which best represents the vector d', then the combination of two columns, three columns, etc. which constitute the best sub-basis for the representation of the vector d'. Let: $S_R'^{(p)}$ be the best sub-basis of dimension p; $\Delta p_R'^{(p)}$ the combination of the corresponding parameters evaluated in the least squares sense and: $d'^{(p)} = S_R'^{(p)} \cdot \Delta p_R'^{(p)}$ the best representation of d' in the sub-basis of dimension p. Let the scalar e be defined as the distance between d' and $d'^{(p)}$ such that:

$$e\% = 100 \, \frac{||d' - d'^{(p)}||}{||d'||} \quad . \tag{10}$$

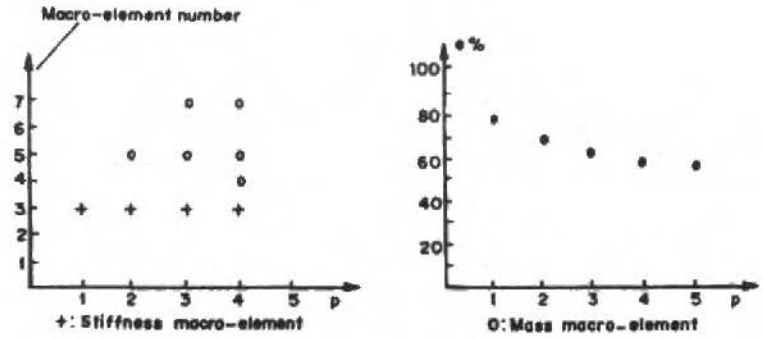

Figure 1. Typical evolution of e as a function of the dimention p of the sub-basis

In example of Figure 1, taking into account the stiffness parameter of the macro-element n° 3 allows a reduction of e from 100% to 80%. The addition of the column corresponding to the mass-parameter of the macro-element n° 5 decreases e to 70%. Then, taking into account the supplementary parameters does not noticeable reduce e. It is clear that, in this example, the regions presenting dominant errors are the macro-elements n° 3 and 5.

If the selected parameters were the "good ones", the error e should tend toward zero. An important residual error can be attributed to either a poor correspondance between the macro-elements and the elements actually bearing the errors, or an incorrect modelization of the errors, or to the influence of the higher order terms not taken into account in the local linearization (method of Gauss-Newton). An approach such as Newton's method based on a local quadratic model (and this including the second derivatives) is presented in a more general manner in the following paragraph. In the relations which follow, in order to return to a resolution of the localization problem by a deterministic Newton-type approach, the values of the matrices P_P and P_R should be taken as: $P_P = 0$; $P_R = I_{cn+n}$.

PARAMETRIC ADJUSTMENT BY NEWTON'S METHOD. BAYESIAN APPROACH

Assuming that the localization phase of the dominant modelization errors has been resolved, the next problem is that of qualitatively correcting the parameters in the regions presenting dominant errors. This problem is resolved by iterative minimization of the following functional:

$$f(p) = \frac{1}{2}\left[{}^T r(p)\, P_r\, r(p) + {}^T(p - p^0)\, P_P\, (p - p^0)\right]$$

in which:

- $r(p) = r^m - r^e(p) \in R^{cn+n,\,1}$ contains the "distances" between the identified and calculated eigensolutions; $r^m = {}^T({}^T z^m; {}^T\lambda^m)$; $r^e(p) = {}^T({}^T z^e; {}^T\lambda^e)$ with: $z^m, z^e \in R^{cn,\,1}$; $\lambda^m, \lambda^e \in R^{n,\,1}$ formed respectively from the n sub-eigenvectors corresponding to the c identified dof and the n eigenvalues.
- $p; p^0 \in R^{q,\,1}$ vectors of dimension q equal to the number of design variables taken into account in the macro-elements presenting the dominant errors; p designates · the vector of sought parameters, p^0 the vector of initial estimations of these parameters.
- $P_r; P_P$ diagonal matrices, positive definite, respectively the covariance matrix of uncertainties in the measured responses and the covariance matrix of uncertainties in the initial estimation of the parameters p^0.

A quadratic model is constructed of $f(p)$ in the neighborhood of $p = p^0$, then the minimization of $f(p)$ is approximated by the minimization of this quadratic model. Letting: $\Delta p = p - p^0$, the minimization problem is written: $Min\, f(\Delta p)$ and the necessary condition for a minimim: $\frac{\partial f}{\partial \Delta p} = 0$ leads to:

$$\Delta p = [{}^T S(p^0)\, P_r\, S(p^0) + P_p + V(p^0)]^{-1}\, {}^T S(p^0)\, P_r\, r(p^0) \ ,$$

with:

$$S(p^0) = \frac{\partial r}{\partial p}\Big|_{p^0} \in R^{cn+n,\,q} \ ,$$

with the general element i,j: $\frac{\partial r_i}{\partial p_j}\Big|_{p^0}$

$V(p^0) \in R^{q,q}$ with the general element i,j:

$$V_{ij} = \left[\frac{\partial^2 r_1}{\partial p_i\, \partial p_j}\ ;\ \ldots\ ;\ \frac{\partial^2 r_{cn+n}}{\partial p_i\, \partial p_j}\right] P_r\, r(p^0)$$

The approximation of $f(p)$ by a quadratic model does not allow convergence to be obtained in a single calculation step. The calculation thus proceeds in an iterative fashion with, on the one hand, a verification of the norm of the solution Δp and, on the other hand, an updating of the sensitivity matrix S and of matrix of second derivatives at each iteration.

Normalization of the Solution Δp. This normalization can be made by multiplying the solution Δp by a reduction coefficient or by introducing a weighting coefficient limiting the norm of Δp. Tests have shown that the two methods lead to similar results and the first technique is used as it is simpler to apply. Let h be the maximum norm allowed for Δp (in pratice $h \leq 1$, which sets the upper limit on the variation of parameters at 100%). The normalized solution Δp is obtained by:

$$\hat{\Delta p} = \frac{\Delta p\, h}{||\Delta p||} \quad \text{if: } h < ||\Delta p|| \ ; \quad \hat{\Delta p} = \Delta p \quad \text{if: } h => ||\Delta p|| \ .$$

Updating of the Sensitivity Matrix S. The sensitivity matrix involves the parameters as well as the eigenvalues and eigenvectors of the F.E. problem. As for the parameters, p is replaced by $p + \Delta p$. For Λ^e, Y^e it is impractical to re-make a F.E. analysis after each

iteration. However, it is possible to make an approximate calculation working in the modal basis Y^e. Letting, as before:

$$K^e = \sum_i s_i K_i^e \ , \quad M^e = \sum_i m_i M_i^e \ .$$

For the initial F.E. Model:

$$\underset{(0)}{K^e} = \sum_i K_i^e \ , \quad \underset{(0)}{M^e} = \sum_i M_i^e$$

The first iteration yields $ds_i^{(1)}, dm_i^{(1)}$. The new eigenvalue problem becomes:

$$[\sum_i K_i^e + \sum_i ds_i^{(1)} K_i^e - \lambda^{(1)} (\sum_i M_i^e + \sum_i dm_i^{(1)} M_i^e)] y^{(1)} = 0$$

Let: $\underset{(1)}{Y^e} = \underset{(0)}{Y^e} q^{(1)}$ be the new modal basis. By using an extended basis of N modes and multiplying on the left hand side by ${}^T\underset{(0)}{Y^e}$, the following equation is obtained, having taken into account the orthonormality relation:

$$\left[\underset{(0)}{\Lambda^e} + \sum_i ds_i \, {}^T\underset{(1)}{Y^e} \underset{(0)}{K_i^e} \underset{(0)}{Y^e} - \lambda^{(1)} \left(I + \sum_i dm_i \, {}^T\underset{(1)}{Y^e} \underset{(0)}{M_i^e} \underset{(0)}{Y^e}\right)\right] q^{(1)} = 0$$

which can be rewritten:

$$[\Lambda^e + \hat{\Delta K}^{(0)} - \lambda^{(1)} (I + \hat{\Delta M}^{(0)}] \, q^{(1)} = 0 \qquad (11)$$

The matrices are strongly diagonal dominant. A resolution by the method of Jacobi is particularly well adapted to this problem.

The resolution of (11) yields Λ^e and $Q^{(1)}$ such that:

$${}^TQ^{(1)} \left(\underset{(0)}{\Lambda^e} + \sum_i ds_i \, {}^T\underset{(1)}{Y^e} \underset{(0)}{K_i^e} \underset{(0)}{Y^e}\right) Q^{(1)} = \Lambda^{(1)}$$

$${}^TQ^{(1)} \left(I + \sum_i dm_i \, {}^T\underset{(1)}{Y^e} \underset{(0)}{M_i^e} \underset{(0)}{Y^e}\right) Q^{(1)} = I \ .$$

The new eigenvalues are defined by $\Lambda^{(1)}$, the new eigenvectors by: $\underset{(1)}{Y^e} = \underset{(0)}{Y^e} Q^{(1)}$.

The sensitivity matrix uses the matrices ${}^{T}Y^{e}_{(j)} K^{e}_{i} Y^{e}_{(j)}$; ${}^{T}Y^{e}_{(j)} M^{e}_{i} Y^{e}_{(j)}$; where j is the iteration number. It is thus not necessary to calculate the new Y^{e}, and the matrices can be updated using the following relations:

$$ {}^{T}Y^{e}_{(j)} M^{e}_{i} Y^{e}_{(j)} = {}^{T}Q^{(j)} \left({}^{\cdot}Y^{e}_{(j-1)} M^{e}_{i} Y^{e}_{(j-1)} \right) Q^{(j)} $$

$$ {}^{T}Y^{e}_{(j)} K^{e}_{i} Y^{e}_{(j)} = {}^{T}Q^{(j)} \left({}^{\cdot}Y^{e}_{(j-1)} K^{e}_{i} Y^{e}_{(j-1)} \right) Q^{(j)} $$

The sensitivity matrix can thus be updated at each iteration. The parameters at iteration j are deduced from those of iteration $j-1$ by the relation: $p_i^{(j)} = p_i^{(j-1)} (1 + \Delta p_i^{(j)})$.

APPLICATION TO THE TEST CASE GARTEUR Nº 1

The method of parametric adjustment proposed above is applied to an initial test case developed by R. Ohayon et H. Berger, Onera, in the context of the activities of the "Action Group: Refinement of Structural Dynamics Computational Models, GARTEUR". The test case consists of a pure numerical simulation. The "identified" eigensolutions are generated by a calculation using the initial F.E. estimation M^{e}, K^{e} perturbed by localized parametric modifications which the participants in the case test must attempt to find.

The considered structure is a bidimensional frame in plane vibrations (Figure 2). Each of the 83 finite element segments is considered as a superposition of a bar element in axial deformation with the mass concentrated at the nodes and a beam element in bending deformation and with zero mass and inertia. The model has 3 dof per node, 78 nodes, giving a total of 234 dof.

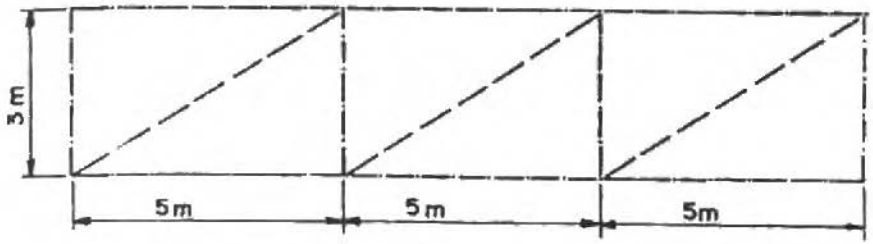

Figure 2. Geometry of the structure and finite element mesh

The Following Data are furnished by the Onera. a) Initial estimation: geometrical and mechanical characteristics: $E = .75\,10^{11}\,Pa, \rho = 2800 kg/m^3, I$ moment of inertia = $= .756\,10^{-1}\,m^4$; cross-sections of the vertical elements: $.6\,10^{-2}\,m^2$; of the horizontal elements: $.4\,10^{-2}\,m^2$; of the diagonal elements: $.3\,10^{-2}\,m^2$. In order to verify the dynamic characteristics of this model, the first 20 eigenfrenquencies provided along with the first 5 sub-eigenvectors on 78 dof (whose positions are indicated in Figure 5) and the first 5 generalized masses.

b) Identified eigensolutions: the first eigenfrequencies of the structure: $M^m = M^e$; $K^m = K^e + \Delta K$; the first 5 sub-eigenvectorson the 78 preceeding dof; the generalized masses associated with the first 5 eigenmodes. In the test case, the parametric modifications have only been introduced in the design variables influencing the stiffness matrix.

Results obtained from the Localization Parametric Adjustment. Three analyses, differing by the dimension of the macro-element introduced are performed.For each of these analyses, the method of Gauss-Newton has been used with: $P_p = 0; P_r = I$.

Analysis Nº 1: Partitioning into 13 "physical" beams defined by the plan of the structure. The following design variables have been introduced for the localization: 1 parameter I per beam; 1 parameter S per beam; giving a total of 26 parameters.

The results of the localization and of the parametric correction are reported in Figure 3 and the residual differences in the eigenfrequencies after the parametric correction in Figure 6.1.

Analysis Nº 2: Partitioning into 26 half-beams (each physical beam from analysis nº 1 is divided in two parts). The following design variables have been introduced: 1 parameter I per half-beam; 1 parameter S per half-beam, giving a total of 52 parameters.

The results of the localization and of the parametric correction are reported in Figure 4 and the residual differences in the eigenfrequencies after the parametric correction in Figure 6.2.

Analysis Nº 3: The partitioning corresponds to the 83 finite elements of the model. The following design parameters are introduced: One parameter I per finite element; one parameter S per finite element; giving a total of 166 parameters.

The results of the localization and of the parametric correction are reported in Figure 5 and the residual differences in the eigenfrequencies after the parametric correction in Figure 6.3a and 6.3b.

Treatment Nº 1: 13 Macroelements; one macroelement = one beam
One parameter I per beam; one parameter S per beam. Total Nb. of parameters: 26

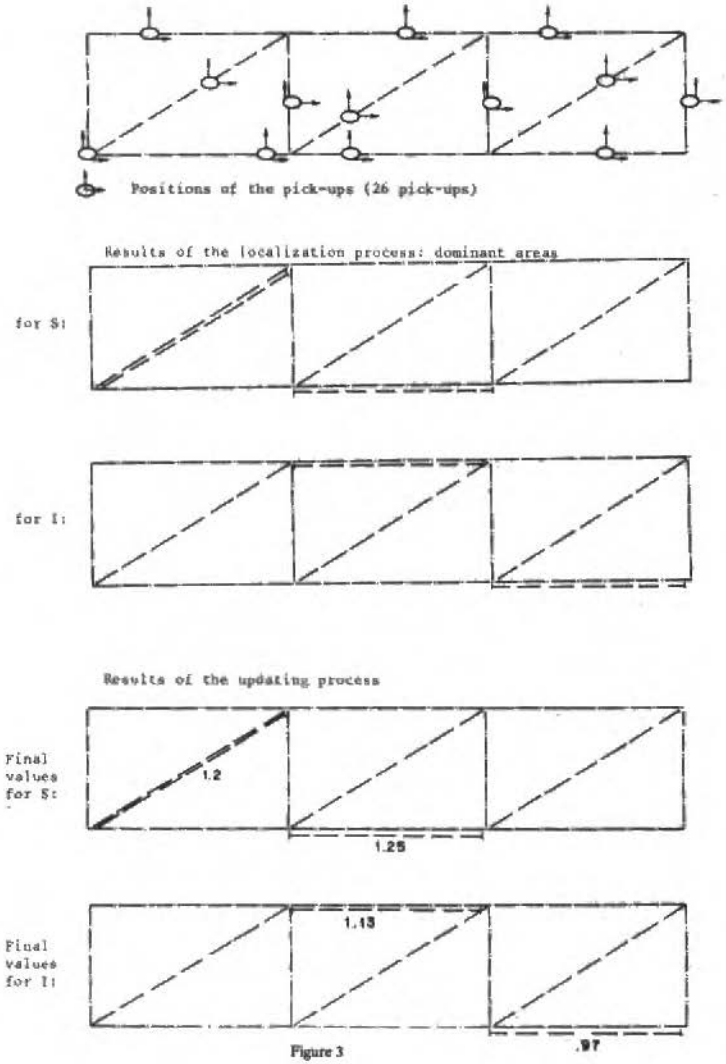

Figure 3

Figure 3

Treatment Nº 2: 26 Macroelements; one macroelement = half a beam
One parameter I per half beam; one parameter S per half beam. Total Nb. parameters: 52

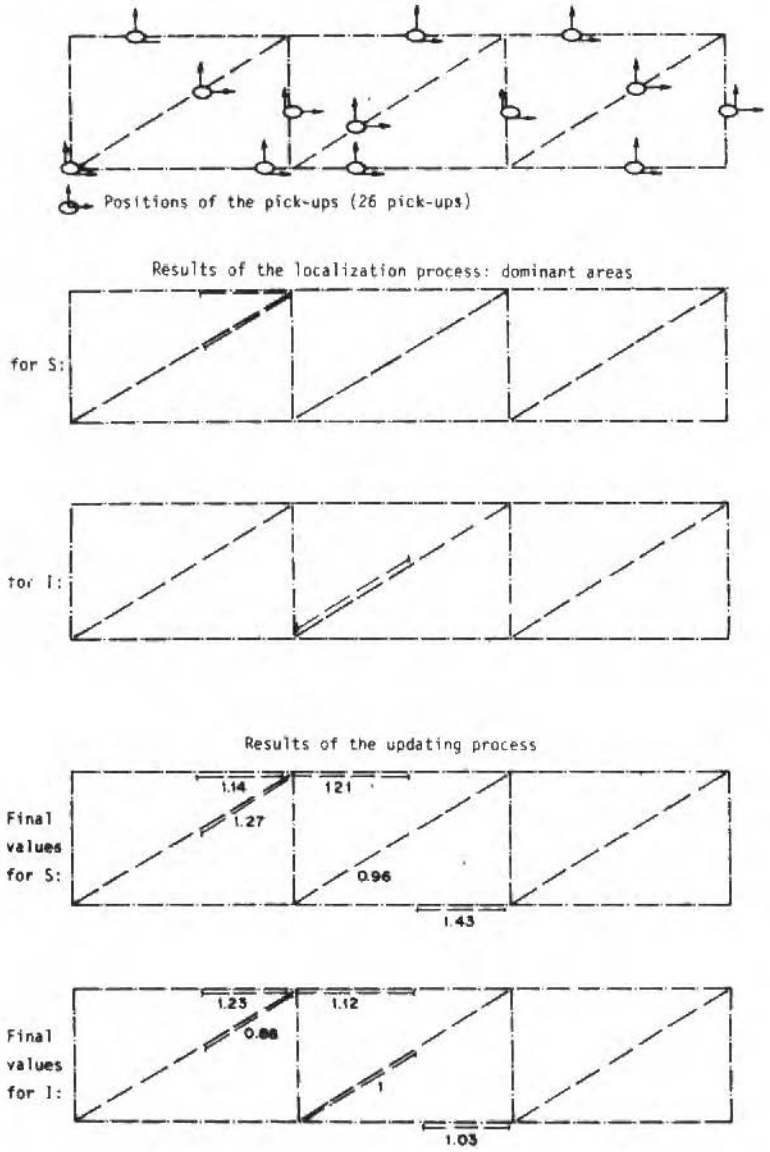

Figure 4

Treatment Nº 3: 83 Macro-elements: one finite-element = one macro-element
One parameter I per finite element; one parameter S per finite element. Total Nb. of parameters = 166

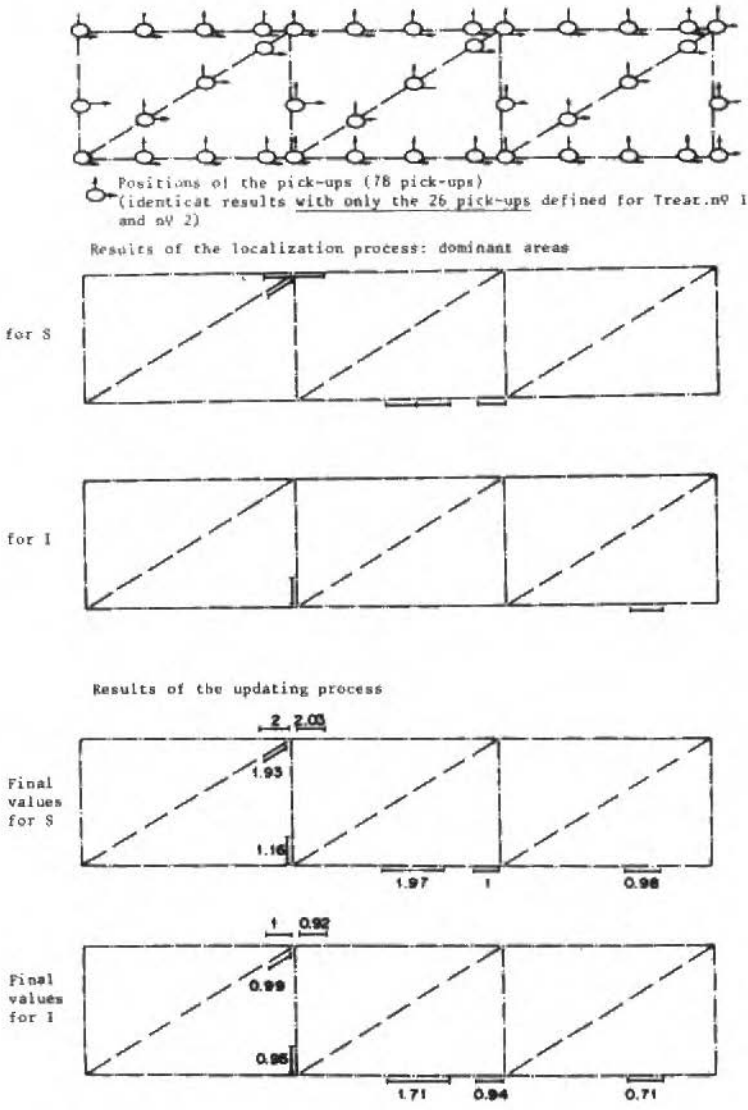

Figure 5

Synthesis of the Results. The following data have been taken into account in the three performed analyses:

- number of identified eigensolutions exploited in the localization and parametric correction: 5
- number of calculated eigensolutions exploited in the evaluation of the first derivations of the eigenvectors: 15
- number c of pick-up degrees of freedom: analyses n° 1 and n° 2: $c = 26$; analysis n° 3: $c = 78$.

The positions of these degrees of freedom have been **arbitrarily** chosen. A method for optimizing the repartition of the pick-ups is currently under development, but has not been applied to this test case.

Figure 6 and Table 1 regroup the values of the "distances" between the calculated and identified eigensolution before and after the parametric correction. These "distances" are defined as follows:

a) Distances relative to the eigenfrequencies:

$$\frac{\Delta f_\nu}{f_\nu}\,\% \overset{\Delta}{=} \frac{f_\nu^{(m)} - f_\nu^{(e)}}{f_\nu^{(m)}} \times 100$$

where: $f_\nu^{(m)}$ is the ν^{th} identified eigenfrequency, $f_\nu^{(e)}$ is the ν^{th} eigenfrequency calculated using the finite element model and matched to $f_\nu^{(m)}$.

b) Distances relative to the sub-eigenvectors:

Let C designate the total number of degrees of freedom of the finite element model. The calculated eigenvector $\hat{y}_\nu^{(e)} \in R^{C,1}$ is normalized such that:

$$^T\hat{y}_\nu^{(e)}\, M^{(e)}\, \hat{y}_\nu^{(e)} = 1 \ , \qquad \nu = 1, 2, \ldots$$

The associated eigenvector $\hat{y}_\nu^{(m)}$ of the structure is also normalized, using a definition which is coherent with the preceeding one:

$$^T\hat{y}_\nu^{(m)}\, M^{(m)}\, \hat{y}_\nu^{(m)} = 1 \ , \qquad \nu = 1 \text{ to } 5$$

Let $y_\nu^{(m)} \in R^{c,1}$ designate the sub-eigenvector of $\hat{y}_\nu^{(m)}$ identified from tests on the structure and $y_\nu^{(e)} \in R^{c,1}$ the homologous sub-eigenvector extracted from $\hat{y}_\nu^{(e)}$. The distances between the sub-eigenvectors are defined by:

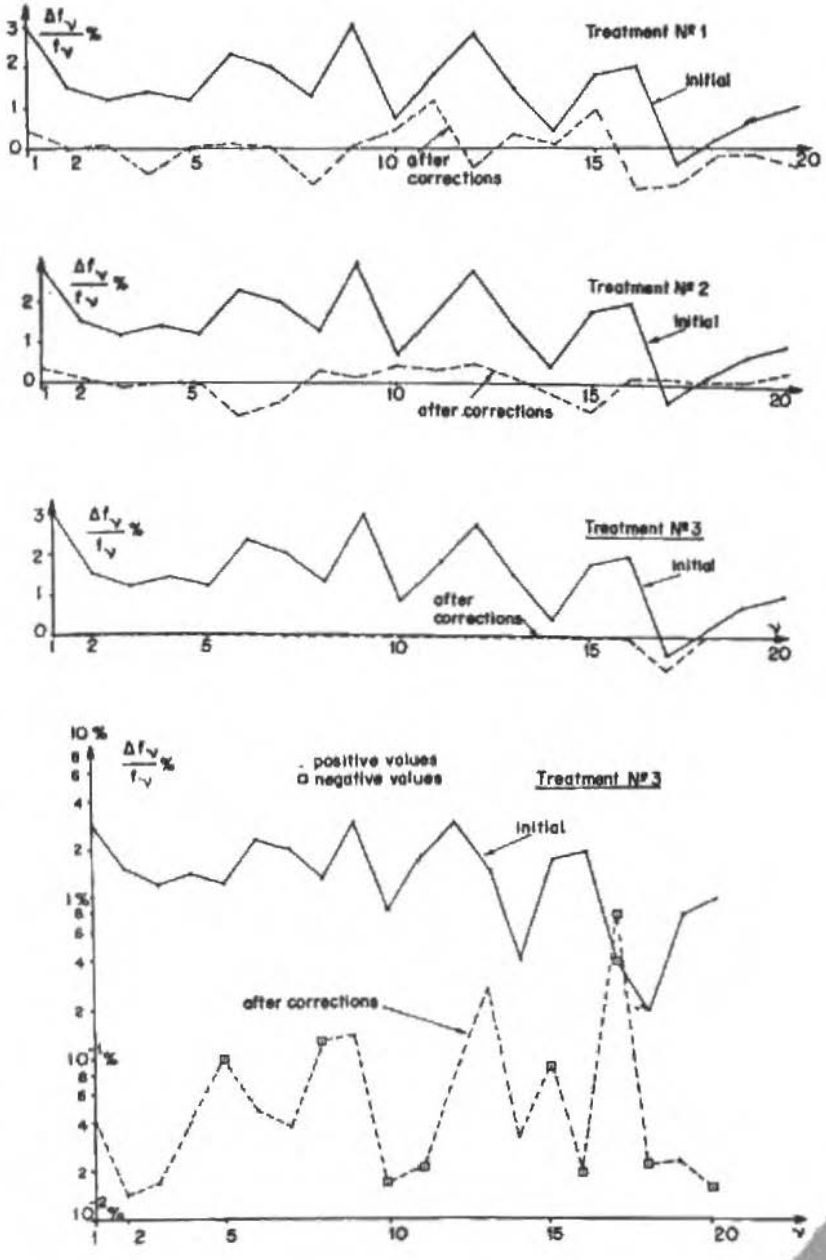
Treatment N° 1
initial
after corrections
Treatment N° 2
initial
after corrections
Treatment N° 3
initial
after corrections
positive values
negative values
Treatment N° 3
initial
after corrections

Figure 6

$$\frac{\Delta y_\nu}{y_\nu}\,\% \overset{\Delta}{=} \frac{||y_\nu^{(m)} - y_\nu^{(e)}||}{||y_\nu^{(m)}||} \times 100$$

$$(1 - MAC_\nu)\,\% = \left(1 - \frac{{}^T y_\nu^{(m)}\, y_\nu^{(e)}}{||y_\nu^{(m)}|| \cdot ||y_\nu^{(e)}||}\right) \times 100$$

Table 1 summarizes the distances between the eigensolutions:

- in column n° 2, the initial distances (with $y_\nu^{(m)}$ and $y_\nu^{(e)} \in R^{26,1}$)
- in column n° 3, the initial distances (with $y_\nu^{(m)}$ and $y_\nu^{(e)} \in R^{78,1}$)
- in column n° 4, the initial distances after the parametric correction of analysis n° 1 ($y_\nu^{(m)}$ and $y_\nu^{(e)} \in R^{26,1}$)
- in column n° 5, the residual distances after the parametric correction of analysis n° 2 ($y_\nu^{(m)}$ and $y_\nu^{(e)} \in R^{26,1}$)
- in column n° 6, the residual distances after the parametric correction of analysis n° 3 ($y_\nu^{(m)}$ and $y_\nu^{(e)} \in R^{78,1}$).

Finally, Figure 6 reports in detail, mode by mode for the first 20 modes, the distances in the eigenfrequencies respectively before and after the parametric corrections.

Note again that only the first 5 "identified" eigenmodes have been exploited for the localization and for the parametric correction.

As the distances in the eigenfrequencies becomes very small after analysis n° 3, they have been simultaneously plotted using both a linear scale (Figure 6.3a) and a logarithmic scale (Figure 6.3b).

Comparison with the Exact Solution. Conclusions. The relative parametric variations effectively introduced (defining the model $M^m; K^m$ sought) and furnished by the Onera after the participants returned their solution are represented in Figure 7. In comparison with the results obtained here, the following remarks can be made:

- **Analysis n° 1**: the macro-element partitioning was much too crude and does not lead to a good solution. The localized regions however are not altogether erroneous.
- **Analysis n° 2**: the localization is not perfect, but by and large concern the regions effectively perturbed. The reduction of the "distances" between the eigensolutions is already fairly satisfactory.

In order to augment the efficiency and the applicability of parametric correction methods to technical problems, current research is directed towards:

a) the development of methods allowing the measured frequency (or time) responses to be treated directly,

b) improving the robustness of the methods with respect to the errors contained in the measured data,

c) the optimal definition of the measurement points (pick-up mesh),

d) the elimination of the matching problems between calculated and observed eigensolutions.

ACKNOWLEDGEMENTS

This study has been financially supported by the DGA-DRET (research contract n° 85/125) and we would like to thank all the individuals concerned, especially Mr. GRELLIER, for their support.

REFERENCES

[1] Equipe Vibrations du LMA - Notice d'utilisation du programme d'identification modale Modan, UFR Sciences et Techniques, Besancon, Juin 1987.

[2] ZHANG, Q.; LALLEMENT, G. - Selective structural modifications. Applications to the problems of eigensolutions sensitivity and model adjustment, Mechanical Systems and Signal Processing, 2(4), Oct. 1988.

[3] LALLEMENT, G.; ZHANG , Q. - Inverse sensitivity based on the eigensolutions: analysis of some difficulties encountered in the problem of parametric correction of finite element models, Proc. 13th Int. Sem. on Modal Analysis, Leuven, Belgium, pp. 19-23, Sept. 1988.

Analysis nº 3: overall, the localizations are good, except in the region of the nodes nº 71, 74 and 76 which is completely hidden. In fact, this region has very low strain energies for the five observed modes and thus, by the method presented here, is practically unobservable.

Table 1. Synthesis of the "distances" between eigensolutions

	Initial c=26	Initial c=78	Analysis Nº 1 c=26	Analysis Nº 2 c=26	Analysis Nº 3 c=78
$\frac{1}{5}\sum_{\nu=1}^{5}\left\|\frac{\Delta f_\nu}{f_\nu}\right\|$ %	1.66	1.66	.22	.11	.04
$\frac{1}{20}\sum_{\nu=1}^{20}\left\|\frac{\Delta f_\nu}{f_\nu}\right\|$ %	1.51	1.51	.41	.27	.13
$\frac{1}{5}\sum_{\nu=1}^{5}\frac{\lvert\Delta y_\nu\rvert}{y_\nu}$ %	14.72	13.90	5.84	3.46	.86
$\frac{1}{5}\sum_{\nu=1}^{5}(1-MAC_\nu)$ %	2.82	2.64	.22	.08	$6.4\ 10^{-3}$

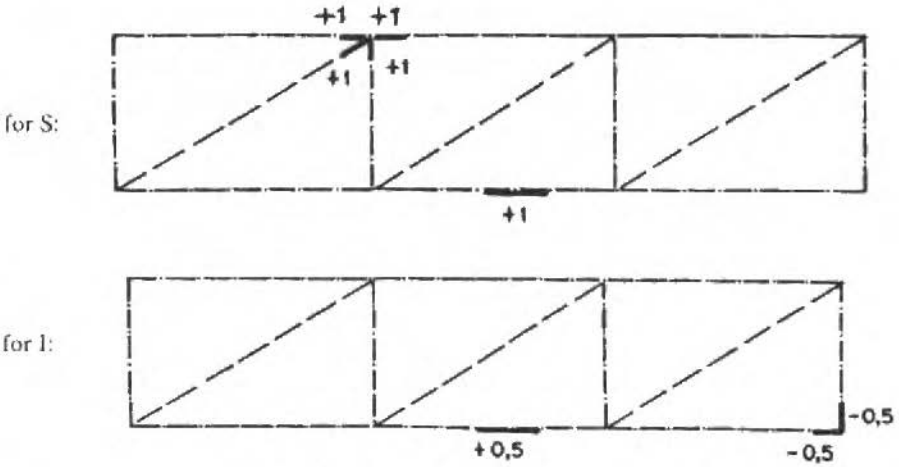

Figure 7. Perturbed regions defining the model K^m. Relative variations of S and of I. $\left(\frac{S^m - S^e}{S^e} ; \frac{I^m - I^e}{I^e}\right)$

OBJETIVO E ESCOPO

A Revista Brasileira de Ciências Mecânicas visa a publicação de trabalhos voltados ao projeto, pesquisa e desenvolvimento nas grandes áreas das Ciências Mecânicas. É importante apresentar os resultados e as conclusões dos trabalhos submetidos de forma que sejam do interesse de engenheiros, pesquisadores e docentes.

O escopo da Revista é amplo e abrange as áreas essenciais das Ciências Mecânicas, incluindo interfaces com a Engenharia Civil, Elétrica, Metalúrgica, Naval, Nuclear, Química e de Sistemas. Aplicacões de Física e de Matemática à Mecânica também serão consideradas.

Em geral, os Editores incentivam trabalhos que abranjam desenvolvimento e a pesquisa de métodos tradicionais bem como a introdução de novas idéias que possam potencialmente ser aproveitadas na pesquisa e na indústria.

AIMS AND SCOPE

The Journal of the Brazilian Society of Mechanical Sciences of concerned primarily with the publication of papers dealing with design, research and development relating to the general areas of Mechanical Sciences. It is important that the results and the conclusions of the submitted papers are presented in a manner which is appreciated by practising engineers, researchers, and educationalists.

The escope of the Journal is broad and encompasses essential areas of Mechanical Engineering Sciences. In addition, interface with Civil, Eletrical, Metallurgical, Naval, Nuclear, Chemical and System Engineering as well as in the areas of Physics and Applied Mathematics, are welcomed.

In general, the Editors are looking for papers covering both development and research of traditional methods and the introductions of novel ideas which have potential in science and manufacturing industry.

Note and Instructions To Contributors

1. The Editors are open to receive contributions from all parts of the world, and manuscripts for publication should be sent to the Editor-in-Chief or to the appropriate Associate Editor.
2. (i) Papers offered for publication must contain unpublished materials and will be refereed and assessed by reference to the aims of the Journal as stated above. (ii) Reviews should constitute outstanding critical appraisals of published materials and will be published by suggestion of the Editors. (iii) Letters and communications to the Editor should not exceed 400 words in length and may be: Criticisms of articles recently published in the Journal; Preliminary announcements of original work of importance warranting immediate publications; Comments on current engineering matters of considerable moment.
3. Only papers not previously published will be accepted and authors must agree not to publish elsewhere a paper submitted to and accepted by the Journal. Exception can be made in some cases of papers published in annals or proceedings of conferences. The decision on acceptance of papers is taken by the Editors on behelf of two reviews of outstanding scientists and will take into consideration their originality, contribution to science and/or technology.
4. All contribution are to be in English or portuguese. However Spanish will also be considered.
5. Manuscripts should begin with the title of the article, always including the english title the author's name, and the address from which communication comes. In the case of co-autors, respective addresses should be clearly indicated. Follow with the abstract in the paper's language; if different from english an extended summary in this language shell be included. Give also key words for the paper. Next, it possible, the nomenclature list shell be presented.
6. Manuscripts should be typed with double spacing with ample margins, in accordance to other published material submitted in triplicate. Pages should be numbered consecutively.
7. Figures and line drawing should be originals and include all relevant details; only excelent photocopies should be sent. Photographs should be enlarged sufficiently to permit clear reproduction in half-tone. If words or numbers are to appear on a photograph then they should be sufficiently large to permit the necessary reduction in size. Figure captions should be typed on a separate sheet and placed at the end of the manuscript.

REVISTA BRASILEIRA DE CIÊNCIAS MECÂNICAS
JOURNAL OF THE BRAZILIAN SOCIETY OF MECHANICAL SCIENCES

Vol. XI - Nº 4 *1989*

ÍNDICE / CONTENTS